



UNIVERSIDADE FEDERAL DE SANTA CATARINA
CENTRO DE CIÊNCIAS FÍSICAS E MATEMÁTICAS
PROGRAMA DE PÓS-GRADUAÇÃO EM QUÍMICA

Felipe Silveira de Souza Schneider

**Quantitative computational contributions to the
elucidation of chemical reaction mechanisms**

Florianópolis, Santa Catarina

6 de janeiro de 2023

Felipe Silveira de Souza Schneider

**Quantitative computational contributions to the
elucidation of chemical reaction mechanisms**

Tese submetida ao Programa de Pós-graduação em Química da Universidade Federal de Santa Catarina como requisito parcial para obtenção do título de Doutor em Química, na área de concentração em Físico-Química.

Orientador: Prof. Dr. Giovanni Finoto Caramori
Coorientador: Prof. Dr. Faruk José Nome Aguilera (*in memoriam*)

Florianópolis, Santa Catarina

6 de janeiro de 2023

Ficha de identificação da obra elaborada pelo autor,
através do Programa de Geração Automática da Biblioteca Universitária da UFSC.

Schneider, Felipe Silveira de Souza
Quantitative computational contributions to the
elucidation of chemical reaction mechanisms / Felipe
Silveira de Souza Schneider ; orientador, Giovanni Finoto
Caramori, coorientador, Faruk José Nome Aguilera, 2023.
140 p.

Tese (doutorado) - Universidade Federal de Santa
Catarina, Centro de Ciências Físicas e Matemáticas,
Programa de Pós-Graduação em Química, Florianópolis, 2023.

Inclui referências.

1. Química. 2. Química computacional. 3. Elucidação de
mecanismos de reação. 4. Desenvolvimento de software. I.
Caramori, Giovanni Finoto. II. Aguilera, Faruk José Nome.
III. Universidade Federal de Santa Catarina. Programa de
Pós-Graduação em Química. IV. Título.

Felipe Silveira de Souza Schneider

Quantitative computational contributions to the elucidation of chemical reaction mechanisms

O presente trabalho em nível de Doutorado foi avaliado e aprovado, em 6 de janeiro de 2023, pela banca examinadora composta pelos seguintes membros:

Prof. Dr. Maximiliano Segala
IQ/UFRGS

Prof. Dr. Amir A. M. de Oliveira Jr.
EMC/UFSC

Prof. Dr. Ataulpa A. C. Braga
IQ/USP

Prof. Dr. Luciano N. Vidal
DAQBI/UFTPR

Certificamos que esta é a versão original e final do trabalho de conclusão que foi julgado adequado para obtenção do título de Doutor em Química, na área de concentração em Físico-Química.

Prof. Dr. Daniel Lázaro G. Borges
Coordenação do
Programa de Pós-Graduação

Prof. Dr. Giovanni Finoto Caramori
Orientador

Florianópolis, Santa Catarina
6 de janeiro de 2023

*Este trabalho é dedicado ao Prof. Dr. Faruk José Nome Aguilera (in memoriam),
motivador original destas ideias.*

Acknowledgements

I would like to acknowledge the following people for their support in the development of this thesis.

Prof. Dr. Giovanni Finoto Caramori for his confidence and trust in myself and in this work, and for the opportunity he gave me to pursue these ideas. Prof. Dr. Faruk José Nome Aguilera (*in memoriam*) for his kind support at a time where this work was in its infancy. I thank both for their support, kindness, advice and mentoring. I am truly honored for the opportunity to have worked with them.

The thesis committee for taking the time and effort to read, evaluate and discuss the present thesis.

To all professors in the Chemistry Department and in the Graduate Programme, and to the Federal University of Santa Catarina as a whole for the high-quality education and excellent work. A special thanks goes to Prof. Dr. Josiel D. Barbosa and Dr. Bernardo de Souza for their enthusiasm and outstanding collaboration, advice and support.

To all the members of our research group, colleagues and friends at GEEM for their support. I would like to thank particularly the following people: Alechania Misturini, Alexandre Osmar Ortolan, Denner Ferreira, Letícia Maria Pequeno Madureira, Marina Briese, Matheus Colaço, Rômulo Peixoto, Vinícius Glitz, and Vinícius Port. Without you I could not have made it until here.

To Scheila and Manssur for helping me when I most needed it.

To my parents (Edson Schneider and Laureci Silveira de Souza Schneider) for their love and support in all these years.

To Deise Munaro for being so kind and special, and for standing on my side for so long and in such difficult times;

I am also grateful for the funding and resources provided by the following institutions. CNPq, for a PhD scholarship (grant number 140485/2017-1), and FAPESC, FAPESP, and CESUP/UFRGS, whose valuable resources make, directly or indirectly, our computing facilities viable.

To the developers of software I have used throughout these years, in special for the developers of the following projects: Julia, NumPy/SciPy, Helix, Vim/Neovim, L^AT_EX and abnT_EX, and cclib.

“We’re in the position of a visitor from another dimension who comes to earth and sees a chess match. Assuming he knows it’s a game, he’s got two problems: first, figure out the rules, and second, figure out how to win. Ninety percent of science (including virtually all of chemistry) is in that second category. They’re trying to apply the laws that are already known.”

(Sheldon Lee Glashow, 1979)

Resumo

Esta tese tem como objetivo explorar a aplicação da química computacional na elucidação de mecanismos de reações químicas complexas. Duas investigações computacionais-experimentais usando cálculos de teoria do funcional de densidade para entender mecanismos de reações químicas são apresentadas na tese, bem como uma publicação sobre o desenvolvimento de um pacote de *software* para simular redes complexas de reações químicas. A primeira publicação consiste em uma investigação híbrida experimental-computacional sobre o desproteção bioortogonal mediado por Pd(II) de grupos hidroxila protegidos por propargila para o propósito de ativação de pró-fármacos (COELHO, S. E. et al. Mechanism of Palladium(II)-Mediated Uncaging Reactions of Propargylic Substrates. **ACS Catalysis**, American Chemical Society (ACS), v. 9, n. 5, p. 3792–3799, Mar. 2019. ISSN 2155-5435. DOI: [10.1021/acscatal.9b00210](https://doi.org/10.1021/acscatal.9b00210). Available from: <http://dx.doi.org/10.1021/acscatal.9b00210>). Na segunda publicação, também uma colaboração computacional-experimental conjunta, investigamos a despropargilação mediada por Pt(II) de amida de pentinoíla e N-propargila para liberação e ativação de fármacos na terapia do câncer (OLIVEIRA, B. L. et al. Platinum-Triggered Bond-Cleavage of Pentynoyl Amide and N-Propargyl Handles for Drug-Activation. **Journal of the American Chemical Society**, American Chemical Society (ACS), v. 142, n. 24, p. 10869–10880, May 2020. ISSN 1520-5126. DOI: [10.1021/jacs.0c01622](https://doi.org/10.1021/jacs.0c01622). Available from: <http://dx.doi.org/10.1021/jacs.0c01622>). Cálculos de mecânica quântica foram fundamentais para apoiar os mecanismos de reação química propostos em ambos os casos. Na terceira publicação, descrevemos o desenvolvimento do *overreact*, um programa de código aberto e fácil de usar que pode ser usado para realizar automaticamente modelagem microcinética de reações químicas complexas em solução ou fase gasosa usando dados de cálculos químicos quânticos de primeiros princípios (SCHNEIDER, F. S. S.; CARAMORI, G. F. Overreact, an *in silico* lab: Automative quantum chemical microkinetic simulations for complex chemical reactions. **Journal of Computational Chemistry**, Wiley, Apr. 2022. ISSN 1096-987x. DOI: [10.1002/jcc.26861](https://doi.org/10.1002/jcc.26861). Available from: <http://dx.doi.org/10.1002/jcc.26861>). As limitações dos resultados são discutidas, e trabalhos futuros potenciais são sugeridos.

Palavras-chave: catálise. química computacional. mecanismos de reação química. microcinética. Python. DFT.

Resumo Expandido

Introdução

Esta tese tem como objetivo explorar a aplicação da química computacional para a elucidação de mecanismos de reações químicas complexas, utilizando cálculos de teoria do funcional da densidade (DFT) e modelagem microcinética. Ao longo do trabalho, são apresentadas duas investigações computacional-experimentais, bem como o desenvolvimento de um pacote de *software* para simular redes de reações químicas complexas.

Objetivos

O principal objetivo desta tese é investigar e desenvolver métodos computacionais para entender mecanismos de reações químicas complexas, utilizando cálculos de DFT e modelagem microcinética. Além disso, a tese busca contribuir com o desenvolvimento de um pacote de *software* para simular redes de reações químicas complexas, facilitando a aplicação dos métodos computacionais desenvolvidos.

Metodologia

No primeiro capítulo, é realizada uma introdução aos conceitos fundamentais de química computacional, teoria do funcional da densidade e microcinética de reação química. Além disso, são apresentadas as principais técnicas e métodos empregados ao longo do desenvolvimento da tese, incluindo a aplicação de cálculos de DFT para a investigação de mecanismos de reação, e a utilização de modelagem microcinética para análise de redes de reações.

No segundo capítulo, são introduzidas as contribuições científicas desta tese, destacando os principais resultados e o impacto das publicações geradas ao longo do trabalho. São apresentadas tanto as contribuições menores, quanto as principais contribuições em cada um dos estudos realizados.

Resultados e Discussão

Na primeira investigação, apresentada no Capítulo 3 (COELHO, S. E. et al. Mechanism of Palladium(II)-Mediated Uncaging Reactions of Propargylic Substrates. **ACS Catalysis**, American Chemical Society (ACS), v. 9, n. 5, p. 3792–3799, Mar. 2019. ISSN 2155-5435. DOI: [10.1021/acscatal.9b00210](http://dx.doi.org/10.1021/acscatal.9b00210)). Available from: <<http://dx.doi.org/10.1021/acscatal.9b00210>>), foi realizado um estudo híbrido experimental-computacional sobre o descascamento bioortogonal de grupos hidroxila protegidos por propargila mediado por Pd(II) com o objetivo de ativar pró-drogas. Os cálculos mecânicos quânticos foram fundamentais para apoiar os mecanismos de reação propostos, oferecendo uma visão detalhada das etapas envolvidas no processo e contribuindo para o entendimento geral da reação.

A análise dos resultados permitiu a identificação das principais barreiras energéticas e intermediários envolvidos no mecanismo de reação.

Na segunda investigação, apresentada no Capítulo 4 (OLIVEIRA, B. L. et al. Platinum-Triggered Bond-Cleavage of Pentynoyl Amide and N-Propargyl Handles for Drug-Activation. **Journal of the American Chemical Society**, American Chemical Society (ACS), v. 142, n. 24, p. 10869–10880, May 2020. ISSN 1520-5126. DOI: [10.1021/jacs.0c01622](https://doi.org/10.1021/jacs.0c01622). Available from: <http://dx.doi.org/10.1021/jacs.0c01622>), foi realizada uma colaboração computacional-experimental com foco na despropargilação mediada por Pt(II) de amida de pentinoíla e alças de N-propargila para entrega e ativação de medicamentos em terapia contra câncer. Mais uma vez, os cálculos mecânicos quânticos desempenharam um papel crucial na elucidação dos caminhos de reação e na compreensão dos resultados experimentais obtidos, permitindo a identificação das principais espécies envolvidas e a descrição detalhada do processo de ativação dos fármacos.

No Capítulo 5 (SCHNEIDER, F. S. S.; CARAMORI, G. F. Overreact, an *in silico* lab: Automative quantum chemical microkinetic simulations for complex chemical reactions. **Journal of Computational Chemistry**, Wiley, Apr. 2022. ISSN 1096-987x. DOI: [10.1002/jcc.26861](https://doi.org/10.1002/jcc.26861). Available from: <http://dx.doi.org/10.1002/jcc.26861>), é descrito o desenvolvimento do pacote de *software overreact*, um programa de código aberto e fácil de usar que pode ser utilizado para realizar modelagem microcinética de reações químicas complexas em solução ou fase gasosa de maneira automática, utilizando dados de cálculos químicos quânticos de primeiros princípios. O *software* é aplicado em diversos estudos de caso, demonstrando sua versatilidade e utilidade para pesquisadores da área, além de facilitar a aplicação dos métodos computacionais desenvolvidos.

Considerações Finais

Por fim, no sexto capítulo, são discutidas as conclusões, limitações dos resultados obtidos e sugeridos trabalhos futuros potenciais. Destaca-se a importância dos estudos realizados e o impacto dos resultados obtidos na compreensão dos mecanismos de reação química e no desenvolvimento de novas estratégias para ativação de pró-drogas e terapias contra câncer. Além disso, são apontadas possíveis direções para pesquisas futuras, tanto na área de química computacional quanto na aplicação prática dos resultados obtidos, incluindo a extensão dos métodos desenvolvidos para outros sistemas e a investigação de novos mecanismos de ativação de fármacos.

Palavras-chave: catálise. química computacional. mecanismos de reação química. microcinética. Python. DFT.

Abstract

This thesis aims to explore the application of computational chemistry to the elucidation of complex chemical reaction mechanisms. Two computational-experimental investigations using density functional theory calculations to understand chemical reaction mechanisms are presented in the thesis, as is a publication on the development of a software package for simulating complex chemical reaction networks. The first publication consists of an experimental-computational hybrid investigation on the Pd(II)-mediated bioorthogonal uncaging of propargyl-protected hydroxyl groups for the purpose of activating prodrugs (COELHO, S. E. et al. Mechanism of Palladium(II)-Mediated Uncaging Reactions of Propargylic Substrates. **ACS Catalysis**, American Chemical Society (ACS), v. 9, n. 5, p. 3792–3799, Mar. 2019. ISSN 2155-5435. DOI: [10.1021/acscatal.9b00210](https://doi.org/10.1021/acscatal.9b00210). Available from: <http://dx.doi.org/10.1021/acscatal.9b00210>). In the second publication, a joint computational-experimental collaboration as well, we investigated the Pt(II)-mediated depropargylation of pentynoyl amide and N-propargyl handles for drug-activation delivery in cancer therapy (OLIVEIRA, B. L. et al. Platinum-Triggered Bond-Cleavage of Pentynoyl Amide and N-Propargyl Handles for Drug-Activation. **Journal of the American Chemical Society**, American Chemical Society (ACS), v. 142, n. 24, p. 10869–10880, May 2020. ISSN 1520-5126. DOI: [10.1021/jacs.0c01622](https://doi.org/10.1021/jacs.0c01622). Available from: <http://dx.doi.org/10.1021/jacs.0c01622>). Quantum mechanical calculations were key to support the proposed chemical reaction pathways in both cases. In the third publication we describe the development of **overreact**, a user-friendly, open-source program that can be used to automatically perform microkinetic modelling of complex chemical reactions in solution or gas-phase using data from first-principles quantum chemical calculations (SCHNEIDER, F. S. S.; CARAMORI, G. F. Overreact, an *in silico* lab: Automative quantum chemical microkinetic simulations for complex chemical reactions. **Journal of Computational Chemistry**, Wiley, Apr. 2022. ISSN 1096-987x. DOI: [10.1002/jcc.26861](https://doi.org/10.1002/jcc.26861). Available from: <http://dx.doi.org/10.1002/jcc.26861>). Limitations of the findings are discussed, and potential future work is suggested.

Keywords: catalysis. computational chemistry. chemical reaction mechanisms. microkinetics. Python. DFT.

Contents

I	STATE OF THE ART AND THEORY	23
1	METHODS AND TECHNIQUES	25
1.1	Practical theoretical background	25
1.1.1	Choice of computational method	26
1.2	Molecular thermodynamics	28
1.2.1	Thermochemical partition functions	29
1.2.1.1	Low-lying imaginary vibrational frequencies	30
1.2.1.2	Corrections to low-frequency vibrational modes	31
1.2.2	Molecular symmetries	31
1.2.3	Standard state corrections	32
1.3	General representation of chemical kinetic equations	33
1.3.1	Representing equilibria	34
1.3.2	Reaction and activation Gibbs' free energies	34
1.3.2.1	Reaction symmetry	35
1.4	Calculation of reaction rate constants	35
1.4.1	Error propagation with respect to energies	36
1.4.2	Adjustment of systematic errors with respect to energies	36
1.4.3	Approximations for quantum tunnelling transmission coefficients	37
1.5	First-principles microkinetic modelling	38
1.5.1	Representation and solution of the chemical kinetic ordinary differential equations	38
1.5.1.1	Concentration constraints	39
1.5.1.1.1	Application: acid-base equilibria	39
II	PUBLICATIONS	41
2	SCIENTIFIC CONTRIBUTIONS	43
2.1	Minor contributions	43
2.2	Major contributions	44
3	PAPER I: MECHANISM OF PALLADIUM-MEDIATED UNCAGING REACTIONS OF PROPARGYLIC SUBSTRATES	45
3.1	Full text	47

4	PAPER II: PLATINUM-TRIGGERED BOND-CLEAVAGE OF PEN- TYNOYL AMIDE AND <i>N</i> -PROPARGYL HANDLES FOR DRUG- ACTIVATION	57
4.1	Full text	59
5	PAPER III: OVERREACT, AN <i>IN SILICO</i> LAB: AUTOMATIVE QUANTUM CHEMICAL MICROKINETIC SIMU- LATIONS FOR COMPLEX CHEMICAL REACTIONS	73
5.1	Full text	75
6	CONCLUDING REMARKS AND CLOSING	87
	References	89
	APPENDICES	111
	Appendix A – LIST OF WORKS	113
	ANNEXES	117
	Annex A – RIGHTS FOR CHAPTER 1	119
	Annex B – RIGHTS FOR CHAPTER 2	121
	Annex C – RIGHTS FOR CHAPTER 3	131

Introduction

The development of catalysis in general, and fine-tuned control of chemical reactions in particular, has truly shaped the world we live in today. A striking example is the development of the Haber-Bosch process, a “synthesis of ammonia from its elements” [4], which Otto Haber had developed in the early 1900s [5, 6], receiving the Nobel Prize for it in 1918 [4]. Carl Bosch later improved the industrial reaction through high pressure methods, which awarded him the Nobel Prize in 1931 [7]. Together, development and precise control were so impressive that it is often used as an example of the geological impact of human actions, a key defining milestone for the era we live in, the Anthropocene [6, 8, 9].

Human activity profoundly affects the environment, from Earth's major biogeochemical cycles to the evolution of life. For example, the early twentieth-century invention of the Haber-Bosch process, which allows the conversion of atmospheric nitrogen to ammonia for use as fertilizer, has altered the global nitrogen cycle so fundamentally that the nearest suggested geological comparison refers to events about 2.5 billion years ago [6].

More than a century later, with the advent of climate change and other environmental and energetic challenges [10], the rational design of chemical reactions is more important than ever before. This is not only due to the impact of human actions, but also precisely because of it: humans have the decision power to start making positive impact on the environment we live in by transitioning to a greener economy. On the other hand, today's economy demands fast and efficient chemical reactions: catalysts are employed in the production of over 80% of all chemical goods of industrial importance [11, 12], and make up a considerable piece of human activity. In fact, the 2014 global market share of catalysts was evaluated in US\$ 33.5 billion, with an annual share in the global economy estimated to be worth US\$ 10 trillion [12].

The apparent conflict between these two requirements can be reconciled by the rational design of green, fast and efficient chemical transformations and catalysts, in particular, with precise prediction of chemical reactions from first principles [13]. The ability to accurately predict and account for the kinetics and thermodynamics associated with chemical procedures remains an immense challenge, yet a central objective in various scientific sectors, with broad implications for the future. Since complex reaction networks can critically inform our interpretation of experimental results, and enable the design of efficient chemical production processes, a broad interest in efficient modelling of the corresponding prediction methods exists. Such rational modelling provides the basis for process improvement and the optimised design of new processes that is demanded today.

Various techniques have been applied for this purpose [14–17]. Computer-aided strategies, such as density functional theory (DFT), provide theoretical models for map-

ping out even complex reaction pathways from initial starting material [18–20]. Additionally, electronic structure calculations of the transition state (TS) or intermediates can be used to determine the reaction rate constants, which are key in the interpretation of experimental data [1, 2, 21, 22]. Recent studies have also explored the use of machine learning algorithms to predict chemical reaction rate constants, providing a useful tool for accelerating reaction catalyst design [23, 24]. Finally, quantum mechanics and statistical mechanics techniques, such as molecular dynamics and Monte Carlo methods, can be employed to obtain thermodynamic and kinetic information for many reactions [25].

On the other hand, there is natural room for improvement: despite the recent great efforts [26], currently industrially employed catalysts do not reach near the throughput, atomic economy, selectivity and efficiency that are so frequently attained by natural enzymes [27]. If we are to rationally design chemical reactions on par with natural enzymes' billion years worth of evolution, we need to be able to predict chemical reactions from first principles with a high degree of accuracy. Such predictions must go beyond simple Gibbs' free energy diagrams and consider important aspects of complex chemical reaction networks such as concentrations, quantum tunnelling, diffusion effects and others [28]. Such modelling provides a significantly improved understanding of the reaction mechanisms underlying the manufacture of valuable chemical products.

Although much of the chemical and industrial breakthroughs were serendipitous, and they were largely based on inspiration, intuition and empirical testing, definition of rational principles of design have involved an increasing amount of computational chemistry [13]. Indeed, nowadays, the role of computational chemistry for industrial applications can hardly be replaced by any other means, as it is often used to boost experimental efforts. Understanding what the global energy landscape of the reaction network looks like, and how it depends on the reaction conditions is thus instrumental in providing a guiding hand towards making efficient, industrially viable improvements. Detailed chemical kinetic modelling of catalytic processes is an emerging area of research and key stepping stone for the future.

Scope

This thesis attempts to formalize a review of methods for predicting chemical kinetics and thermodynamics from first principles. It starts with a brief introduction to the general state of the art in quantum chemistry and state-of-the-art applications to the study of chemical reactions. It then goes on to describe the methods employed in `overreact` [3], a software package for predicting chemical kinetics and simulating microkinetics automatically from first principles.

We pursue methods for predicting and designing reaction mechanisms and equilib-

rium schemes for the chemical machines of the future, with the aim to provide an efficient way to design, understand, evaluate and optimize reactions and their conditions. The focus is in methods and techniques that both aid experimental work and can be validated by it. Such framework allows first-principles microkinetic simulations, by predicting the reaction mechanism from first principles, taking into account most relevant effects influencing chemical reactions in homogeneous media at both room and body temperatures, impacting the design of novel, compact and highly integrated future chemical processes.

Outline

The present thesis is organized in two parts. Part I encompasses a brief overview of the current state of the art in the area of computational elucidation of reaction mechanisms. Part II is divided into three chapters, each of which presents an application or development to certain problems in the field.

The chapters in Part I provide a detailed account of the field. Chapter 1 describes the methods available to computationally investigate reaction mechanisms and, in particular, the methods used in the present thesis. In Section 1.5, attention is paid to methods that led to the design of `overreact` [3, 29], a software package developed by the author for the purpose of automating the investigation of reaction mechanisms in general.

The chapters in Part II revolve around papers that have been published in the field and co-authored by the author. The applications are intertwined in the sense that they contribute to the elucidation of more complex reaction mechanisms. Chapter 3 deals with computational-experimental collaboration on the elucidation of the Palladium(II)-mediated uncaging reaction of propargylic substrates, with applications to the activation of prodrug molecules. It was published in COELHO, S. E. et al. Mechanism of Palladium(II)-Mediated Uncaging Reactions of Propargylic Substrates. **ACS Catalysis**, American Chemical Society (ACS), v. 9, n. 5, p. 3792–3799, Mar. 2019. ISSN 2155-5435. DOI: [10.1021/acscatal.9b00210](https://doi.org/10.1021/acscatal.9b00210). Available from: <http://dx.doi.org/10.1021/acscatal.9b00210>. Chapter 4 provides an account of another computational-experimental collaboration on prodrug activation, this time on the Platinum(II)-triggered bond-cleavage of pentynoyl amide and N-propargyl handles. The relevant publication is OLIVEIRA, B. L. et al. Platinum-Triggered Bond-Cleavage of Pentynoyl Amide and N-Propargyl Handles for Drug-Activation. **Journal of the American Chemical Society**, American Chemical Society (ACS), v. 142, n. 24, p. 10869–10880, May 2020. ISSN 1520-5126. DOI: [10.1021/jacs.0c01622](https://doi.org/10.1021/jacs.0c01622). Available from: <http://dx.doi.org/10.1021/jacs.0c01622>. Finally, Chapter 5 introduces the `overreact` package, a software that performs microkinetic simulations from first principles in an automated way. It was published under SCHNEIDER, F. S. S.; CARAMORI, G. F. Overreact, an *in silico*

lab: Automative quantum chemical microkinetic simulations for complex chemical reactions. **Journal of Computational Chemistry**, Wiley, Apr. 2022. ISSN 1096-987x. DOI: [10.1002/jcc.26861](https://doi.org/10.1002/jcc.26861). Available from: <<http://dx.doi.org/10.1002/jcc.26861>>. In all three chapters, the papers are presented in full text. These encompass what the author believes to be his most relevant contributions to the field, as detailed in Section 2.2. Other minor contributions that tangentially relate to the field are commented on in the text (see Section 2.1). Furthermore, works not directly related to the field, but were nevertheless published during the thesis are presented in Appendix A.

A brief, closing perspective is given in Chapter 6, where the author concludes the thesis with an eye on what he believes to be the future of the field.

Part I

State of the art and theory

1 Methods and techniques

This chapter provides detailed information about the computational methodologies that are applied in the research contributions described in Chapters 3 to 5 to elucidate reaction mechanisms, as well as insights into relevant fundamental concepts of theoretical and computational chemistry. The exposition of all presented formulae follows a standard approach and closely references the pertinent literature. A basic background on computational chemistry applied to mechanistic elucidation is given in Section 1.1 with special emphasis on the proper choice of computational methods (Section 1.1.1). A detailed account on molecular thermodynamics is given in Section 1.2 covering both the rigid-rotor harmonic oscillator approximation (RRHO, Section 1.2.1) and *quasi*-RRHO models (Section 1.2.1.2). We provide a general representation for chemical kinetic equations in Section 1.3 (with special treatment for equilibria in Section 1.3.1) and its role in the systematic calculation of reaction and activation Gibbs' free energies in Section 1.3.2. A treatment on reaction rate constants is done in Section 1.4 with a special account on error propagation (Sections 1.4.1 and 1.4.2) as well as approximations to quantum tunnelling transmission coefficients (Section 1.4.3). Finally, details about solving the differential equations of microkinetic models are given in Section 1.5 including a simple account on concentration constraints (Section 1.5.1.1).

1.1 Practical theoretical background

In order to computationally model a chemical reaction, one needs to collect certain types of information about each participating species. The conceptual information of interest is stored as a potential energy surface (PES), which can be regarded as a function from the atomic coordinates to molecular potential energy, i.e., using the Born-Oppenheimer (BO) approximation, the electronic properties of a molecule depend on the nuclear coordinates only parametrically [30]. In this sense, the model treats nuclei as classical particles as far as geometry optimizations are concerned, which is reasonable for most problems of interest in chemistry. This limitation is mostly relevant to chemical kinetics when we discuss quantum tunnelling effects (Section 1.4.3).

Modelling of a reaction mechanism is performed by first optimizing the structures of the reactants, transition states (TSs), intermediates, and products. While the first one and the last two are minima on the potential energy surface, transition states represent saddle points and special methods must be used to find them [31–43]. Once properly optimized structures are obtained, the region around them on the potential energy surface holds all the information needed for the prediction of chemical reaction kinetics and

thermodynamics (Sections 1.2 and 1.4).

In any case, one needs a potential energy surface. There are many methods available to estimate the potential energy given atomic coordinates, ranging from simple and low-cost semiempirical methods, all the way through highly accurate and expensive multideterminantal wavefunction calculations [44]. Most of these techniques consist of self-consistent field approximations, and a thorough comparison of them is out of the scope of this presentation. In Section 1.1.1, an account on the choice of method is given specifically for the problem of computational chemical kinetics. The interested reader is invited to explore references: on density functional theory [45–61], wavefunction methods [62–64], semi-empirical methods [65, 66], potential additive terms such as solvation approximations [67, 68], atom-centered basis sets [62, 69–83], and quantum chemistry packages [84, 85].

1.1.1 Choice of computational method

As we shall see later, good levels of theory for chemical kinetics must produce 1. energies, 2. geometries, and 3. vibrational frequencies ¹ of suitable quality. Those three requirements have different demands. One needs to choose a computational level of theory to calculate molecular properties with accuracy. It is important to choose a good method for the job at hand. Many reviews are available to help one make a good decision [61, 86–89]. It is also plausible to use a combination of different levels of theory, such as calculating geometries and vibrational frequencies with one method, then using single-point energies with a more costly and precise one; this is performed the works presented in Chapters 3 to 5. Reviewing geometry optimization techniques is out of scope in the present thesis, so we invite the reader to the references on *quasi*-Newton optimization methods [31, 36], single-structure eigenvector-following methods for transition state optimizations [31, 36, 42], and other multi-structure methods for transition state optimizations [32–35, 37–41, 43].

The works presented in this thesis made use of the most popular technique nowadays, the density functional theory (DFT) method [45, 50–52, 54] for that. As such, a brief discussion on the choice of density functional is warranted.

Geometries obtained using recent density functionals are good enough for most purposes. For instance, Bühl; Kabrede observed typical deviations around ± 1.6 pm for metal-ligand bond lengths for 50 transition metal complexes for which precise gas-phase geometries are known from electron diffraction or microwave spectroscopy, when using double- or tripe-zeta basis sets [90]. Minenkov et al. observed that DFT geometries are

¹ Additionally, the calculation of vibrational frequencies is important for characterizing optimized geometries as local minima (reactants, intermediates and products) or saddle points (transition states are first-order saddle points).

systematically expanded when compared with single-crystal X-ray diffraction structures, which is expected, but the deviations are acceptably small in general [49]. Sirianni et al. compared DFT geometries of bimolecular van der Waals complexes using double-zeta basis sets against reference geometries at CCSD(T)/CBS and reported that all functionals analyzed produced geometries within ± 0.1 Å in terms of root-mean-squared displacements. All this leads us to conclude that, in general, modern density functionals deliver molecular geometries of reasonable quality.

In terms of vibrational frequencies, Katari et al. showed that most density functionals predict wavenumbers within ± 10 – 20 cm^{-1} on average for an experimental database of organometallic complexes [92]. Similar deviations were found by Howard; Enyard; Tschumper when comparing against reference CCSD(T)/CBS calculations on small water clusters [93]. As such, we can expect vibrational frequencies to be reasonably delivered by DFT methods.

When it comes to the electronic energy, the situation is different. Goerigk; Grimme compared the performance of 47 density functionals in many different applications within the GMTKN30 dataset, comprising 1218 single point calculations and 841 data points of relative energies [61] (covering general main group thermochemistry, kinetics, and noncovalent interactions). In general, LDAs perform worse of all in all applications, and won't be discussed further here. Overall, GGAs showed errors around 5.3 ± 0.8 $\text{kcal}\cdot\text{mol}^{-1}$, with meta-GGAs presenting 4.4 ± 0.6 $\text{kcal}\cdot\text{mol}^{-1}$. Conventional hybrid functionals performed 3.4 ± 0.8 $\text{kcal}\cdot\text{mol}^{-1}$, with Minnesota hybrids following with 3.1 ± 0.9 $\text{kcal}\cdot\text{mol}^{-1}$, and range-separated hybrids showing 3.3 ± 0.5 $\text{kcal}\cdot\text{mol}^{-1}$. Double hybrids presented errors around 1.7 ± 0.2 $\text{kcal}\cdot\text{mol}^{-1}$. All calculations were performed at essentially complete basis set ((aug-)def2-QZVP). For comparison, different variations of MP2 presented errors around 3.5 ± 0.4 $\text{kcal}\cdot\text{mol}^{-1}$. Mardirossian; Head-Gordon performed a similar benchmark with 200 density functionals and the MGCDB84 dataset consisting of nearly 5000 data points [87] (covering noncovalent interactions, isomerization energies, thermochemistry, and barrier heights), obtained similar results.

These observations reflect on the choice of method when using DFT. Bursch et al. have assembled a series of best-practices in choosing functionals for a variety of applications [89]. Molecular structures can be calculated with triple-zeta basis sets (def2-TZVP) or even well-balanced double-zeta basis sets (def2-SVP). Geometric counterpoise (gCP, for mitigating BSSE) and dispersion corrections are recommended in all cases (D3 or D4). (m)GGAs are typically adequate. Vibrational frequencies have similar demands, as calculation has to be performed with an already optimized geometry.

When modelling reactions, one is often interested in reaction barrier heights. Barrier heights refer to the amount of energy needed to move from the starting point of a reaction to the transition state, which is the point of highest energy in the course of an

elementary reaction. As such, one needs accurate energies for both reactants and transition state. Transition states are challenging to calculate because they often involve weakly bound electrons in near-degenerate molecular orbitals due to stretched bonds, which can lead to an underestimation of the energy barrier heights when using semi-local (m)GGA functionals. The error is dependent on the character of bonds being broken in the transition state, with larger errors associated with dissociation reactions, and smaller ones with pericyclic reactions, for instance [89]. Bursch et al. [89] recommends the use of range-separated hybrids functionals for the calculation of reaction barriers, as well as global hybrids (with a high amount of Fock exchange) and double hybrids, as they mitigate self-interaction errors. Additionally, basis sets should be chosen carefully (oftentimes requiring triple- and quadruple-zeta basis sets) and the London dispersion energy should be taken into account [89]. Finally, for the initial search for transition states, lower-level methods such as hybrid-based composite methods (e.g., PBEh-3c [94]) or semi-empirical methods can be used. Further refinement can then be performed afterwards.

Finally, in order to overcome the errors in electronic energies inherent to density functional theory, one can employ more precise wavefunction methods (e.g., CCSD(T)). In general, such methods are costly, but there are recent developments that attempt at overcoming this limitation. For instance, DLPNO-CCSD(T) [63, 64] can be used to obtain accurate electronic energies, oftentimes as good as CCSD(T), in a cost-effective way. Given that DFT geometries and vibrational frequencies are oftentimes already reasonable, one can employ such cost-effective, precise wavefunction methods to correct the electronic energy only. For instance, [95] observed for DLPNO-CCSD(T) deviations of $0.5 \text{ kcal}\cdot\text{mol}^{-1}$ on average from CCSD(T)/CBS for activation and reaction energies of some enzymatic reactions [95]. Similar conclusions were drawn by [96] when comparing deviations for reaction barriers, although some challenging reactions presented errors as large as $1.2 \text{ kcal}\cdot\text{mol}^{-1}$, outside the chemical accuracy threshold of $1 \text{ kcal}\cdot\text{mol}^{-1}$, but much smaller than the ones expected from density functionals [96].

1.2 Molecular thermodynamics

In order to investigate chemical reactions, one requires knowledge of the absolute Gibbs' free energies from each compound at a given temperature. Those values are calculated from 1. electronic energies, 2. geometry coordinates, and 3. vibrational frequencies of each chemical species.

The `overreact` software, described in Chapter 5, automatically obtains those quantities by parsing computational chemistry output files, using the excellent `cclib` library [97]. Internally, the `overreact` assigns a natural number for each of the m chemical species, and stores a vector G of length m , where each entry is an absolute Gibbs' energy

for that particular compound. Without such a tool, one would have to do this tedious and error-prone data collection by hand. By having such a tool, one can investigate larger and more complex systems in less time. Absolute Gibbs' energies are processed through the usual gas-phase partition-function treatment, as explained in the subsection below.

1.2.1 Thermochemical partition functions

This section briefly presents the process of calculating the absolute Gibbs' free energies as a function of the data collected from computational chemistry output files described above (Section 1.2). In order to do that, thermochemical partition functions have to be estimated. This is already routinely achieved by most standard computational chemistry packages, in an automated way, but as we shall see later, it is advantageous to perform the calculations separately, since one can have complete control over the results.

The canonical gas-phase partition-function, $q(V, T)$, from statistical mechanics is employed for obtaining thermochemical properties of molecules and whole systems, which has been recommended for species in solution as well [98]. Specifically, the rigid-rotor harmonic oscillator (RRHO) ideal gas approximation is used, where energy levels can be decomposed into translational, rotational, vibrational and electronic contributions [99],

$$q(V, T) = \sum_j^{\text{states}} \exp\left(\frac{\epsilon_j}{k_B T}\right) = q_{\text{trans}} q_{\text{rot}} q_{\text{vib}} q_{\text{elec}} \quad (1.1)$$

where ϵ_j is an energy state, k_B is Boltzmann's constant, V is the volume, T is the temperature, and q_{trans} , q_{rot} , q_{vib} and q_{elec} are the aforementioned total partition function contributions (with ω_0 denoting spin multiplicity),

$$\begin{aligned} q_{\text{trans}} &= \left(\frac{2\pi m k_B T}{h^2}\right)^{\frac{3}{2}} \frac{k_B T}{p} \\ q_{\text{rot}} &= \begin{cases} \frac{T}{\Theta_1^{\text{rot}}} & \text{if linear} \\ \sqrt{\pi} \frac{T^3}{\prod_{i=1}^3 \Theta_i^{\text{rot}}} & \text{otherwise} \end{cases}, \quad \Theta_i^{\text{rot}} = \frac{\hbar^2}{2I_i k_B} \\ q_{\text{vib}} &= \sum_{i=1}^{n_\nu} \frac{\exp\left(-\frac{\Theta_i^{\text{vib}}}{2T}\right)}{1 - \exp\left(-\frac{\Theta_i^{\text{vib}}}{T}\right)}, \quad \Theta_i^{\text{vib}} = \frac{h\nu_i}{k_B}, \quad n_\nu = \begin{cases} 3N - 5 & \text{if linear} \\ 3N - 6 & \text{otherwise} \end{cases} \\ q_{\text{elec}} &= \omega_0 \end{aligned} \quad (1.2)$$

Observe that, in the equations above, molecular symmetry is not included. They will be discussed separately below (Section 1.2.2). Furthermore, q_{elec} can in general contain other contributions, only spin multiplicity is currently implemented in `overreact`.

From the partition functions above, we can extract enthalpic and entropic contributions to the Gibbs' free energy, according to the well-known relations. In practice,

vectors U , H and S , of length m , are constructed to store contributions for each species,

$$\begin{aligned} H_i &= U_i + pV \\ G_i &= H_i - TS_i \end{aligned} \quad (1.3)$$

The exact contributions are given below,

$$U_{\text{trans}} = \frac{3}{2}RT \quad U_{\text{rot}} = \begin{cases} RT & \text{if linear} \\ \frac{3}{2}RT & \text{otherwise} \end{cases} \quad (1.4a)$$

$$U_{\text{vib}} = R \sum_{i=1}^{n_\nu} \Theta_i^{\text{vib}} \left(\frac{1}{2} + \frac{1}{\exp\left(\frac{\Theta_i^{\text{vib}}}{T}\right) - 1} \right) \quad U_{\text{elec}} = \epsilon_{\text{elec}} \quad (1.4b)$$

$$S_{\text{trans}} = R \left(\frac{5}{2} + \ln q_{\text{trans}} \right) \quad S_{\text{elec}} = R \ln q_{\text{elec}} \quad (1.4c)$$

$$S_{\text{rot}} = \begin{cases} R(1 + \ln q_{\text{rot}}) & \text{if linear} \\ R\left(\frac{3}{2} + \ln q_{\text{rot}}\right) & \text{otherwise} \end{cases} \quad (1.4d)$$

$$S_{\text{vib}} = R \sum_{i=1}^{n_\nu} \left[\frac{\Theta_i^{\text{vib}}}{T} \frac{1}{\exp\left(\frac{\Theta_i^{\text{vib}}}{T}\right) - 1} - \ln \left(1 - \exp\left(-\frac{\Theta_i^{\text{vib}}}{T}\right) \right) \right] \quad (1.4e)$$

where ϵ_{elec} stands for the final electronic energy as obtained from the output files, which eventually includes all contributions such as dispersion and continuum solvation free energy corrections.

The big advantage of performing such calculations oneself is the complete control over variations of them. Such further refinements, details and other treatments are detailed in the following.

1.2.1.1 Low-lying imaginary vibrational frequencies

It is not unusual to observe one or two imaginary vibrational frequencies of small magnitude in vibrational analyses, as they are especially susceptible to numerical noise [100]. This is particularly common in calculations for host-guest complexes, weakly interacting molecules, and other structures with flat PESs. They can often be removed by tightening grid sizes and convergence criteria for geometry and electronic energy minimisation procedures. In case of failure, it is advisable to consider the absolute value of such vibrational frequencies and use the corresponding thermodynamical contributions, since excluding low-lying vibrational frequencies effectively discards whole degrees of freedom and can result in errors as large as $2 \text{ kcal}\cdot\text{mol}^{-1}$ at room temperature [100]. In order to avoid this pitfall, it is thus advisable to make use of their absolute value, which is oftentimes small,

and proceed normally. As such, the automatic software described in Chapter 5 highlights imaginary vibrational frequencies of small magnitude ($< 50 \text{ cm}^{-1}$) in its output, warning the user in the process that their absolute values are being taken.

1.2.1.2 Corrections to low-frequency vibrational modes

Vibrational frequencies below 150 cm^{-1} strongly contribute to entropy and must be carefully treated, as they are known to be inaccurately treated under the RRHO approximation, and shifts of a few wave numbers further impact the performance of the model [98, 100–102]. This is due to the breakdown of separability between vibrational and rotational degrees of freedom at such small frequencies, an assumption of the RRHO model. In order to mitigate this effect, `overreact` employs the *quasi*-RRHO (QRRHO) model of Grimme [101], which effectively considers low-frequency vibrational modes as *quasi*-rotations when calculating entropies. In this treatment, contributions of low-lying modes to the entropy are replaced by an interpolation between the original vibrational contributions and a corresponding rotational entropy with the moment of inertia computed for a free-rotor with reduced frequency. The interpolation is calculated using the Head-Gordon damping function [103],

$$S_{\text{rot-vib}, i} = w(\nu_i) S_{\text{vib}, i} + (1 - w(\nu_i)) S_{\text{rot}, i} \quad w(\nu_i) = \frac{1}{1 + \left(\frac{103.6 \text{ cm}^{-1}}{\nu_i}\right)^4} \quad (1.5)$$

$$\mu'_i = \frac{\mu_i B_{\text{av}}}{\mu_i + B_{\text{av}}}, \quad \mu_i = \frac{h}{4\pi\nu_i}, \quad B_{\text{av}} = 10^{-44} \text{ kg m}^2$$

A similar QRRHO treatment is also available for enthalpies [104], where the same interpolation is employed to calculate the equivalent contribution. For the development of `overreact` (Chapter 5), both treatments for entropies and enthalpies were tested against published results (see Figure 1). Both QRRHO approximations for enthalpy and entropy are used by default by `overreact`, but can be deactivated by the user [105].

1.2.2 Molecular symmetries

Molecular point-group symmetries are required for the calculations mentioned above. However, automatically determining point groups for molecules of arbitrary size is error prone due to small perturbations of the molecular coordinates affecting angles more intensely the farther an atom is from the molecular center of mass. As such, standard quantum chemistry packages often require the user to manually indicate point-group symmetries. Our software `overreact` (Chapter 5) does automatic point group detection by using a especially designed, robust algorithm based on clustering of equivalent atoms and rigid rotor classification inspired by Beruski; Vidal [106], which is less sensitive to perturbation of molecular coordinates.

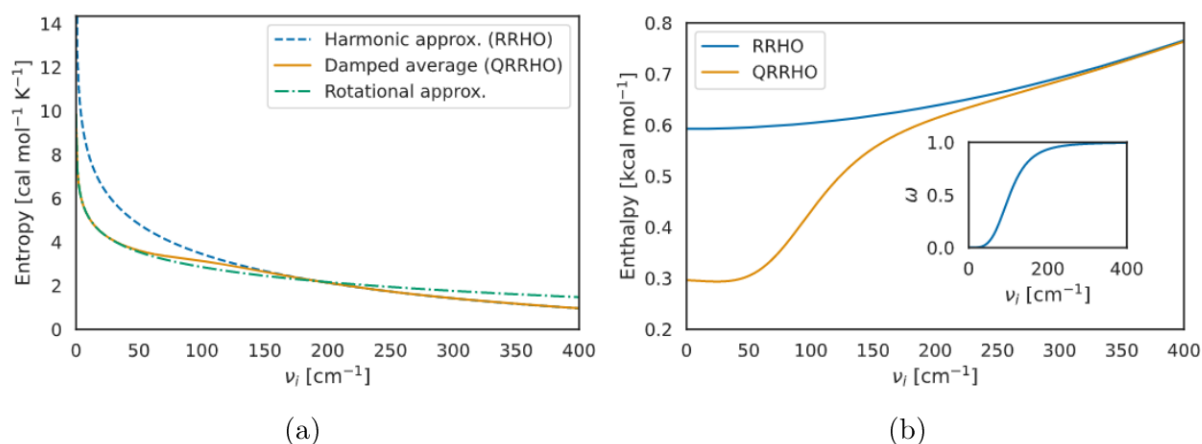


Figure 1 – Computed (a) entropy and (b) enthalpy vibrational contributions at 298.15 K for a single mode under both RRHO and QRRHO [101, 104] models as a function of frequency, as calculated by `overreact`. The cutoff frequency for the QRRHO model was chosen as 103.6 cm^{-1} and $B_{\text{av}} = 10^{-44} \text{ kg m}^2$. Compare to Figures 2 and 7 of Grimme [101] and Li et al. [104], respectively.

In practice, a vector σ of length m is constructed consisting of the symmetry numbers [107, 108] for all compounds, and this vector is used to update all entropies separately,

$$S_i^{\text{sym}} = S_i - R \ln(\sigma_i) \quad (1.6)$$

In any case, extra symmetries other than the detected ones can be informed in the input by the user. The user guide describes the detailed `overreact` input specification [105]. This can be useful for, e.g., undetected symmetries of weakly bound complexes [108] and uncommon reaction path degeneracies [107].

1.2.3 Standard state corrections

Quantum thermochemical quantities are usually reported in standard states, which means 1 M for the solution phase, while first-principle calculation results are reported by standard quantum chemistry packages for the gas phase, whose standard state reference is the ideal gas concentration at 1 atm and thus requires a standard state correction. The software described in Chapter 5 automatically detects (by reading the model input file [105]) the required standard state correction to absolute Gibbs' energies,

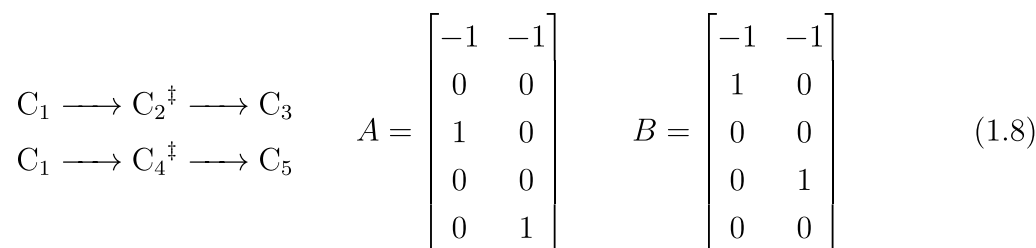
$$S^{1 \text{ M}} = S^{1 \text{ atm}} - R \ln\left(\frac{c_f}{c_i}\right) \quad (1.7)$$

where $c_f = 1 \text{ M}$ and c_i is the concentration of an ideal gas at the given temperature and pressure, and applies it.

1.3 General representation of chemical kinetic equations

Hypothetical reaction mechanisms consist of the interpretation of the available data for chemical reactions in terms of a model that is self-consistent. After being proposed, reaction mechanisms normally do not stay still: they must be compared with each other and with available experimental data. Furthermore, many different hypotheses for the same reaction can exist, and, after pruning the ones in disagreement with the available data, it is still possible to have several different plausible models at hand. In sum, such proposed mechanisms pass through a series of transformations, amendments, and refining. Although simple for small chemical reaction networks, this can be overwhelming for complex ones, with dozens of species and reactions, like some presented in Chapters 3 to 5. As such, it is especially useful to build a mathematical framework with which chemical reaction networks of arbitrary size can be defined and manipulated. This is not yet common practice in the field, though, as can be seen, e.g., in the work of Pérez-Soto; Besora; Maseras whose work represents one of the first complex chemical reaction networks in the literature modelled using first-principles computational chemistry data [109], but employs an *ad hoc* representation, with over 20 equations hard-coded in a Python script. As such, we present in this section a general framework that can be employed in an automatic fashion.

The problem of generally representing arbitrary chemical kinetic equations can be reduced to the definition of two matrices. A general reaction scheme can be represented as a pair of integer-valued $m \times n$ -matrices A and B , where n is the number of reactions and m the number of species, including transition states. Entries in both matrices represent signed stoichiometric coefficients, i.e., negative (positive) values denote species being consumed (produced) in a given reaction. Both matrices A and B store stoichiometric coefficients for reactants, but only A stores information about products, while only B stores information about transition states. For example, the following system of chemical equations, with two reactions and five species, translate into the following matrices:



In this scheme, each matrix column represents a single reaction, while compounds are indicated by row indices. As such, matrices are of size 5×2 . For instance, $A_{11} = A_{12} = -1$, since C_1 is a reactant in both reactions. The same goes for matrix B , since the information regarding reactants is repeated in both matrices. On the other hand, A stores information about products. For instance, $A_{31} = 1$ and $A_{52} = 1$, since C_3 and C_5 are products of the first and second reactions, respectively. In the same vein, B stores information about

transition states, such that $B_{21} = 1$ and $B_{42} = 1$, since C_2^\ddagger and C_4^\ddagger are transition states of reactions one and two, respectively. Observe that rows two and four in A are full of zeros, while rows three and five in B are full of zeros, as expected.

Essentially, this is equivalent of representing a special purpose directed graph, which is an idea that has proven useful in catalysis before [110–112]. Matrices A and B store all the information required for analyzing chemical reaction networks, as far as stoichiometric information is concerned. For instance, as we shall see later, both matrices A and B can be used to generate reaction and activation Gibbs' energies. Our software `overreact` produces those matrices during input parsing in a straightforward and automated way.

1.3.1 Representing equilibria

In this scheme, it is possible to represent both common reactions, whose transition states are explicitly taken into account, and equilibria, represented by pairs of reactions indicating interconvertible reactants and products with no explicit indication of transition states. Having a representation that supports both scenarios is important, as many chemical reaction mechanism proposals encompass rapid equilibria and key reactions of interest, such as the archetypal Michaelis-Menten model [113–116], where it is assumed that equilibria are much faster than the other chemical reactions. This allows phenomena in chemical kinetics such as pH dependencies and equilibrium between conformations to be accounted for in a simple and elegant manner.

In terms of matrix representation, each forward and backward equilibrium half-reaction gives rise to two columns in matrix A and two columns in matrix B . Notwithstanding, while the respective columns in matrix A have the expected form, matrix B holds the same columns as A , except for the backward reaction, which is filled with zeroes. As we shall see later, this allows us to use the same machinery for calculating reaction rate constants described below, since backward rate constants will be unity, while the forward constant will be numerically the same as the equilibrium constant (see Section 1.4 below). In order to guarantee that equilibria are faster than the other reactions in the system, one can multiply all equilibrium half-reaction rate constants by a reasonable constant afterwards, without disturbing the equilibrium relations.

1.3.2 Reaction and activation Gibbs' free energies

Reaction and activation Gibbs' energies can be easily generated from matrices A and B using the G vector of absolute Gibbs' energies introduced in Section 1.2 as

$$\begin{aligned}\Delta G &= A^T G \\ \Delta G^\ddagger &= B^T G\end{aligned}\tag{1.9}$$

where ΔG and ΔG^\ddagger are vectors of length n of reaction and activation Gibbs' energies, respectively, and X^T denotes the transposition of the matrix X . Observe that for an equilibrium forward half-reaction, this produces an “effective” activation Gibbs' free energy that is numerically identical to the reaction Gibbs' free energy, while the effective activation Gibbs' free energy for the associated backward reaction will be numerically equal to zero.

1.3.2.1 Reaction symmetry

In some cases, it is necessary to account for extra entropy contributions due to participating species being indistinguishable in a reaction. This occurs whenever it is possible to interchangeably translate molecules of identical configurations [107, 108]. This is particularly important, for instance, when two identical molecules react with each other [107, 108], or when modelling explicit solvation with more than one solvent molecule (e.g. when modelling the formation of a water cluster, one side of the reaction would contain n indistinguishable, infinitely separated water molecules) [100]. In such cases, an extra term $-R \ln(n!)$ should be added to the total entropy of reactants for reactions such as $n A \longrightarrow$ products. As it is arguably non-intuitive and often neglected, `overreact` (Chapter 5) detects such cases and applies the correction automatically.

1.4 Calculation of reaction rate constants

Once the vector ΔG^\ddagger of activation Gibbs' free energies is constructed (Section 1.3.2), it can be used to calculate a n -vector k of reaction rate constants, using the Eyring-Evans-Polanyi equation [117–119], the key equation of transition state theory [119],

$$k_i = \kappa_i \frac{k_B T}{h} \exp\left(-\frac{\Delta G_i^\ddagger}{RT}\right) \quad (1.10)$$

where κ_i is the quantum tunnelling transmission coefficient of the i -th reaction (see below in Section 1.4.3), k_B is Boltzmann's constant, h is Planck's constant, T is the chosen temperature and R is the ideal gas constant. The transition state theory is based on the idea that the reactant ground state complex is in equilibrium with the transition state structure [119].

Equilibrium half-reactions can be assigned forward and reverse rate constants such that equilibria are ensured,

$$K_{\text{eq}} = \frac{k_i^{\text{forward}}}{k_{i+1}^{\text{reverse}}} = \exp\left(-\frac{\Delta G_i}{RT}\right) \quad (1.11)$$

The slowest equilibrium half-reaction is initially assigned unitary rate constant (as commented above in Section 1.3.1). Later, when all reaction rate constants have been calculated, all equilibrium half-reaction rates can be multiplied by a positive factor greater than

one, such that the slowest equilibrium is safely faster than the fastest non-equilibrium reaction in the model. This is important for properly modelling chemical reaction mechanisms as intended by the proposer (Section 1.5).

1.4.1 Error propagation with respect to energies

The prediction of chemical reactions is an unforgiving problem. Since reaction rate constants depend exponentially on the activation Gibbs' free energies, small deviations on the latter exponentially increase errors on the former. As such, given an activation energy estimate ΔG^\ddagger on the true value $\Delta \widehat{G}^\ddagger$ with error ϵ ,

$$k = \kappa \frac{k_B T}{h} e^{-\frac{\Delta G^\ddagger}{RT}} = \kappa \frac{k_B T}{h} e^{-\frac{(\Delta \widehat{G}^\ddagger + \epsilon)}{RT}} = \widehat{k} e^{-\frac{\epsilon}{RT}} \quad (1.12)$$

where k and \widehat{k} are the predicted and true chemical reaction constants, respectively. Thus, at room temperature, errors in the order of 10–100× in reaction rate constants are produced by energy deviations of 1.36–2.73 kcal·mol⁻¹, with larger errors in reaction rate constants found in lower temperatures. This is particularly important, as popular DFT methods commonly achieve accuracies of 2–3 kcal·mol⁻¹ for many molecules [120, 121] (more in Section 1.1.1 above). In fact, an error as small as 0.41 kcal·mol⁻¹ gives rise to a twofold deviation in the reaction rate constant. This goes to show that the so called “quantum chemical accuracy” of <1 kcal·mol⁻¹ [121] is not enough for the prediction of chemical reactions on par with experimental results. This not only increases the demand for more precise quantum chemical methods, but also for methods aiming at mitigating the effects of such errors in computational predictions of chemical reactions.

Going one step further, errors in reaction rate constants have different relationships to individual errors in activation enthalpies and entropies,

$$k = \kappa \frac{k_B T}{h} e^{-\frac{\Delta H^\ddagger}{RT}} e^{\frac{\Delta S^\ddagger}{R}} = \kappa \frac{k_B T}{h} e^{-\frac{(\Delta \widehat{H}^\ddagger + \chi)}{RT}} e^{\frac{(\Delta \widehat{S}^\ddagger + \sigma)}{R}} = \widehat{k} e^{-\frac{\chi}{RT}} e^{\frac{\sigma}{R}} \quad (1.13)$$

The above suggests that, all things equal, errors in the predicted activation entropy (enthalpy) dominate at high (low) temperatures. The balance between the two will on the other hand depend on the actual reaction at hand. These relationships are crucial for actually controlling and mitigating errors when making computational quantitative predictions for chemical reaction networks.

1.4.2 Adjustment of systematic errors with respect to energies

First-principles microkinetic modelling is powerful and can produce qualitatively correct results. This is in part due to the nature of DFT errors, which tend to be systematic [109]. As such, good levels of theory often guarantee quantitative results for unimolecular reactions, where error cancellation is expected, but errors can deeply affect

predictions for bimolecular reactions [109]. In such cases, further adjustments can be necessary for calculations of microkinetic models to be comparable to experimental results. By shifting absolute Gibbs' free energies by a fixed amount, it is possible to mitigate systematic energy errors, which was shown to be adequate in many cases [109, 122]. In particular, in Chapter 5 we present a reproduction [3] of the numerical results of Pérez-Soto; Besora; Maseras [109] using `overreact`, which encompasses a well-studied and validated imine formation reaction, taking into account a systematic error of 3.2 kcal·mol⁻¹. Using this technique, results on par with the available experimental data are obtained.

1.4.3 Approximations for quantum tunnelling transmission coefficients

Quantum tunnelling effects are often important, in particular for reactions where hydrogen abstractions take place [123], such as the homolysis of C–H bonds by strong oxidants, in which case it is often the rate-limiting step. Notwithstanding, it is hardly known *a priori* whether an elementary step will present quantum tunnelling effects, so it is reasonable to apply approximate quantum tunnelling corrections to all steps in a chemical reaction network to account for this possibility.

Two particularly simple approximations that can be readily applied to any standard computational chemical reaction investigation are the Wigner [124] and Eckart [125] quantum tunnelling corrections. The Wigner correction is the simplest of the two and assumes that most of the tunnelling happens at the top of the reaction barrier,

$$\kappa_i^{\text{Wigner}} = 1 + \frac{1}{24} \left(\frac{h|\nu^\ddagger|}{k_B T} \right)^2 \quad (1.14)$$

where ν^\ddagger , the imaginary vibrational frequency at the transition state, is the only information required.

The unsymmetrical Eckart correction uses information about the shape of the barrier as well

$$\begin{aligned} \kappa_i^{\text{Eckart}} &= \int_{\epsilon_0}^{\infty} P(\epsilon) \exp(-\epsilon) d\epsilon, & \epsilon &= \frac{E - \Delta H_f^{\ddagger,0K}}{k_B T} \\ P(\epsilon) &= 1 - \frac{\cosh(2\pi(a_1 - a_2)) + \cosh(2\pi|d|)}{\cosh(2\pi(a_1 + a_2)) + \cosh(2\pi|d|)} \\ \epsilon_0 &= \begin{cases} -v_1 & \text{if } \Delta H_f^{\ddagger,0K} \leq \Delta H_r^{\ddagger,0K} \\ -v_2 & \text{otherwise} \end{cases}, & v_i &= \frac{\Delta H_i^{\ddagger,0K}}{k_B T} \\ a_i &= \frac{\left[2 \frac{\epsilon + v_i}{\pi u^*} \right]^{-\frac{1}{2}}}{\alpha_1^{-\frac{1}{2}} + \alpha_2^{-\frac{1}{2}}}, & \alpha_i &= 2\pi \frac{\Delta H_i^{\ddagger,0K}}{h\nu^\ddagger}, & u^* &= \frac{h\nu^\ddagger}{k_B T} \\ d &= \frac{1}{2\pi} \sqrt{4\alpha_1\alpha_2 - \pi^2} \end{aligned} \quad (1.15)$$

where $\Delta H_f^{\ddagger,0K}$ and $\Delta H_r^{\ddagger,0K}$ are the activation enthalpies at 0 K for the forward and reverse reactions, respectively. For the integration required by the Eckart approximation, a simple quadrature scheme can be employed.

We implemented both approximations for κ_i in our software `overreact`, with the Eckart approximation being the default for all reactions when estimating Equation (1.10), but the user can choose Wigner or disable quantum tunnelling corrections completely (in which case $\kappa_i = 1$) from the command-line (see a detailed description of the command-line interface in the official guide [126]).

1.5 First-principles microkinetic modelling

Microkinetic modelling is a technique used to predict the outcome of complex chemical reactions. It can be used to investigate the catalytic transformations of molecules by propagating a system of ordinary differential equations that model the chemical reaction network.

The technique can be made first-principle by making use of pure computational chemistry predictions. It is able to take into account effects that the sole use of Gibbs' free energies are not able to, such as concentrations of species and relatively complex time dynamics. In order to perform microkinetic modelling, a system of ordinary differential equations must be first derived, for which a general representation of chemical reaction networks is most helpful (Section 1.3), and then solved over time from starting concentrations.

1.5.1 Representation and solution of the chemical kinetic ordinary differential equations

This section briefly introduces the representation and solution of the system of differential equations, which consists of time-propagating the m -vector $y(t)$ of species concentrations (in mol/L) as follows. First, a n -vector of reaction rates $r(y)$, which in general depends on y , can be defined, component-wise, as

$$r_j = k_j \prod_i^{\text{reactants}} y_i^{-A_{ij}} \quad (1.16)$$

where the negative sign in A_{ij} is due to the reactant stoichiometric coefficients being stored as negative integers (Section 1.3). With this definition, the time derivative of the concentration vector, \dot{y} , is given as

$$\dot{y} = Ar(y) \quad (1.17)$$

where matrix multiplication is implied.

Equation (1.17) describes the entire reaction network dynamics as a set of ordinary differential equations (ODEs) expressing the rate of change of concentration of each species in the given model as a function of the instantaneous concentration of all chemical species. The ODE system above can be solved using any standard methodology widely available in the literature. Notwithstanding, for a numerically robust procedure, one needs to observe certain aspects of this system. First, the system above is only linear if all reactions in the model are unimolecular. Second, it is not unusual to encounter chemical kinetic problems consisting of phenomena with different time scales, which is especially relevant for models containing equilibria. By definition, such problems are oftentimes stiff and the use of solvers purposely built for stiff systems is warranted [127–129]. The implicit Runge-Kutta method of Radau IIA family (of order five) [130] is used by default in `overreact`, but any solver supported by the `SciPy` library [131] can be employed. Furthermore, `overreact` leverages Google’s `JAX` library [132] in order to obtain an analytic Jacobian of the system in Equation (1.17) *via* automatic differentiation, which further increases the robustness and efficiency of the scheme, as no numerical differentiation is required throughout the microkinetic simulation.

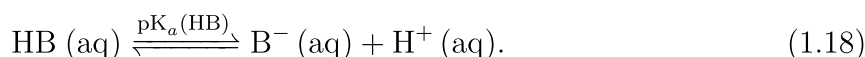
1.5.1.1 Concentration constraints

Within the well-mixed condition approximation, concentration effects are included in microkinetic simulations. However, in many situations, constant concentration effects are important, such as when reactants are used neat or when there is active solvent participation [102]. Our software `overreact` allows fixing the concentration of arbitrary compounds, allowing for simulations of neat reactions, pseudo-first order conditions, pH buffering effects (see below), controlled ionic strengths, and more (Chapter 5).

1.5.1.1.1 Application: acid-base equilibria

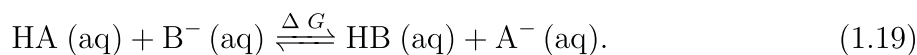
One practical application of constrained concentrations is simulating reactions at buffered pH values, which requires properly estimating acid-base equilibrium constants or, equivalently, their log-scaled counterpart, the pK_a values. This section presents a short account of the method employed in Chapter 5 for mitigating errors in such estimates.

When computationally estimating pK_a values, a direct dissociation approach (Equation (1.18)) is often used. However, this approach leads to issues in the evaluation of the solvated proton. First, conventional electronic calculations are not possible for a zero-electron systems such as a proton [133, 134], and second, due to the covalent nature of the interaction between the H^+ ion and the surrounding aqueous environment, clusters such as H_3O^+ , H_5O_2^+ , etc. are formed [134], which further complicates the problem.



A tentative solution is to employ the experimental proton solvation free energy ($-1104.5 \pm 0.3 \text{ kJ}\cdot\text{mol}^{-1}$ [67, 135]) in a semi-empirical fashion, but the trustworthiness of this method is debatable [136]. In fact, this often produces pK_a values that are far from the expected for simple carboxylic acids, for instance. Errors in the order of 7 pK_a units are not uncommon, and can be found in the literature [133, 137]. It has been pointed out that a major source of error can be attributed to the lack of explicit solute-solvent interactions [137].

An improved approach is to use a relative determination method [133]. This avoids the problems associated with the direct dissociation approach of Equation (1.18) by calculating the auxiliary problem of a proton exchange with a known reference acid, such as acetic acid [138]:



Contrary to Equation (1.18), both sides of Equation (1.19) have the same net charge and likely similar interactions with the solvent, leading to favorable error cancellation in the calculated Gibbs' free energy (ΔG). The $\text{pK}_a(\text{HA})$ in this scheme can thus be written as a function of $\text{pK}_a(\text{HB, exp.})$:

$$\text{pK}_a(\text{HA}) = \text{pK}_a(\text{HB, exp.}) + \frac{\Delta G}{\ln(10)RT}. \quad (1.20)$$

Such semi-empirical estimates often lead to errors of less than 1 pK_a unit for many solutes and solvents [133].

Part II

Publications

2 Scientific contributions

This chapter lists all articles and software co-authored by the author during the course of his PhD (March 2017–December 2022) at the Federal University of Santa Catarina that are relevant to the field of computational elucidation of reaction mechanisms. There are two groups of contributions: minor and major. Minor contributions describe works investigating mechanisms where the impact or main conclusions do not substantially draw from such elucidations. In the author’s view, major contributions are the ones that either contribute substantially to the field, investigate rather complex mechanisms, or the impact of the study would not have been possible without considerable computational mechanistic analysis. Other unrelated works and software can be found in Appendix A.

2.1 Minor contributions

The following articles were co-authored by the author during his PhD and are relevant to the field of computational elucidation of reaction mechanisms, but are considered minor contributions according to the above criteria. As such, they will not be further discussed in this thesis:

- GROSS, I. P. et al. Polylactic acid, maleic anhydride and dicumyl peroxide: NMR study of the free-radical melt reaction product. **Polymer Degradation and Stability**, Elsevier BV, v. 155, p. 1–8, Sept. 2018. ISSN 0141-3910. DOI: [10.1016/j.polymdegradstab.2018.06.016](https://doi.org/10.1016/j.polymdegradstab.2018.06.016). Available from: <http://dx.doi.org/10.1016/j.polymdegradstab.2018.06.016>),
- SCHNEIDER, F. S. et al. A theoretical investigation on the aminolysis of pyromellitic and 1,4,5,8-naphthalenetetracarboxylic dianhydrides. **Computational and Theoretical Chemistry**, Elsevier BV, v. 1147, p. 13–19, Jan. 2019. ISSN 2210-271x. DOI: [10.1016/j.comptc.2018.11.008](https://doi.org/10.1016/j.comptc.2018.11.008). Available from: <http://dx.doi.org/10.1016/j.comptc.2018.11.008>), and
- ALMERINDO, G. I. et al. Kinetics and adsorption calculations: insights into the MgO-catalyzed detoxification of simulants of organophosphorus biocides. **Journal of Materials Chemistry A**, Royal Society of Chemistry (RSC), v. 8, n. 36, p. 19011–19021, 2020. ISSN 2050-7496. DOI: [10.1039/c9ta14028j](https://doi.org/10.1039/c9ta14028j). Available from: <http://dx.doi.org/10.1039/C9TA14028J>).

2.2 Major contributions

The next three chapters describe all articles and software that the author has co-authored during his PhD that are considered major contributions towards the field of computational elucidation of reaction mechanisms, given the definition above. Such works are either directly relevant to the elucidation of rather complex reaction mechanisms, or the scientific impact would likely not have been possible without a computational mechanistic investigation:

- COELHO, S. E. et al. Mechanism of Palladium(II)-Mediated Uncaging Reactions of Propargylic Substrates. **ACS Catalysis**, American Chemical Society (ACS), v. 9, n. 5, p. 3792–3799, Mar. 2019. ISSN 2155-5435. DOI: [10.1021/acscatal.9b00210](https://doi.org/10.1021/acscatal.9b00210). Available from: <http://dx.doi.org/10.1021/acscatal.9b00210> (Chapter 3),
- OLIVEIRA, B. L. et al. Platinum-Triggered Bond-Cleavage of Pentynoyl Amide and N-Propargyl Handles for Drug-Activation. **Journal of the American Chemical Society**, American Chemical Society (ACS), v. 142, n. 24, p. 10869–10880, May 2020. ISSN 1520-5126. DOI: [10.1021/jacs.0c01622](https://doi.org/10.1021/jacs.0c01622). Available from: <http://dx.doi.org/10.1021/jacs.0c01622> (Chapter 4), and
- SCHNEIDER, F. S. S.; CARAMORI, G. F. Overreact, an *in silico* lab: Automatic quantum chemical microkinetic simulations for complex chemical reactions. **Journal of Computational Chemistry**, Wiley, Apr. 2022. ISSN 1096-987x. DOI: [10.1002/jcc.26861](https://doi.org/10.1002/jcc.26861). Available from: <http://dx.doi.org/10.1002/jcc.26861> (Chapter 5).

The following software, associated by the last above publication, was developed during the author's PhD as well:

- SCHNEIDER, F. S. S. **geem-lab/overreact: overreact v1.0.2**. [S.l.]: Zenodo, Nov. 2021. <https://doi.org/10.5281/ZENODO.5730603>. Accessed: 2022-07-29. DOI: [10.5281/zenodo.5730603](https://doi.org/10.5281/zenodo.5730603). Available from: <https://zenodo.org/record/5730603> (Chapter 5).

3 Paper I: Mechanism of Pd(II)-mediated uncaging reactions of propargylic substrates

COELHO, S. E. et al. Mechanism of Palladium(II)-Mediated Uncaging Reactions of Propargylic Substrates. *ACS Catalysis*, American Chemical Society (ACS), v. 9, n. 5, p. 3792–3799, Mar. 2019. ISSN 2155-5435. DOI: [10.1021/acscatal.9b00210](https://doi.org/10.1021/acscatal.9b00210). Available from: <http://dx.doi.org/10.1021/acscatal.9b00210>

This work contributes to the development of better Pd(II)-based C–O bond cleavage promoters in the context of bioorthogonal catalysis. These bioorthogonal approaches, involving transition metals and biocompatible conditions, have been recently added to the arsenal of tools for chemical biology and medicinal chemistry for the purpose of activating proteins and prodrugs outside or inside living cells.

Following the literature, the most common mechanism for this process is the formation of a Pd(0) catalyst, which then undergoes an oxidative addition with the propargyl group to form an allenylpalladium intermediate. This intermediate can then be hydrolyzed to produce acetol as a side product and to regenerate the Pd(0). A less common mechanism is through a Pd(II)-mediated hydration, which can form an intermediate that can decompose to form Pd(II) by hydrolysis.

This study consisted of an experimental-computational hybrid investigation on the uncaging of propargyl-protected hydroxyl groups (from the prodrug compound DNPPE in particular) using Pd(II) salts in a phosphate-buffered aqueous medium. The reactions were monitored by UV-vis spectroscopy and discovered to have a biexponential regime, consistent with biphasic kinetics. Two distinct rate constants, k_1 and k_2 , were determined — k_1 , with a half-life of 1 hour, being $15\times$ faster than k_2 . k_1 was responsible for two turnovers (at around 20 mol% of the catalyst), with k_2 showing a sharp increase after two turnovers.

According to what was expected from the literature, the reaction mechanism was thus hypothesized to consist of either an intramolecular ligand exchange reduction or nucleophilic attack by solvent, either followed by reductive elimination to form Pd(0) or completing the reaction to form hydrolysed carbopalladate intermediates. Experiments ruled out that the reaction proceeded through Pd(0) and showed that the catalyst was likely inhibited by the product.

We thus turned to computational calculations, making use of data from mass spec-

trosopies (ESI-HRMS with CID-MS/MS were used) to support the hypothesis that the reaction proceeds through biphasic kinetics with different rates and involves a Pd(II)-mediated anti-Markovnikov hydration of the propargyl group, followed by C–O bond breaking by β -O elimination. Markovnikov keto intermediates were found to be significantly less favourable than those of the anti-Markovnikov route. In total, 21 rest states and 23 elementary reactions and equilibria were modelled. A summarized diagram of the proposed reaction mechanism can be seen in Figure 2.

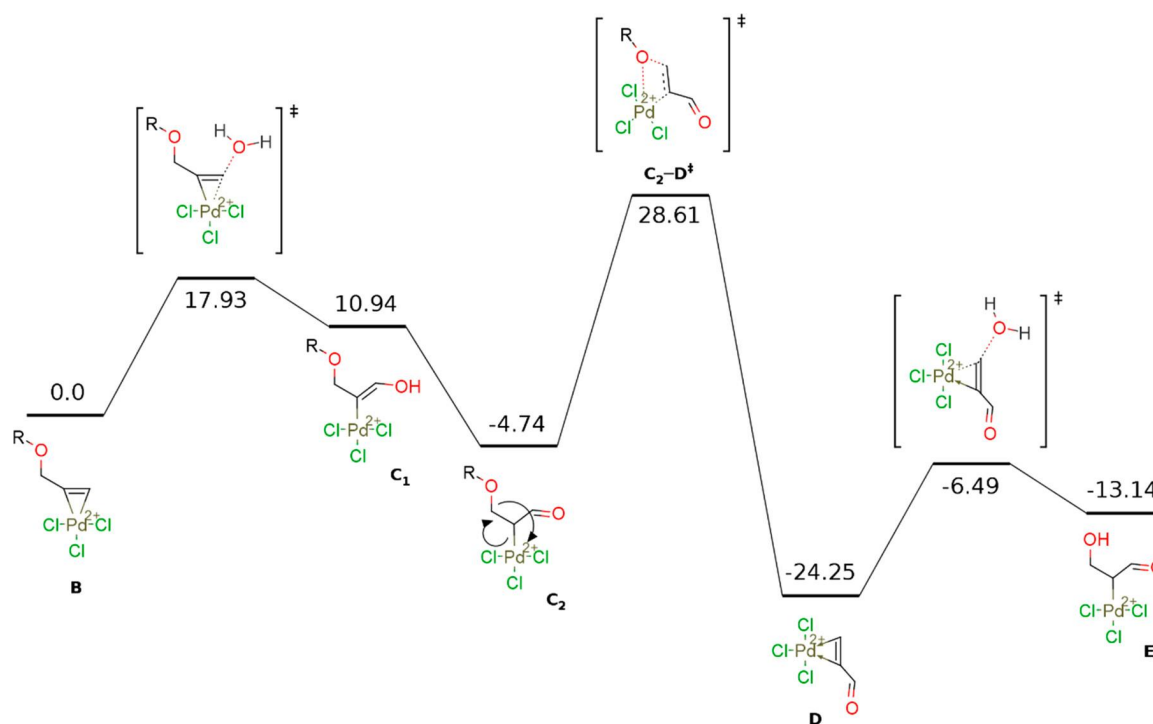


Figure 2 – Summarized diagram of the proposed reaction mechanism in Coelho et al. Energies are in $\text{kcal}\cdot\text{mol}^{-1}$. Reprinted with permission from COELHO, S. E. et al. Mechanism of Palladium(II)-Mediated Uncaging Reactions of Propargylic Substrates. **ACS Catalysis**, American Chemical Society (ACS), v. 9, n. 5, p. 3792–3799, Mar. 2019. ISSN 2155-5435. DOI: [10.1021/acscatal.9b00210](https://doi.org/10.1021/acscatal.9b00210). Available from: <http://dx.doi.org/10.1021/acscatal.9b00210>. Copyright 2019 American Chemical Society.

In conclusion, the study demonstrates that simple Pd(II) salts acted as a catalyst for O-depropargylation with two phases — one fast, but lasting only two turnovers due to product inhibition, and one slow. The mechanism for the faster phase involves Pd(II) insertion with an anti-Markovnikov hydration of the propargyl moiety before the C–O bond is cleaved through β -O elimination. Although a lot of catalyst is needed for the reaction process to be completed due to product inhibition, such shortcomings can be rationally overcome in the future through the design of bulky ligand systems to prevent strong binding of the product.

3.1 Full text

This work was a collaboration between researchers at the Department of Chemistry at the Federal University of Santa Catarina (UFSC), the Brazilian Synchrotron Light Laboratory (LNLS), and the Thomson Mass Spectroscopy Laboratory at the State University of Campinas.

The work was jointly funded by the Brazilian Council for Technological Development (CNPq), grant/award number 140485/2017–1, the Brazilian Synchrotron Light Laboratory (LNLS), grant/award number 20160243/20170351.

The paper was dedicated to the memory of Professor Faruk José Nome Aguilera (1947–2018).

The publication can be read in full next.

Reprinted with permission from COELHO, S. E. et al. Mechanism of Palladium(II)-Mediated Uncaging Reactions of Propargylic Substrates. **ACS Catalysis**, American Chemical Society (ACS), v. 9, n. 5, p. 3792–3799, Mar. 2019. ISSN 2155-5435. DOI: [10.1021/acscatal.9b00210](http://dx.doi.org/10.1021/acscatal.9b00210). Available from: <<http://dx.doi.org/10.1021/acscatal.9b00210>>. Copyright 2019 American Chemical Society.

Mechanism of Palladium(II)-Mediated Uncaging Reactions of Propargylic Substrates

Sara E. Coelho,[†] Felipe S. S. Schneider,[†] Daniela C. de Oliveira,[‡] Guilherme L. Tripodi,[§] Marcos N. Eberlin,[§] Giovanni F. Caramori,[†] Bernardo de Souza,[†] and Josiel B. Domingos^{*,†}

[†]Department of Chemistry, Federal University of Santa Catarina - UFSC, Campus Trindade, C.P. 476, Florianópolis, Santa Catarina 88040-900, Brazil

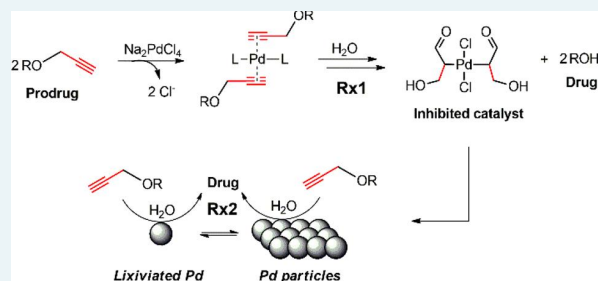
[‡]Brazilian Synchrotron Light Laboratory, LNLS, C.P. 6192, Campinas, São Paulo 13083-970, Brazil

[§]Thomson Mass Spectrometry Laboratory, University of Campinas-UNICAMP, Campinas, São Paulo 13083-872, Brazil

Supporting Information

ABSTRACT: The palladium(II)-mediated chemical uncaging reaction of propargylic substrates is a recent addition to the field of chemical biology and medicinal chemistry in the activation of bio and prodrug molecules. Most of the strategies used involve C–O bond breaking in molecules bearing protected amino and hydroxyl groups. Although this reaction has been known for many decades, its catalytic cycle in aqueous milieu remains unclear. Our mechanistic investigation results unveil that full propargylic substrate conversion occurs through biphasic kinetics of different rates, where the fastest reaction phase involves a Pd(II) anti-Markovnikov hydration of the propargyl moiety, followed by the C–O bond breaking through a β -O elimination and lasts only for two turnovers due to product inhibition. The second slower reaction phase involves the hydrolysis of the substrate promoted by Pd(0) species formed during the first phase of the reaction. These findings are crucial for the potential development of bioorthogonal Pd catalysts for the uncaging of propargylic protected bioactive and drugs molecules.

KEYWORDS: depropargylation reaction, palladium, mechanism, catalysis, hydrolysis



1. INTRODUCTION

The promotion of C–O bond cleavage by transition metals is one of the key strategies recently described for uncaging protected molecules possessing hydroxyl and amino functional groups under biocompatible conditions, extra- or intracellularly.^{1,2} In particular, palladium-mediated bond-cleavage reactions have gained great interest owing to their unique catalytic properties.^{3–8} Cell-surface engineering⁹ and protein^{10,11} and prodrug^{5,12–15} activation outside or inside living cells, through the C–O bond cleavage of propargylic ethers, carbamates, and carbonates (Figure 1a), are examples of the recent applications of palladium-mediated uncaging reactions, taking advantage of a bioorthogonal approach.^{16,17} Although it has been argued that carbamate groups are not truly bioorthogonal because they can be deprotected in vivo through the reaction with various nucleophiles and digestive enzymes, propargylic amines and ethers, while less reactive, are more suitable for in vivo applications.¹⁸ Deallylation reactions are also a common strategy, although they are less efficient with simple palladium catalysts than depropargylation.¹⁰ Whereas the mediation of deallylation by Pd(0) through a π -allylpalladium mechanism is well established,¹⁹ the Pd-mediated depropargylation reaction mechanism remains challenging in the current stage, and no systematic mechanistic

studies have been performed.¹⁶ However, it has been most frequently postulated that even when the initial forms of the catalyst are simple Pd(II) salts, the depropargylation reaction mechanism involves the in situ formation of the catalytic species Pd(0). This process is normally assumed to be promoted by a base through an intramolecular ligand exchange reduction or by an attack of a nucleophilic solvent, followed by a reductive elimination pathway.^{10–13,16,20–23} The Pd(0) is then assumed to undergo an oxidative addition with the propargyl group to form an allenylpalladium intermediate, which can be hydrolyzed to produce acetol as a side product and to regenerate the Pd(0) (pathway (i), Figure 1b). The less common hypothesis is a Pd(II)-mediated hydration mechanism (pathway (ii)) to form an intermediate that can decompose to form Pd(II) by hydrolysis (iii) in a Wacker-like oxidation.^{10,16,24}

However, these uncaging reactions are reported to be relatively slow and present low product yields, requiring high doses of catalyst. The catalyst solubility and toxicity therefore need to be considered when designing a bioorthogonal

Received: January 16, 2019

Revised: February 28, 2019

Published: March 21, 2019

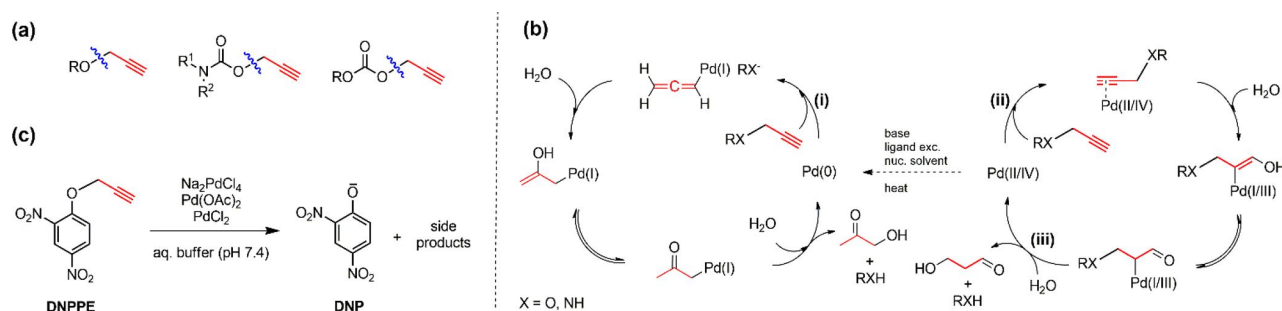


Figure 1. (a) Representative examples of C–O bond cleavage of propargyl protected hydroxyl and amino groups. (b) As suggested in the literature, the mechanism for the depropargylation reaction is mediated by Pd(0) (pathway i) and Pd(II/IV) (pathway ii). (c) Proposed model reaction for the mechanistic studies in this work: prodrug DNPPE uncaging reaction in a phosphate-buffered aqueous medium (pH 7.4) mediated by simple Pd(II) salts.

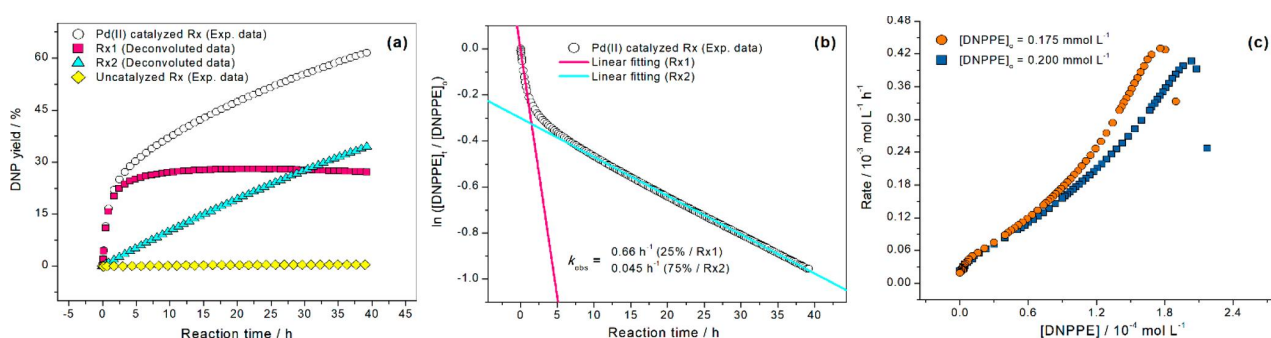


Figure 2. (a) Kinetics profiles of product conversion. (b) Natural log of the normalized experimental kinetic data for the DNPPE depropargylation reaction. (c) RPKA of on-cycle catalyst stability during the conversion of DNPPE (experiment 1: [DNPPE]₀ = 0.2 mmol L⁻¹, [Pd]₀ = 0.05 mmol L⁻¹ and experiment 2: [DNPPE]₀ = 0.175 mmol L⁻¹, [Pd]₀ = 0.05 mmol L⁻¹).

protocol.²⁵ Thus rational designs of highly elaborate transition-metal catalysts for uncaging reactions will rely on the understanding of fundamental organometallic mechanistic pathways, which can be achieved via both experiments and theoretical calculations to determine the coordination and reaction behavior of reactive intermediates.²⁶

In this article, we investigated the mechanism of the C–O bond-cleavage reaction of propargyl protected hydroxyl groups, triggered by the addition of simple Pd(II) salts (Na₂PdCl₄, Pd(OAc)₂, and PdCl₂), without the addition of base or ligands, in phosphate-buffered aqueous medium (pH 7.4). The prodrug compound 2,4-dinitrophenyl propargyl ether (DNPPE) was chosen as a model substrate for these studies (Figure 1c). DNPPE is a caged protonophore that becomes an active mitochondrial uncoupler (DNP)²⁷ after the removal of the propargyl protecting group. DNP is a widely studied pharmacological uncoupling agent used in experimental models of neurodegenerative conditions.^{28–30} Moreover, DNP is a tyrosine analogue, a catalytic residue present in many enzymes, and consequently a model compound for the bioconjugation of proteins.^{11,31} Also, the deprotection yield of DNPPE can be linked directly to UV–vis spectroscopy readouts, which offers a simple approach for an assessment of the reaction progress.

2. RESULTS AND DISCUSSION

In phosphate-buffered aqueous medium (pH 7.4), the reactions mediated by the Pd(II) salts were monitored by UV–vis spectroscopy through the appearance of the product DNP at a wavelength of 400 nm (Figure S1). For all Pd(II)

salts, a deviation from the first-order kinetics was observed (open circles, Figure 2a, for the reaction mediated by Na₂PdCl₄ and Figure S2 for the other salts). The distinct biexponential shape of the curve is not consistent with a simple reaction mechanism. Indeed, these profiles were typical of biphasic kinetics, producing the same product (DNP) at different rates (eq 1).^{32,33} The linear fit of eq 1 enabled the determination of two observed macroscopic rate constants (k_1 and k_2 , Figure 2b).

$$\frac{[\text{DNPPE}]_t}{[\text{DNPPE}]_0} = F^0 e^{-k_1 t} + S^0 e^{-k_2 t} \quad (1)$$

The yield magnitudes of the fast (k_1) and slow (k_2) phases are denoted by F^0 (25%) and S^0 (75%), respectively. On the basis of these macroscopic rate constants, the evolution of the DNP product was deconvoluted into two reaction kinetics profiles (Figure 2a, red squares and blue triangles for the fast and slow phases, respectively), namely, Rx1 and Rx2, respectively. It can be observed that Rx1 was ~15 times faster than Rx2 ($k = 0.66$ and 0.045 h^{-1} , respectively) and ~650 times faster than the uncatalyzed reaction ($k_{\text{unc}} = 1.02 \times 10^{-3} \text{ h}^{-1}$) under the same conditions. The half life for Rx1 is ~1 h, which makes this reaction feasible for bioorthogonal applications.³⁴

It is important to note that the fast phase (Rx1) is responsible for the conversion of ~20 mol % into the product DNP, that is, only two turnovers (Figure S3). Mechanistically, this information shows that although Rx1 is faster than Rx2, it shuts down after two turnovers. In fact, sequential addition of the catalyst after different reaction times leads to a sharp increase in the DNP production, which also lasts for around

two turnovers (Figure S4). We found this to be very important because for many of the Pd catalysts reported herein, the reaction was monitored during a short period, and the turnover, especially intracellularly, was not properly established.¹⁷

For a single-substrate catalytic cleavage reaction, a biphasic time course is consistent with a change in mechanism owed to a change in the activity of the catalyst. Thus an experiment by reaction progress kinetic analysis (RPKA) was performed to establish catalyst stability over the entire reaction course. RPKA can suggest a few initial sets of experiments to find any evidence of catalyst deactivation or product inhibition.³⁵ Therefore, two reactions initiated with different initial concentrations of DNPPE and the same catalyst concentration should display identical rate versus substrate concentration profiles in the absence of catalyst deactivation or product inhibition processes. Consequently, two reactions were performed: experiment 1 with $[\text{DNPPE}]_0 = 0.2 \text{ mmol L}^{-1}$ and experiment 2 with $[\text{DNPPE}]_0 = 0.175 \text{ mmol L}^{-1}$ (Figure 2c). Figure 2c shows an unmatched rate behavior through the graphical overlay, suggesting that $[\text{Pd}]$ is unequal for both experiments. These results indicate that the catalyst is not stable, which is further supported by later experiments revealing that the catalyst is changing to accommodate a switch in the mechanism. Moreover, further kinetic experiments adding DNP or acetol (the most frequently reported byproduct for this reaction) to the reaction medium show that neither affects the reaction profile (Figure S5). Thus a possible inhibition due to the presence of DNP or possibly acetol products is ruled out.

Other parameters can also influence the reaction rate; for instance, increasing the Pd concentration from 2 to 12 mol % of Pd(II) resulted in an increase in the reaction rate by factors of 10 for Rx1 and 45 for Rx2 (Figure S6). The nonlinear response of Rx1/Rx2 reaction rates with changes in Pd concentration suggests a different nuclearity in the catalyst for these two processes. The phosphate buffer concentration also altered the reaction rate for Rx1, with a decrease observed from 0.01 to 0.15 mol L⁻¹, but it had no effect in the case of Rx2 (Figure S7). The amount of cosolvent DMSO affected the reaction rate as well; an increase from 10 to 50% of DMSO almost completely inhibited both reactions (Figure S8). This is important because DMSO is by far the most common cosolvent used in these reactions for substrate solubilization in aqueous solution *in vitro* or *in vivo* experiments. Because of the known coordination capabilities of phosphate and DMSO toward transition metals, the concentrated buffer and cosolvent are probably inhibiting the reaction through complexation with the catalytic species. The stronger inhibition effect of the buffer in the case of Rx1 shows that the Pd species involved in this reaction is a more labile one.

As discussed before, the most general assumption in the literature is that this reaction mechanism occurs via oxidative addition of the propargyl C–O bond to Pd(0) (Figure 1b, pathway i). Thus to investigate the true nature of the catalytic species, we tested the hypothesis that the involvement of Pd(0) formed spontaneously from the reduction of Pd(II) in the reaction medium. First, we performed X-ray absorption spectroscopy (XAS) analysis of the reaction medium after 3 h under the same conditions used during the standard reaction (buffered aqueous medium, pH 7.4, at 48 °C) but without the addition of substrate. The Na₂PdCl₄ salt was chosen due to its higher solubility in water, and the XAS data were collected on a

synchrotron-based setup in transmission mode at the Pd–K edge (24.35 keV). (See the Supporting Information for details of the XAS setup.) As shown in Figure S9, the extended X-ray absorption fine structure (EXAFS) fitting results show an intense Pd(II)–Cl bond signal and the absence of the Pd(0)–Pd(0) or Pd(II)–O bond signals, which would be observed if Pd(0) species or Pd(II) hydrolysis products had been formed in the reaction medium during the 3 h of the experiment.^{36,37} It is clear from these results that under these reaction conditions, no Pd(0) is spontaneously formed, but we do not rule out the possible formation of Pd(0) in the presence of the substrate, for example, due to a Wacker-type reaction. The nature of the catalysts in the presence of substrate was not investigated by XAS due to the low solubility of DNPPE.

Thus two mechanistic scenarios could possibly act in the faster kinetic phase. If Pd(0) was somehow formed in the presence of substrate, then the reaction would occur via an oxidative addition at the propargyl group, or the other scenario would be a hydration of the propargyl group coordinated to a Pd(II) (Figure 1b, pathways i and ii, respectively). To distinguish between these possible pathways, we have performed a kinetic experiment adding CS₂ at 0 h and after 2 h of reaction time. CS₂ acts as a catalyst poison for homogeneous and heterogeneous Pd(0) catalysts at temperatures below 50 °C, whereas Pd(II) species are unaffected.³⁸ As shown in Figure S10, the initial reaction rate for the faster phase in all cases is similar. This result indicates that there is no participation of Pd(0) species in the faster phase (Rx1). On the contrary, the slower phase (Rx2) rate has been intensely affected by the addition of CS₂, most probably due to the participation of Pd(0) in this reaction phase.

Continuing with the aim to unveil the nature of the catalytic species, high-resolution electrospray ionization mass spectrometry (ESI–HRMS) was used to monitor the reaction and possible detection of key reaction intermediates.^{39–42} ESI is a soft ionization technique that can be used to analyze both cations and anions, displays high sensitivity, and allows the immediate transfer to the gas phase of most ionic species present in the reaction solution. Working in negative ion mode, the *in situ* ESI(–)–HRMS monitoring of the reaction, with 20 mol % of Na₂PdCl₄ in phosphate-buffered aqueous solution pH 7.4 (5% DMSO) provided 10 min after the start of the reaction, identified the following proposed species: the product DNP ($m/z = 183$) as the major species (Figure 3a) and three other Pd species interacting with the substrate at m/z 434.8, 416.9, and 638.9 (Figure 3b–d). The species at m/z 434.8 (1, Figure 3b) is a π complex of PdCl₃ with DNPPE, and the Pd signal at m/z 416.9 may be one of the several possible carbopalladate isomers formed from the hydration (Markovnikov or anti-Markovnikov) of the π complex [DNPPE–PdCl₃] (2, Figure 3c). We shall see later that computational calculations revealed that the ketone isomer is more stable ($\sim 16 \text{ kcal mol}^{-1}$).

The third species identified is a hydrolyzed (Markovnikov or anti-Markovnikov) carbopalladate intermediate complexed with another DNPPE molecule through a π interaction (3, Figure 3d). The agreement between the experimental and calculated (Figure S11) isotopologue patterns and exact masses corroborates the proposed structures and elemental compositions. Moreover, the ESI–HRMS analysis after 35 min of reaction shows that species 1 and 2 are still present, but after 120 min, only the DNP product can be observed. In addition, the analysis of a precipitate formed after 35 min of reaction

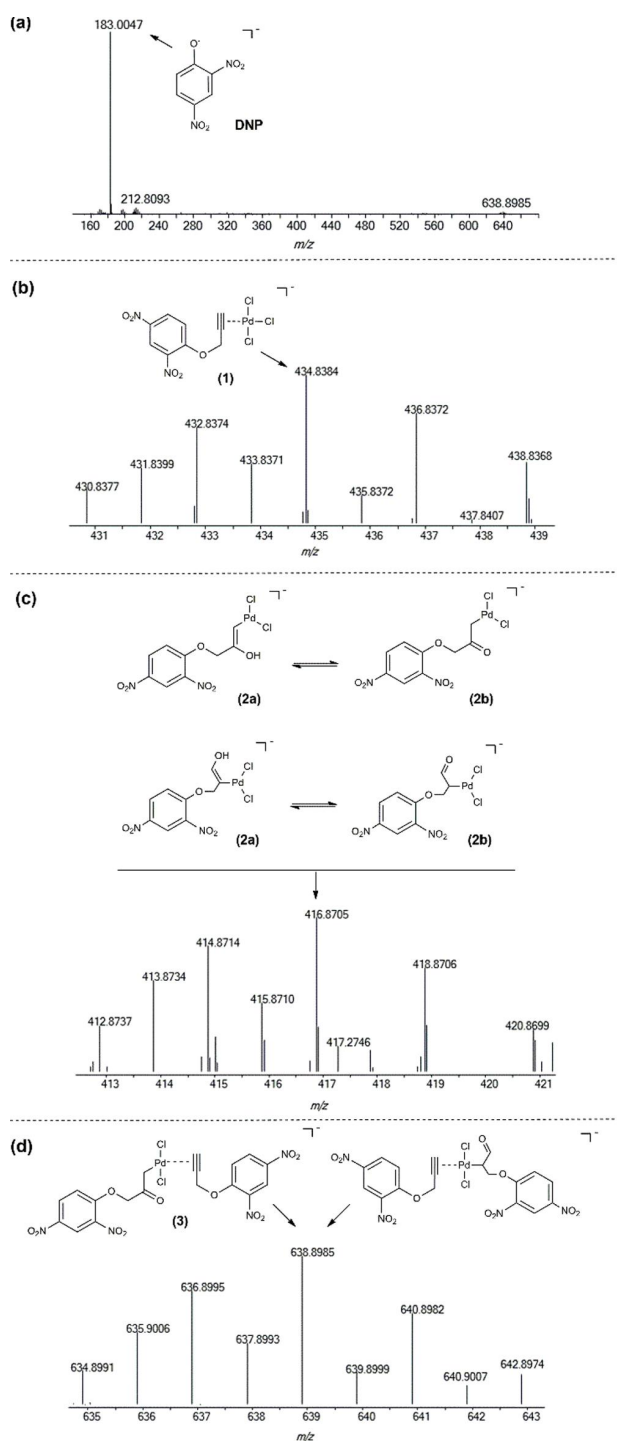


Figure 3. ESI(-)-HRMS of the reaction medium 10 min after the start of the DNPPE depropargylation reaction. The ions at m/z 434.8 (b), m/z 416.9 (c), and m/z 638.9 (d) were detected in lower abundance compared with the product ion DNP (a), so the spectral regions of interest were amplified ($[\text{DNPPE}] = 2.12 \text{ mmol L}^{-1}$, $[\text{Na}_2\text{PdCl}_4] = 20 \text{ mol } \%$, in H_2O (5% DMSO), pH 7.4 at 48°C).

also identified an ion at m/z 473 (Figure S12), corresponding to another hydrolyzed carbopalladate intermediate. Ion 3 was then further characterized by ESI collision-induced dissociation tandem mass spectrometry (ESI-CID-MS/MS). The

observed fragmentation pathways of these reaction intermediates reflect their intrinsic reactivity and support the proposed structures of 3. (See Figure S13 for further discussion.)

These species identified by ESI-HRMS, together with the results from the kinetic studies, align more with an alkyne hydration pathway than with an oxidative addition pathway, at least for the initial part of the reaction, that is, for the faster reaction phase. To explore the details of the fast Rx1 and possibly exploit it in the future, we also performed computational studies. On the basis of the XAS results, the complex $[\text{PdCl}_4]^{2-}$ was used as the catalyst species, and we chose the model substrate methyl-propargyl ether to simplify the calculations. All simulations were performed with an implicit solvent model, and we added two extra water molecules to consider the effect of explicit solvation, one interacting with the enol part and the other interacting with the leaving group. Geometries and frequencies were calculated with the functional PBE0,⁴³ and, to obtain very accurate energetics, DLPNO-CCSD(T)⁴⁴ was used to compute the energies, and the HF-gCP⁴⁵ correction was added to minimize basis set artifacts.

Surprisingly, the energy difference between the Markovnikov and anti-Markovnikov regiochemical hydrations of the Pd-propargyl complex to form enols is low ($<1 \text{ kcal mol}^{-1}$), falling within the error of the method (Figure S14). Thus both pathways to product formation were explored. After the formation of the enol, a tautomerization can occur (also suggested by ESI-HRMS, Figure 3c), and we found that keto tautomers are the most stable. Next, we searched for the C–O bond break step for both regiochemical keto tautomer intermediates. For the anti-Markovnikov keto intermediate (C_2 , Figure S14), the first-expected $\text{S}_{\text{N}}2$ -like hydrolysis is not much faster than the uncatalyzed reaction, with the transition state being stabilized by only ca. 8 kcal mol^{-1} . We then searched for other mechanistic pathways, such as an intramolecular attack of the oxygen ($\Delta G^\ddagger = 58.7 \text{ kcal mol}^{-1}$), β -H elimination of Pd, followed by hydrolysis (this pathway was discarded due to the high acidity of methylene H) and concluded that a β -O elimination mechanism was most likely, with the C–O bond breaking prior to a subsequent attack of water ($\Delta G^\ddagger = 38 \text{ kcal mol}^{-1}$). For the Markovnikov keto intermediate (C'_2 , Figure S14), the $\text{S}_{\text{N}}2$ -like hydrolysis presented much higher activation energy ($\Delta G^\ddagger = 54.02 \text{ kcal mol}^{-1}$) than the β -O elimination of the anti-Markovnikov keto intermediate. The complete calculation for the first reaction turnover of the main mechanism is depicted in Figure 4.

Thus we propose that the most probable operating reaction pathway for Rx1 involves the coordination of DNPPE molecules to Pd(II), followed by an anti-Markovnikov attack of water molecules at the propargyl moiety, prior to the C–O bond breaking by β -O elimination and hydration (Figure 5). The proposed pathways for Rx1 shown in Figure 5 involve the stepwise C–O bond cleavages ($2 \rightarrow 4 \rightarrow 5 \rightarrow 6 \rightarrow 7 \rightarrow 8$). In this scenario, the final products are two equivalents of DNP and the bis(1-hydroxy-3-oxopropan-2-yl)palladium(II) chloride, the carbopalladate complex 8. Although the formation of 8 could not be confirmed by analytical tools such as ESI-HRMS or even by ^1H NMR (Figure S15), its existence is supported by the detection of only two turnovers during Rx1 because the binding of a third DNPPE molecule is less likely due to steric hindrance.

The K_{eq} values calculated for two insertions of the propargyl ether substrate are 4.9×10^{-4} for the first and 6.3×10^{-4} for

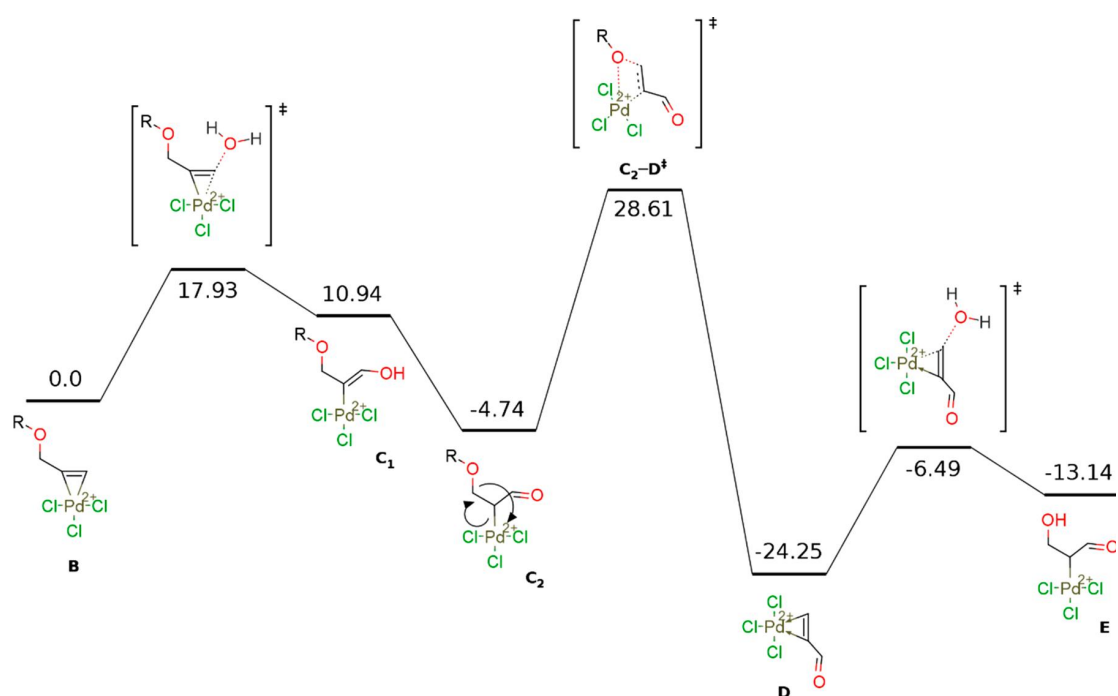


Figure 4. Energy profile (kcal mol^{-1}) calculated for the first turnover of the depropargylation reaction catalyzed by $[\text{PdCl}_4]^{2-}$ in water.

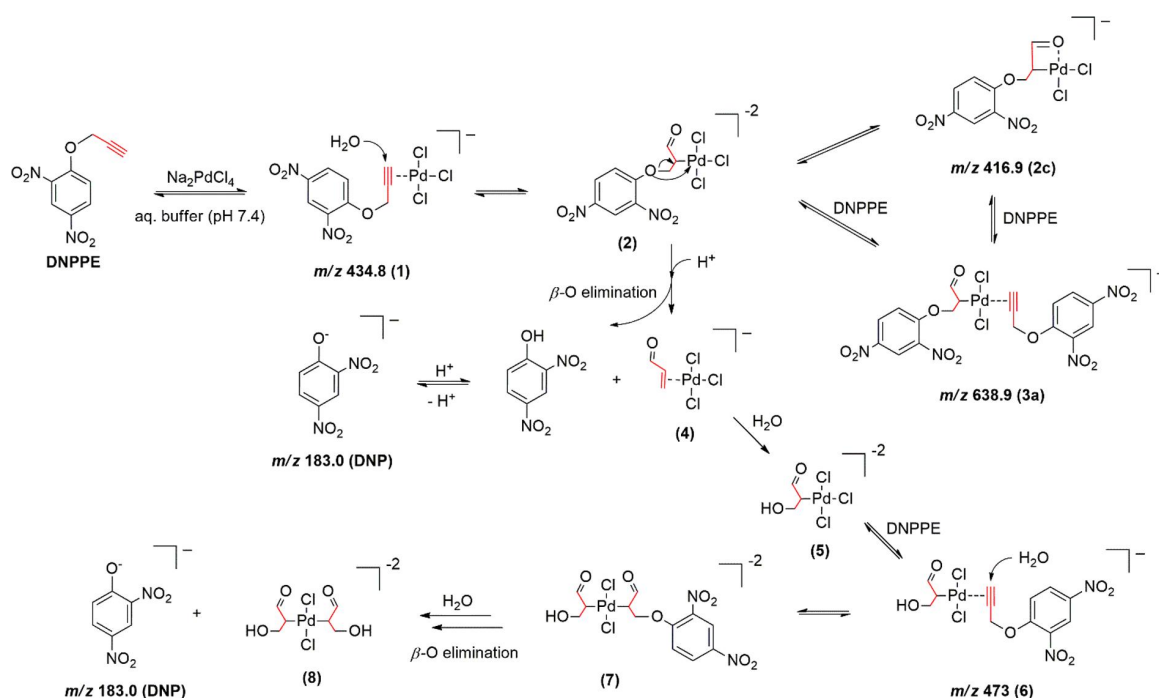


Figure 5. Proposed pathways for Rx1 in the depropargylation reaction of DNPPE mediated by Pd(II) salts.

the second insertion, but the binding of a third molecule, displacing a chloride, has a constant of 7.6×10^{-8} (Figure S14) and probably does not happen at all; in this case, complex 8 can be considered a product-inhibited Pd catalyst. Indeed, when 50 mol % of Pd is used, the quantitative formation of DNP is reached in <2 h in a monophasic first-order kinetic profile (Figure S16) for all three Pd(II) salts used in this study. As can be seen, the role of the metal in this first step is two-

fold: It facilitates the hydration of the triplet bond and stabilizes the keto tautomer intermediate during the C–O bond breaking. We assume that when a second substrate is coordinated, the same hydrolytic mechanism is followed.

To test the hypothesis of complex 8 formation, we added propargyl alcohol in the reaction medium and waited for 2 h before the addition of the substrate. The idea is that under this time, the propargyl alcohol, complexed with Pd(II), would be

hydrolyzed and inhibit further complexation of DNPPE molecules. In fact, as shown in Figure S17, Rx1 was much slower with the addition of propargyl alcohol. This result corroborates the proposed mechanism for Rx1.

On the basis of the kinetic evidence and poisoning studies (see below), it is more likely that after these first two turnovers, Rx2 is undergoing a different mechanism. When the reaction was performed with a higher substrate concentration, a dark precipitate was observed after the reaction completion. This precipitate was analyzed by transmission electron microscopy (Figure S18) and synchrotron-based X-ray absorption spectroscopy (XANES/EXAFS) (Figure S19). These experiments revealed the presence of 5 nm Pd nanoparticles (Pd NPs) and palladium with a mixed oxidation state. (See the Supporting Information for further details and discussion.) The reaction was then monitored by dynamic light scattering (DLS, Figure S20), and the presence of nanoparticles (hydrodynamic ratio between 8 and 15 nm) was observed beginning at 5 min of reaction, although in very low concentration.

These observations motivated us to perform further poisoning experiments to determine the catalytically active species for Rx2. Figure S21 shows the reaction kinetic profiles with CS₂ and Hg(0) added after 120 min of reaction compared with the reactions without the additives. As discussed before, CS₂ acts as a catalyst poison for homogeneous and heterogeneous catalysts,³⁸ whereas Hg(0) poisons metal-particle heterogeneous catalysts by amalgamating the metal or adsorbing onto the metal surface, especially palladium, with homogeneous complexes remaining unaffected.⁴⁶ The addition of CS₂ completely inhibits the catalytic activity of Rx2, but the presence of mercury inhibits the DNP formation by ~60%. These results indicate that the catalytic activity of the slower phase of the reaction (Rx2) is mainly a result of Pd(0) NPs formed during the reaction or lixiviated Pd(0) atoms from the NPs (Figure 6); the formation of these Pd(0) species from the Pd(II) complex **8** may explain why this product has not been detected by any analytical tools employed. In fact, when the reaction was performed in the presence of as-synthesized Pd(0) NPs, the reaction was extremely slow (Figure S22), supporting the nature of the Rx2 phase of the reaction.

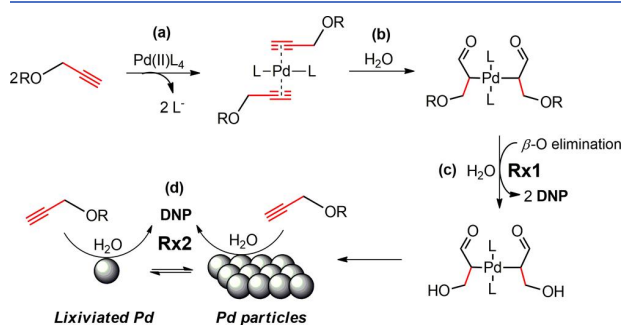


Figure 6. Pd(II) catalytic fate in the DNPPE *O*-depropargylation reaction. The full substrate conversion is a consequence of two different catalytic cycles: (i) Two equivalents of substrate are converted in a fast reaction, where the initial step is a ligand exchange (a), followed by hydration of the triple bond (b) and C–O bond cleavage by β -O elimination, followed by hydration (c). (ii) The second and less effective cycle might be the result of a Pd(0) nanoparticles/lixiviated catalytic species formed after the first cycle (d). L = ligand (e.g., Cl[−] and AcO[−]). R = 2,4-dinitrophenyl group.

3. CONCLUSIONS

We have shown that simple Pd(II) salts can effectively act as catalysts for the *O*-depropargylation reaction under biocompatible conditions, but the reaction is biphasic, presenting a fast and a slow phase, revealing that the catalyst is changing to accommodate a switch in the mechanism. The faster phase ends after two turnovers due to product inhibition. This explains the frequently reported need for high doses of these catalysts for a fast full conversion of the substrate. The mechanism for the faster phase involves key intermediates where the Pd(II) is inserted with anti-Markovnikov orientation at the propargyl moiety prior to the C–O bond cleavage by a β -O elimination, as suggested by theoretical modeling, whereas the slow phase involves the hydrolysis of the substrate promoted by Pd(0) species formed during the first phase of the reaction. These findings will help to design and control the selective reactivity of new palladium catalysts for uncaging reactions of *O*-propargyl substrates, especially discrete Pd complexes.⁴⁷ For example, we envision that Pd complexes with bulky ligands may be a better choice for this reaction because the expulsion of the reaction product can be tuned by the steric bulkiness of the ligands, avoiding the inhibition of the catalyst by the reaction product derived from the propargyl moiety. These studies are currently underway in our laboratory.

■ ASSOCIATED CONTENT

Supporting Information

The Supporting Information is available free of charge on the ACS Publications website at DOI: 10.1021/acscatal.9b00210.

Detailed experimental procedures, reaction kinetics profiles, and spectroscopic analysis (PDF)

■ AUTHOR INFORMATION

Corresponding Author

*E-mail: josiel.domingos@ufsc.br.

ORCID

Sara E. Coelho: 0000-0001-9145-5657

Felipe S. S. Schneider: 0000-0001-8090-2976

Giovanni F. Caramori: 0000-0002-6455-7831

Josiel B. Domingos: 0000-0002-6001-4522

Notes

The authors declare no competing financial interest.

■ ACKNOWLEDGMENTS

We are grateful to CNPq and CAPES for the financial support received for this study. We also thank the Brazilian Synchrotron Light Laboratory (LNLS) team for XAS experiments carried out under proposals 20160243/20170351 on the XDS beamline, using the experimental station developed for the EMA beamline at SIRIUS source, the Central Laboratory of Electron Microscopy (LCME) at UFSC (for the TEM analysis), and the Brazilian National Center for Supercomputing (CESUP/UFRGS). This paper is dedicated in memory of Professor Faruk José Nome Aguilera (1947–2018).

■ REFERENCES

- Li, J.; Chen, P. R. Development and Application of Bond Cleavage Reactions in Bioorthogonal Chemistry. *Nat. Chem. Biol.* **2016**, *12*, 129–137.
- Pérez-López, A. M.; Rubio-Ruiz, B.; Sebastián, V.; Hamilton, L.; Adam, C.; Bray, T. L.; Irusta, S.; Brennan, P. M.; Lloyd-Jones, G. C.;

- Sieger, D.; Santamaría, J.; Unciti-Broceta, A. Gold-Triggered Uncaging Chemistry in Living Systems. *Angew. Chem., Int. Ed.* **2017**, *56*, 12548–12552.
- (3) Yusop, R. M.; Unciti-Broceta, A.; Johansson, E. M. V.; Sánchez-Martín, R. M.; Bradley, M. Palladium-Mediated Intracellular Chemistry. *Nat. Chem.* **2011**, *3*, 239–243.
- (4) Yang, M. Y.; Li, J.; Chen, P. R. Transition Metal-Mediated Bioorthogonal Protein Chemistry in Living Cells. *Chem. Soc. Rev.* **2014**, *43*, 6511–6526.
- (5) Völker, T.; Meggers, E. Transition-Metal-Mediated Uncaging in Living Human Cells — an Emerging Alternative to Photolabile Protecting Groups. *Curr. Opin. Chem. Biol.* **2015**, *25*, 48–54.
- (6) Dumas, A.; Couvreur, P. Palladium: A Future Key Player in the Nanomedical Field? *Chemical Science* **2015**, *6*, 2153–2157.
- (7) Chankeshwara, S. V.; Indrigo, E.; Bradley, M. Palladium-Mediated Chemistry in Living Cells. *Curr. Opin. Chem. Biol.* **2014**, *21*, 128–135.
- (8) Jbara, M.; Maity, S. K.; Brik, A. Palladium in the Chemical Synthesis and Modification of Proteins. *Angew. Chem., Int. Ed.* **2017**, *56*, 10644–10655.
- (9) Wang, J.; Cheng, B.; Li, J.; Zhang, Z.; Hong, W.; Chen, X.; Chen, P. R. Chemical Remodeling of Cell-Surface Sialic Acids through a Palladium-Triggered Bioorthogonal Elimination Reaction. *Angew. Chem., Int. Ed.* **2015**, *54*, 5364–5368.
- (10) Li, J.; Yu, J.; Zhao, J.; Wang, J.; Zheng, S.; Lin, S.; Chen, L.; Yang, M.; Jia, S.; Zhang, X.; Chen, P. R. Palladium-Triggered Deprotection Chemistry for Protein Activation in Living Cells. *Nat. Chem.* **2014**, *6*, 352–361.
- (11) Wang, J.; Zheng, S.; Liu, Y.; Zhang, Z.; Lin, Z.; Li, J.; Zhang, G.; Wang, X.; Li, J.; Chen, P. R. Palladium-Triggered Chemical Rescue of Intracellular Proteins Via Genetically Encoded Allene-Caged Tyrosine. *J. Am. Chem. Soc.* **2016**, *138*, 15118–15121.
- (12) Weiss, J. T.; Dawson, J. C.; Macleod, K. G.; Rybski, W.; Fraser, C.; Torres-Sánchez, C.; Patton, E. E.; Bradley, M.; Carragher, N. O.; Unciti-Broceta, A. Extracellular Palladium-Catalysed Dealkylation of 5-Fluoro-1-Propargyl-Uracil as a Bioorthogonally Activated Prodrug Approach. *Nat. Commun.* **2014**, *5*, 3277.
- (13) Weiss, J. T.; Dawson, J. C.; Fraser, C.; Rybski, W.; Torres-Sánchez, C.; Bradley, M.; Patton, E. E.; Carragher, N. O.; Unciti-Broceta, A. Development and Bioorthogonal Activation of Palladium-Labile Prodrugs of Gemcitabine. *J. Med. Chem.* **2014**, *57*, 5395–5404.
- (14) Tonga, G. Y.; Jeong, Y.; Duncan, B.; Mizuhara, T.; Mout, R.; Das, R.; Kim, S. T.; Yeh, Y.-C.; Yan, B.; Hou, S.; Rotello, V. M. Supramolecular Regulation of Bioorthogonal Catalysis in Cells Using Nanoparticle-Embedded Transition Metal Catalysts. *Nat. Chem.* **2015**, *7*, 597–603.
- (15) Stenton, B. J.; Oliveira, B. L.; Matos, M. J.; Sinatra, L.; Bernardes, G. J. L. A Thioether-Directed Palladium-Cleavable Linker for Targeted Bioorthogonal Drug Decaging. *Chemical Science* **2018**, *9*, 4185–4189.
- (16) Martínez-Calvo, M.; Mascareñas, J. L. Organometallic Catalysis in Biological Media and Living Settings. *Coord. Chem. Rev.* **2018**, *359*, 57–79.
- (17) Bai, Y.; Chen, J.; Zimmerman, S. C. Designed Transition Metal Catalysts for Intracellular Organic Synthesis. *Chem. Soc. Rev.* **2018**, *47*, 1811–1821.
- (18) Vinogradova, E. V. Organometallic Chemical Biology: An Organometallic Approach to Bioconjugation. *Pure Appl. Chem.* **2017**, *89*, 1619–1640.
- (19) Garner, A. L.; Song, F.; Koide, K. Enhancement of a Catalysis-Based Fluorometric Detection Method for Palladium through Rational Fine-Tuning of the Palladium Species. *J. Am. Chem. Soc.* **2009**, *131*, 5163–5171.
- (20) Amatore, C.; Jutand, A.; Thuilliez, A. Formation of Palladium(0) Complexes from Pd(OAc)₂ and a Bidentate Phosphine Ligand (Dppp) and Their Reactivity in Oxidative Addition. *Organometallics* **2001**, *20*, 3241–3249.
- (21) Pal, M.; Parasuraman, K.; Yeleswarapu, K. R. Palladium-Catalyzed Cleavage of O/N-Propargyl Protecting Groups in Aqueous Media under a Copper-Free Condition. *Org. Lett.* **2003**, *5*, 349–352.
- (22) Rambabu, D.; Bhavani, S.; Swamy, N. K.; Basaveswara Rao, M. V.; Pal, M. Pd/C-Mediated Depropargylation of Propargyl Ethers/Amines in Water. *Tetrahedron Lett.* **2013**, *54*, 1169–1173.
- (23) Wei, C. S.; Davies, G. H. M.; Soltani, O.; Albrecht, J.; Gao, Q.; Pathirana, C.; Hsiao, Y.; Tummala, S.; Eastgate, M. D. The Impact of Palladium(II) Reduction Pathways on the Structure and Activity of Palladium(0) Catalysts. *Angew. Chem., Int. Ed.* **2013**, *52*, 5822–5826.
- (24) Liu, B.; Wang, H.; Wang, T.; Bao, Y.; Du, F.; Tian, J.; Li, Q.; Bai, R. A New Ratiometric Espt Sensor for Detection of Palladium Species in Aqueous Solution. *Chem. Commun. (Cambridge, U. K.)* **2012**, *48*, 2867–2869.
- (25) Sletten, E. M.; Bertozzi, C. R. Bioorthogonal Chemistry: Fishing for Selectivity in a Sea of Functionality. *Angew. Chem., Int. Ed.* **2009**, *48*, 6974–6998.
- (26) Murahashi, T.; Ogoshi, S.; Kurosawa, H. New Direction in Organopalladium Chemistry: Structure and Reactivity of Unsaturated Hydrocarbon Ligands Bound to Multipalladium Units. *Chem. Rec.* **2003**, *3*, 101–111.
- (27) Chalmers, S.; Caldwell, S. T.; Quin, C.; Prime, T. A.; James, A. M.; Cairns, A. G.; Murphy, M. P.; McCarron, J. G.; Hartley, R. C. Selective Uncoupling of Individual Mitochondria within a Cell Using a Mitochondria-Targeted Photoactivated Protonophore. *J. Am. Chem. Soc.* **2012**, *134*, 758–761.
- (28) Wu, B.; Jiang, M.; Peng, Q.; Li, G.; Hou, Z.; Milne, G. L.; Mori, S.; Alonso, R.; Geisler, J. G.; Duan, W. 2,4-Dnp Improves Motor Function, Preserves Medium Spiny Neuronal Identity, and Reduces Oxidative Stress in a Mouse Model of Huntington's Disease. *Exp. Neurol.* **2017**, *293*, 83–90.
- (29) Khan, R. S.; Dine, K.; Geisler, J. G.; Shindler, K. S. Mitochondrial Uncoupler Prodrug of 2,4-Dinitrophenol, Mp201, Prevents Neuronal Damage and Preserves Vision in Experimental Optic Neuritis. *Oxid. Med. Cell. Longevity* **2017**, *2017*, 1–10.
- (30) Geisler, J. G.; Marosi, K.; Halpern, J.; Mattson, M. P. Dnp, Mitochondrial Uncoupling, and Neuroprotection: A Little Dab'll Do Ya. *Alzheimer's Dementia* **2017**, *13*, 582–591.
- (31) Trader, D. J.; Carlson, E. E. Chemoselective Hydroxyl Group Transformation: An Elusive Target. *Mol. Biosyst.* **2012**, *8*, 2484–2493.
- (32) Kayastha, A. M.; Gupta, A. K. An Easy Method to Determine the Kinetic-Parameters of Biphasic Reactions. *Biochem. Educ.* **1987**, *15*, 135–135.
- (33) Anderson, T. G.; McConnell, H. M. Interpretation of Biphasic Dissociation Kinetics for Isomeric Class II Major Histocompatibility Complex-Peptide Complexes. *Biophys. J.* **1999**, *77*, 2451–2461.
- (34) Devaraj, N. K. The Future of Bioorthogonal Chemistry. *ACS Cent. Sci.* **2018**, *4*, 952–959.
- (35) Blackmond, D. G. Reaction Progress Kinetic Analysis: A Powerful Methodology for Mechanistic Studies of Complex Catalytic Reactions. *Angew. Chem., Int. Ed.* **2005**, *44*, 4302–4320.
- (36) Yao, Y.; Patzig, C.; Hu, Y.; Scott, R. W. J. In Situ X-Ray Absorption Spectroscopic Study of Fe@Fexoy/Pd and Fe@Fexoy/Cu Nanoparticle Catalysts Prepared by Galvanic Exchange Reactions. *J. Phys. Chem. C* **2015**, *119*, 21209–21218.
- (37) Chang, S. Y.; Grunder, Y.; Booth, S. G.; Molleta, L. B.; Uehara, A.; Mosselmanns, J. F. W.; Cibin, G.; Pham, V. T.; Nataf, L.; Dryfe, R. A. W.; Schroeder, S. L. M. Detection and Characterisation of Sub-Critical Nuclei During Reactive Pd Metal Nucleation by X-Ray Absorption Spectroscopy. *CrystEngComm* **2016**, *18*, 674–682.
- (38) Charbonneau, M.; Addoumieh, G.; Oguadinma, P.; Schmitzer, A. R. Support-Free Palladium-Nhc Catalyst for Highly Recyclable Heterogeneous Suzuki–Miyaura Coupling in Neat Water. *Organometallics* **2014**, *33*, 6544–6549.
- (39) Santos, L. S. In *Reactive Intermediates*; Wiley-VCH Verlag GmbH & Co. KGaA: 2010; pp 133–198.
- (40) Roglans, A.; Pla-Quintana, A. In *Reactive Intermediates*; Wiley-VCH Verlag GmbH & Co. KGaA: 2010; pp 229–275.

- (41) Qian, R.; Zhou, J.; Yao, S.; Wang, H.; Guo, Y. In *Reactive Intermediates*; Wiley-VCH Verlag GmbH & Co. KGaA: 2010; pp 113–131.
- (42) Nachtigall, F. M.; Eberlin, M. N. In *Reactive Intermediates*; Wiley-VCH Verlag GmbH & Co. KGaA: 2010; pp 63–111.
- (43) Adamo, C.; Barone, V. Toward Reliable Density Functional Methods without Adjustable Parameters: The Pbe0Model. *J. Chem. Phys.* **1999**, *110*, 6158–6170.
- (44) Riplinger, C.; Sandhoefer, B.; Hansen, A.; Neese, F. Natural Triple Excitations in Local Coupled Cluster Calculations with Pair Natural Orbitals. *J. Chem. Phys.* **2013**, *139*, 134101–134113.
- (45) Kruse, H.; Grimme, S. A Geometrical Correction for the Inter- and Intra-Molecular Basis Set Superposition Error in Hartree-Fock and Density Functional Theory Calculations for Large Systems. *J. Chem. Phys.* **2012**, *136*, 154101–154116.
- (46) Widegren, J. A.; Finke, R. G. A Review of the Problem of Distinguishing True Homogeneous Catalysis from Soluble or Other Metal-Particle Heterogeneous Catalysis under Reducing Conditions. *J. Mol. Catal. A: Chem.* **2003**, *198*, 317–341.
- (47) Martínez-Calvo, M.; Couceiro, J. R.; Destito, P.; Rodríguez, J.; Mosquera, J.; Mascareñas, J. L. Intracellular Deprotection Reactions Mediated by Palladium Complexes Equipped with Designed Phosphine Ligands. *ACS Catal.* **2018**, *8*, 6055–6061.

4 Paper II: Pt-triggered bond-cleavage of pentynoyl amide and *n*-propargyl handles for drug-activation

OLIVEIRA, B. L. et al. Platinum-Triggered Bond-Cleavage of Pentynoyl Amide and N-Propargyl Handles for Drug-Activation. **Journal of the American Chemical Society**, American Chemical Society (ACS), v. 142, n. 24, p. 10869–10880, May 2020. ISSN 1520-5126. DOI: [10.1021/jacs.0c01622](https://doi.org/10.1021/jacs.0c01622). Available from: <http://dx.doi.org/10.1021/jacs.0c01622>

In this work, we investigated the platinum-mediated depropargylation of pentynoyl amide and N-propargyl handles for drug-activation delivery. They were studied for their application to metallocatalysis in a joint computational-experimental collaboration [2]. Such catalysts have potential to be used in cancer therapy as powerful drugs to target cancerous cells using antibody-drug conjugates (ADCs). ADCs consist of an antibody that transports the drug to the tumor cells and releases their arsenal by external triggers. One way to do this is by using the body's own triggers, such as low pH or reduction of disulfide bonds. However, different external triggers, such as small molecules, are advantageous because they don't rely on the body's own triggers and can thus be used across different patients.

Metal-mediated decaging of prodrugs is a process that uses transition metals, such as palladium, ruthenium, gold, and copper, to activate drugs. These metals need to be used in small amounts to reduce the risk of toxicity and side reactions. Recently, platinum has been explored as a potential metal for drug activation, as it is highly reactive and accumulates in tumors [2, 142]. Compared to palladium-mediated decaging [1], the use of platinum complexes allows the use of substoichiometric amounts of metal and is less susceptible to the presence of nucleophiles in cell cultures. Additionally, platinum is not present in human biology, thus it can activate prodrugs specifically in tumor cells.

Our study revealed that the reaction takes place *via* an intramolecular attack of carbonyl oxygen to the pentynoyl moiety, forming a five-membered ring primary intermediate that then undergoes hydration, decomposition and release of a free amine. The reaction can be done at room temperature in aqueous solutions. In collaboration with Oliveira et al., noninternalizing antibody-drug conjugates (ADC) were then synthesized and the generalized developed methodology using platinum complexes as decaging catalysts was tested. In order to test the *in vivo* efficacy of the reaction, a zebrafish larvae xenograft model was used with measurements of proliferation, apoptosis and tumor size.

Computational studies suggested a stepwise reaction pathway with an intramolecular attack of the Pt-coordinated substrate giving a five-membered ring intermediate, leading to hydration, decomposition and release of the amine product. Our computational model matched well the LC-MS characterization of the reaction intermediates, identifying the key CS₀ structure in particular. In total, two sets of 14 rest states and 14 reactions and equilibria were modelled. A summarized diagram of the proposed reaction mechanism can be seen in Figure 3.

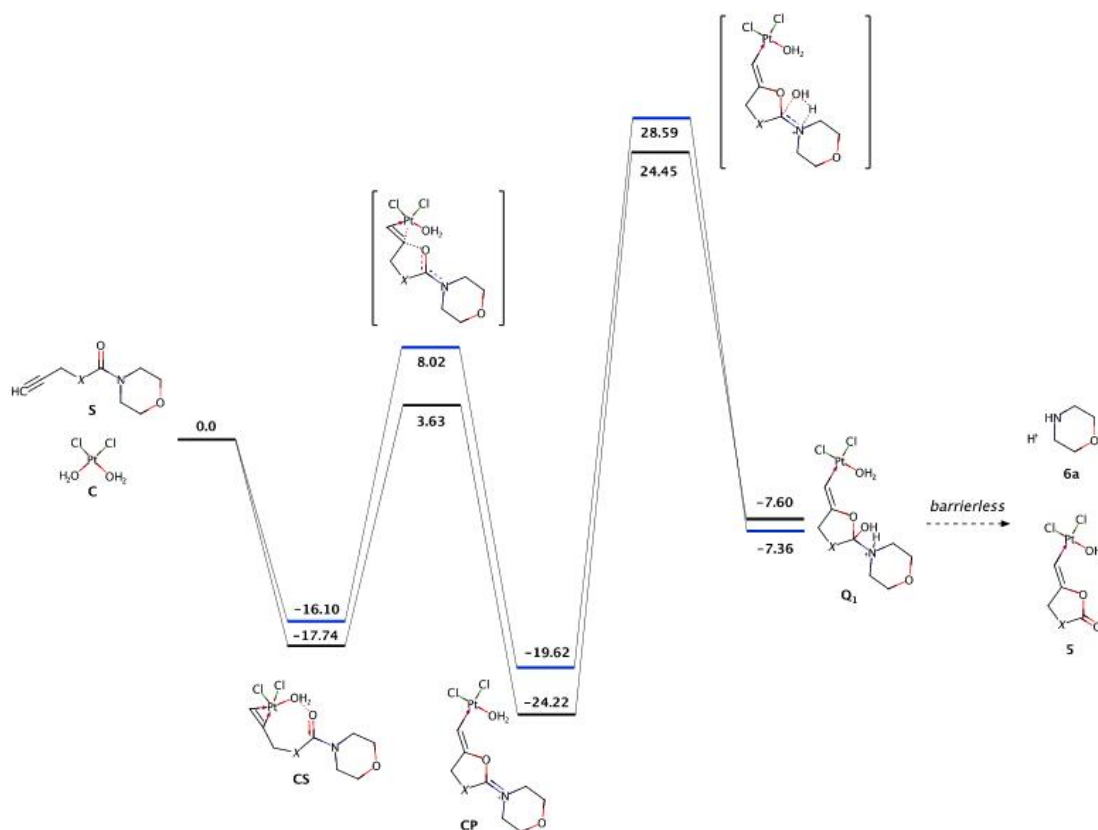



Figure 3 – Summarized diagram of the proposed reaction mechanism in Oliveira et al. Energies are in kcal·mol⁻¹. Licensed under a Creative Commons CC-BY license [143].

We discussed a new reaction of alkynes with platinum complexes that can be used to release secondary amines from tertiary amides, which can be used to activate prodrugs. This reaction was shown to occur through a platinum-mediated intramolecular cyclization mechanism, and water was found to be a necessary metal-activating agent. The reaction was also tested in mammalian cells and a colorectal cancer zebrafish xenograft model and it was found to be successful in both cases. The reaction was also adapted to work with N-propargyl groups and was used to synthesize a noninternalizing ADC. To conclude, our work revealed the suitability of platinum complexes for prodrug activation in physiological conditions, demonstrating the potential of platinum-mediated decaging reactions and paving the way for future developments and *in vivo* applications.

4.1 Full text

This work was a collaboration between researchers at the Department of Chemistry at the University of Cambridge, the Molecular Medicine Institute at the University of Lissabon, the Champalimaud Center for the Unknown at the Champalimaud Foundation, the Department of Chemistry at the Federal University of Santa Catarina (UFSC), and the FT-ICR and Structural Mass Spectroscopy Laboratory at the University of Lissabon.

The work was partially funded by the Brazilian Council for Scientific and Technological Development (CNPq), grant/award numbers 140485/2017-1 and 311963/2017-0, Coordination for the Improvement of Higher Education Personnel (CAPES), PRINT programme call number 88887.310560-00. See the acknowledgements session in the full print (available at the end of this chapter) for the complete list of international financial aids.

The publication can be read in full next. Given that this work was featured in the journal's cover, it has received some local media coverage as well [144]. Oliveira et al. [2] is licensed under a Creative Commons CC-BY license  [143]. A video showing the initial metadynamics simulation for the reaction is available at YouTube ¹.

¹ <https://youtu.be/k5ptn50Zjkc>

Platinum-Triggered Bond-Cleavage of Pentynoyl Amide and *N*-Propargyl Handles for Drug-Activation

Bruno L. Oliveira,^{*,∇} Benjamin J. Stenton,[∇] V. B. Unnikrishnan, Cátia Rebelo de Almeida, João Conde, Magda Negrão, Felipe S. S. Schneider, Carlos Cordeiro, Miguel Godinho Ferreira, Giovanni F. Caramori, Josiel B. Domingos, Rita Fior,^{*} and Gonçalo J. L. Bernardes^{*}

Cite This: *J. Am. Chem. Soc.* 2020, 142, 10869–10880

Read Online

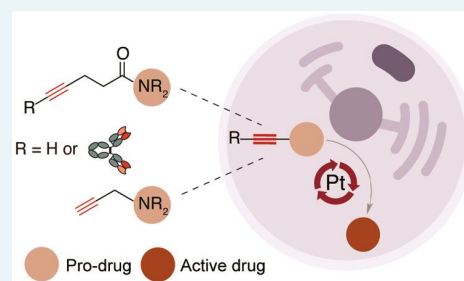
ACCESS |

Metrics & More

Article Recommendations

Supporting Information

ABSTRACT: The ability to create ways to control drug activation at specific tissues while sparing healthy tissues remains a major challenge. The administration of exogenous target-specific triggers offers the potential for traceless release of active drugs on tumor sites from antibody–drug conjugates (ADCs) and caged prodrugs. We have developed a metal-mediated bond-cleavage reaction that uses platinum complexes [K_2PtCl_4 or Cisplatin (CisPt)] for drug activation. Key to the success of the reaction is a water-promoted activation process that triggers the reactivity of the platinum complexes. Under these conditions, the decaying of pentynoyl tertiary amides and *N*-propargyls occurs rapidly in aqueous systems. In cells, the protected analogues of cytotoxic drugs 5-fluorouracil (5-FU) and monomethyl auristatin E (MMAE) are partially activated by nontoxic amounts of platinum salts. Additionally, a noninternalizing ADC built with a pentynoyl traceless linker that features a tertiary amide protected MMAE was also decaged in the presence of platinum salts for extracellular drug release in cancer cells. Finally, CisPt-mediated prodrug activation of a propargyl derivative of 5-FU was shown in a colorectal zebrafish xenograft model that led to significant reductions in tumor size. Overall, our results reveal a new metal-based cleavable reaction that expands the application of platinum complexes beyond those in catalysis and cancer therapy.



INTRODUCTION

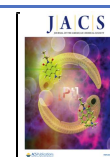
The targeting of potent drugs with tumor-specific ligands is an essential feature of drug delivery and cancer therapy.¹ Notable in this field are antibody–drug conjugates (ADCs) that use an antibody to transport a drug to cancerous cells and endogenously release it by hydrolysis (low pH, reduction of disulfide bonds) or by proteolysis (e.g., cathepsin B protease).^{2,3} Although the cleavage of ADC linkers with endogenous triggers is the simplest method for drug release, external small-molecule triggers for extracellular drug release may be more advantageous because they avoid any disparity in cleavage rates caused by variable biology across subjects, and drug release is not dependent on the concentrations of cellular triggers.^{4–7} In fact, ADCs built with protease cleavable linkers for drug release have been shown recently to not depend on the cathepsin B protease function for efficient and targeted cancer-cell killing.⁴ The promise of controlled prodrug activation has fueled research into new triggers that enable bond-cleavage reactions to unleash bioorthogonal protecting groups, which deactivate otherwise potent drugs.⁸ Robillard and co-workers pioneered the development of tetrazine-triggered drug delivery from ADCs.⁹ By using a non-internalizing ADC consisting of a diabody conjugated to *trans*-cyclooctene-linked drug monomethyl auristatin E (MMAE),¹⁰ the allylic carbamate-containing linker can rapidly

react with a tetrazine through an inverse-electron-demand Diels–Alder reaction.^{10,11} The drug is released within the extracellular tumor environment and showed efficacy in delaying tumor growth in xenograft mice models.¹⁰ Other chemical- or light-mediated decaging reactions have also been developed with an array of applications that range from in situ activation of prodrugs to the gain-of-function study on proteins.^{12–15}

Although the recent results with noninternalizing ADCs for click-triggered drug release show promise, there are several issues that remain to be improved, such as the lack of tumor-selectivity of the chemical triggers or their short in vivo retention times that may result in reduced release of the cytotoxic payloads and thus lower efficacy. Additionally, in such applications the tumor payload concentration is determined by the cell-surface antigen expression, which in some cases may be too low to achieve a useful therapeutic

Received: February 10, 2020

Published: May 26, 2020



response.^{7,16} This contrasts with the use of internalizing ADCs that have an accumulative effect inside the tumor cells.^{7,16,17}

Metal-mediated decaging of prodrugs has been more extensively reported than small-molecule-mediated decaging.¹⁸ Unlike chemical triggers, transition metals can be catalytic, which allows their use in substoichiometric amounts. In these cases, only very small amounts of catalytic metal are required to achieve the desired pharmacologic effect, thereby reducing toxicity and side reactions.^{19,20} This feature was recently demonstrated by Weissleder and co-workers using palladium nanoparticles that accumulate in tumor cells and serve as cellular catalysts for the activation of different model prodrugs and resulted in tumor growth inhibition.²¹

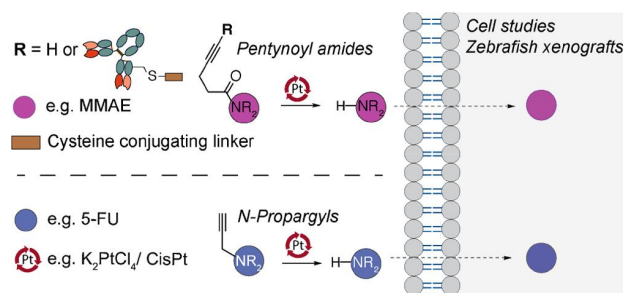
Palladium-mediated decaging is indeed the most studied method for prodrug activation, which relies on the cleavage of terminal propargylic and allylic carbamates moieties introduced into small molecule drugs.^{21–26} Recently, our group developed an internal bifunctional thioether propargyl carbamate linker with a conjugating unit for protein modification and MMAE for palladium-mediated drug release from a nanobody-drug conjugate in cellular systems.²⁷ Other metals, such as ruthenium^{28–30} and gold,^{31,32} have been also explored for cleavage and drug release. One of the latest additions to this field was the recent report by Peng Chen and co-workers³³ on a copper-releasable reaction for protein gain-of-function and drug activation. Together, these examples highlight the potential of metal-mediated cleavage as a means to achieve controlled and chemically defined drug release.

Whereas the utility of the above-mentioned metals for decaging applications has been extensively demonstrated, other metals have not yet been sufficiently explored. For instance, platinum is widely used in catalysis,³⁴ but has found few applications in chemical biology, possibly as a result of its intrinsic cytotoxicity. However, in the context of cancer therapy, we hypothesized that the use of platinum complexes [e.g., Cisplatin (CisPt) used in the clinic]^{35,36} as catalysts for cleavage reactions could be propitious for bioorthogonal activation of prodrugs in tumor cells.

“Bioorthogonal” is perhaps unfitting terminology for a compound known to react with water, nucleic acids, amino acids, and proteins.^{37,38} However, CisPt is one of the most commonly used chemotherapy drugs, being used to treat up to 20% of cancer patients.^{39,40} CisPt was deemed a suitable reagent for the development of a drug decaging reaction because it is highly reactive (half-life in humans of ~30 min),^{41,42} accumulates in the tumor, and most importantly, is not present in human biology.^{43,44} In this way, the activation of prodrugs at the tumor site when the chemical trigger has already accumulated may represent a major achievement. It may be conceivable for metal concentrations to reach 0.25 to 3.7 μg per g of tumor.^{41,45,46} For a 1 cm^3 tumor (approximately 1 g wet weight), the concentration of CisPt is estimated to be 0.83–12.3 μM .⁴⁷

Therefore, we were interested in investigating new bioorthogonal cleavage reactions catalyzed by platinum for applications in prodrug activation. Here, we demonstrate that pentynoyl tertiary amide and *N*-propargyl handles introduced into small-molecule drugs are successfully decaged in aqueous solution and cell media using nontoxic amounts of platinum salts (Scheme 1). This strategy was successfully applied to small molecule prodrug activation (MMAE and 5-FU) and further extended to drug release from a noninternalizing ADC in cancer cells. Finally, we show that CisPt-mediated bond

Scheme 1. Platinum-Mediated Bioorthogonal Bond Cleavage⁴⁷



“Secondary amines protected in the form of a tertiary pentynoyl amide (top) or *N*-propargyl (bottom) can be selectively deprotected by platinum reagents like the chemotherapeutic drug CisPt. This strategy was explored for drug activation of the protected MMAE and 5-FU drugs and extended for drug release from an ADC in cancer cells. Ultimately, CisPt-mediated activation of a “5-FU-propargyl prodrug” was evaluated in a zebrafish xenograft model for treatment of colorectal cancer.

cleavage can be used to activate a 5-FU prodrug in a zebrafish xenograft model for treatment of colorectal cancer.

RESULTS AND DISCUSSION

Engineering of a Platinum-Mediated Decaging Reaction. From studies on the reactivity of platinum complexes, it is apparent that platinum shares many of its reactions with similar complexes of gold.⁴⁸ We therefore searched the literature for reactions with Au and Pt that would function at room temperature, in aqueous media, and with likely fast kinetics to adapt for CisPt-mediated bioorthogonal decaging reactions. The cyclization of 4-pentynoic acid is well-known to proceed quickly in aqueous media with reaction times ranging from minutes to a few hours^{49,50} and has even been demonstrated with platinum (II and IV) anticancer complexes (Figure 1a).⁵¹ Given the previous studies, a metal-catalyzed mechanism was devised whereby a carbamate carbonyl could be used as an internal nucleophile to cause carbocyclization followed by release of a secondary amine (Figure 1b). Working on this hypothesis, we synthesized the terminal propargyl carbamate **3a** (Figure 1c) to verify if the carbonyl could act as a nucleophile and attack the alkyne to subsequently release morpholine **6a** in the presence of K_2PtCl_4 . We observed conversions of 20% and 61% for reactions carried out in $\text{D}_2\text{O}/\text{CD}_3\text{OD}$ (3:1) with 0.1 and 2 equiv of metal salt, respectively (Figure 1d, Entries 1 and 2; Figures S1 and S2 of the Supporting Information, SI). Similar yields were found for the reaction with NaAuCl_4 (Figure S3). In contrast, if an aliphatic carbamate with no propargyl handle is used (compound SI S1) under the same decaging conditions the free amine is not released (Figures S4 and S5, respectively).

According to these observations, it should also be possible to decage tertiary amides to release secondary amines (Figure 1c). This was an attractive prospect because amides are often much more stable than their corresponding carbamates.⁵² Decaging of pentynoyl tertiary amide **4a** was monitored by NMR spectroscopy over time and was proven to have comparable rates and yields to the corresponding carbamate **3a** (Figure 1d, Entry 4; Figure 1e). Importantly, the reaction proceeds with substoichiometric amounts of the metal complex (Figure 1d, Entry 3; Figure S6). The reactions were also

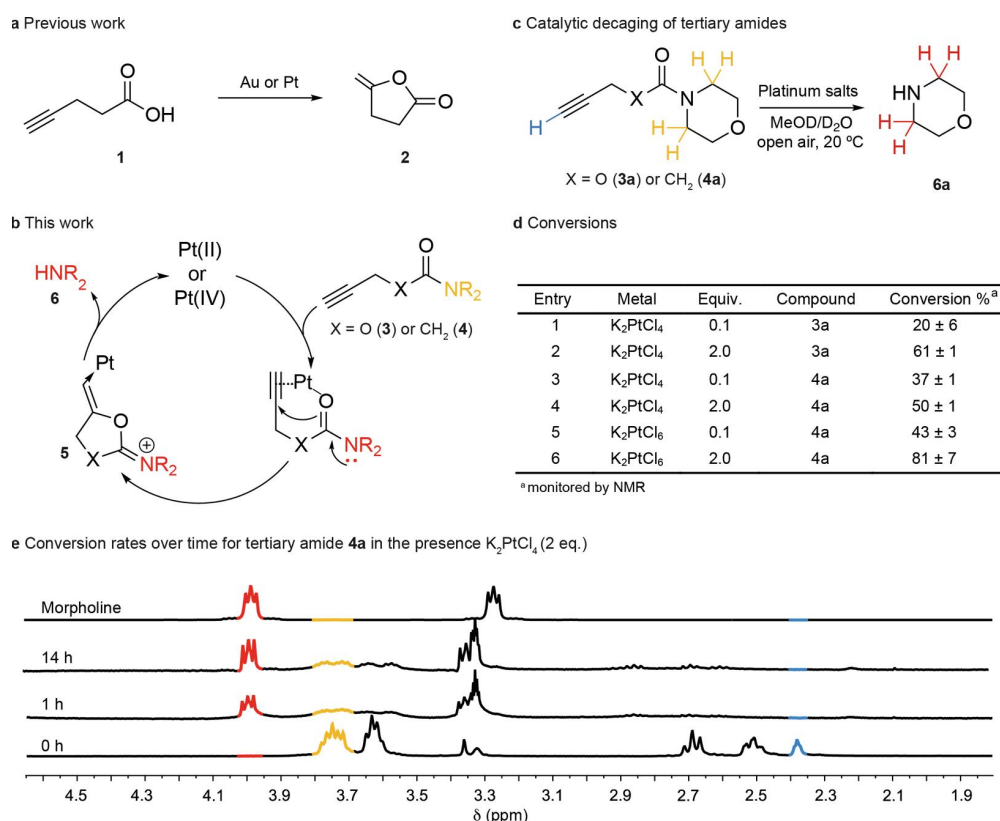


Figure 1. Platinum-mediated decaging reaction engineering. **a.** The cyclization of 4-pentynoic acid is known to proceed rapidly in aqueous media with gold and platinum complexes. **b.** The proposed reaction uses a carboxamide as an internal nucleophile that cyclizes and displaces the secondary amine leaving group, which could be a drug or a fluorophore. **c.** Model compounds with alkyne amide or carbamate were used to survey the decaging reaction. **d.** Efficiency of the cleavage reaction under different conditions was assessed by ¹H NMR spectroscopy. **e.** ¹H NMR spectroscopy of the decaging of the tertiary amide **4a** in the presence of a catalytic amount of K₂PtCl₄. The reaction generates a cyclized intermediate that undergoes hydrolysis to release morpholine **6a**. General procedure for determining decaging conversion by ¹H NMR spectroscopy: carbamate and amide compounds (10 mg) were dissolved in MeOD (0.2 mL) and metal complexes (0.1 or 2 equiv) were added in D₂O (0.6 mL) at room temperature in an open vessel for 14 h. The reactions were transferred to an NMR spectroscopic tube and sealed. Conversion was calculated based on the relative ratios of methylene peaks resulting from the starting material and the released amine product. Numerical data are the mean of 2 or 3 replicates.

successfully trialed with K₂PtCl₆ as a representative Pt(IV) species (Figure 1d, Entries 5 and 6; Figure S7) and NaAuCl₄ (Figure S8) with good yields.

Overall, these results are important because they demonstrate a decaging reaction of stable protected tertiary amides by using substoichiometric amounts of platinum complexes that could function in water, open air, and without need of extreme temperatures or complex ligands. It is important to note that even after all of the starting material has been consumed (as evidenced by loss of terminal alkyne proton), not all of it has decomposed to release the amine (Figure 1e). This lack of conversion is likely due to side reactions, and nucleophilic attack on the alkyne, which seems the most plausible mechanism. To elucidate this a pentynoyl secondary amide (compound **S2**) was reacted with K₂PtCl₄ and NaAuCl₄ under similar conditions (Figures S9 and S10). We found that the reaction proceeds with much lower extents of decaging, likely due to the amide nitrogen competing as a nucleophile to yield a stable cyclized product, and thus a smaller yield of released amine.

Mechanistic and Kinetic Studies of the Platinum-Mediated Decaging Reaction. To further study the platinum decaging reaction, the pentynoyl tertiary amide was

conjugated to a naphthalimide-based fluorophore to generate fluorescent quenched probe **7** (Figure 2a, see SI for synthetic details).^{S3,S4} The reaction was then monitored by the increase in fluorescence upon removal of the protecting group to form fluorescent probe **8**. With 50 equiv of K₂PtCl₄ or CisPt, we found that the fluorescence was restored over a period of 200 min for K₂PtCl₄ and 300 min for CisPt (Figure 2b), with complete consumption of **7** and formation of corresponding “turned ON fluorophore”, as indicated by LC–MS analysis (Figure S11). For both metals the conversion was accompanied by an initial steady state followed by a marked increase of the fluorescence, which suggested the formation of an activated intermediate. Indeed, it is known that platinum complexes form a series of reactive intermediates by successive replacement of the chloro ligands by water or hydroxyl groups.^{S5–S7} We hypothesized that formation of such an aqua intermediate early on could be responsible for the activation of the platinum complexes. This hypothesis was verified using LC–MS studies to follow formation of K₂PtCl₄– and CisPt–aqua complexes over time, which occurred within 6 h (Figures S12 and S13). Consistent with this hypothesis, platinum salts failed to form the aqua complexes when incubated in the presence of *N,N*-dimethylformamide (DMF). On the basis of

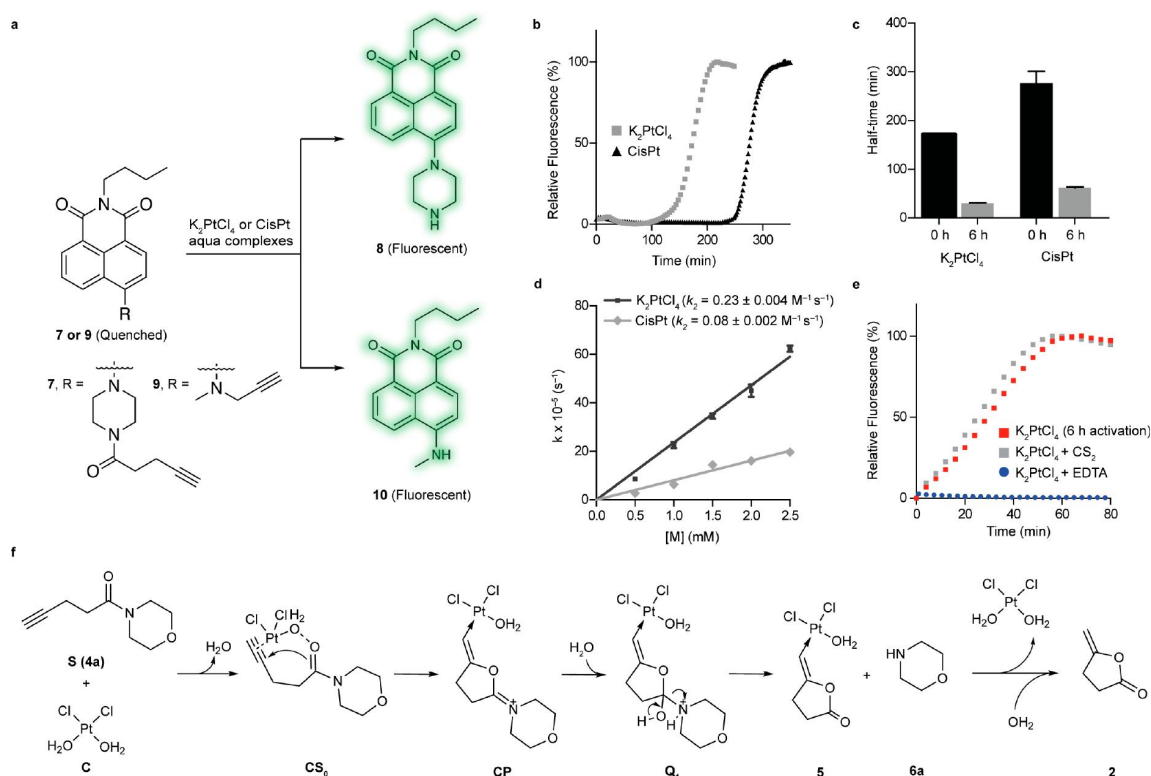


Figure 2. Examination of the platinum-catalyzed bioorthogonal cleavage reaction. a. Naphthalimide-based fluorogenic probes were used to study the cleavage efficiency of the platinum reaction for decaging alkyne-containing molecules. The caged naphthalimide derivatives exhibited high stability in solution and cell media and their quenched fluorescence could be reactivated upon removal of the caging group ($\lambda_{\text{ex}} = 445 \text{ nm}$, $\lambda_{\text{em}} = 545 \text{ nm}$). b. Changes in fluorescence intensity during the time course of the decaging reaction between fluorogenic probe 7 and platinum salts ($\text{K}_2\text{PtCl}_4/\text{CisPt}$). c. Determined half-time for the reaction of 7 with activated and nonactivated platinum salts. d. Decaging kinetics for the pentynoyl amide fluorophore. Rate constants were determined under pseudo first order conditions with a $50 \mu\text{M}$ final concentration of probe 7 and 10–50 equiv of aqua platinum metals. e. Kinetics profiles of the decaging reaction in the presence of the metal poisons CS_2 and EDTA. Error bars represent \pm s.d. ($n = 3$). All experiments were repeated 3 independent times. f. Calculated mechanism for the depropargylation reaction catalyzed by Pt with model substrate 4a. Calculations were performed with an implicit solvent model for water. Geometries and frequencies were calculated with the functional revPBE and, to obtain very accurate energetics, single point energy calculations with DLPNO–CCSD(T) and counterpoise corrections were employed to suppress basis set superposition errors.

these observations, we further studied the kinetics of the releasing reaction after formation of the aqua complexes (6 h in water/DMF at 37°C). As expected, activation of the platinum salts significantly accelerated the turn-on half-time from $t_{1/2} = 171 \text{ min}$ to $t_{1/2} = 30 \text{ min}$ for K_2PtCl_4 and from $t_{1/2} = 276 \text{ min}$ to $t_{1/2} = 60 \text{ min}$ for “CisPt” (Figure 2c and Table S1). Accordingly, if the reaction was performed in pure DMF, then formation of the decaged probe was not observed (50 equiv of K_2PtCl_4 or CisPt for 14 h at 37°C). This result is in agreement with previous LC–MS studies that suggested the requirement of water to generate the active catalyst. The activation of metal chloride in aqueous solvents has few precedents but has been reported for gold complexes.⁵⁸ This effect is explained by facilitated ionization of the M–Cl bonds in water.⁵⁸

In terms of catalytic activity, the reaction of 7 with 0.3 equiv of activated K_2PtCl_4 complex yielded decaged probe 8 in 98% yield after 72 h at 37°C (catalyst turnover number 3.3). Upon moving to 2 equiv of the metal complex, the decaged product was obtained in quantitative yield after 4 h at 37°C (Figure S14). As a comparison, the same study was performed with $\text{Pd}(\text{OAc})_2$, a standard palladium complex for *N*-depropargylation.⁵⁹ Interestingly, the Pd-reaction proceeded with

comparable efficiency, although with slightly better rates of conversion (>98% yield in 1 h, LC–MS analysis). Of relevance, palladium decaging of alkyne amides has never been reported before. Finally, the compatibility and efficiency of the reactions were tested under physiological conditions. The activated aqua complexes were first shown to persist in complete DMEM cell media for at least 16 h at 37°C , as assessed by LC–MS analysis, although a significant decrease in their concentration was observed over time (Figure S15). Later, the reactions were shown to proceed in cell media with conversions of 69% for K_2PtCl_4 (50 equiv) and 17% for CisPt (150 equiv) after 14 h at 37°C (Figures S16 and S17). Similarly, the reaction was also trialed in high salt concentration buffers with high efficiency ($t_{1/2} = 36 \text{ min}$ for 50 equiv of K_2PtCl_4 and $t_{1/2} = 105 \text{ min}$ for 100 equiv of CisPt, 37°C in E3 medium, Figures S18 and S19).

Having found an efficient platinum complex for decaging pentynoyl tertiary amides, we turned our attention to the determination of the rate constant of the reaction (Figure 2d). By fitting the appearance of 8 in the presence of increasing amounts of metal complexes and by using pseudo-first order conditions, the reactions were found to have second order rate constants of $0.230 \pm 0.004 \text{ M}^{-1} \text{ s}^{-1}$ for K_2PtCl_4 and $0.080 \pm$

0.002 M⁻¹ s⁻¹ for CisPt (Figure 2d). These reaction rates are similar to those reported for other metal-assisted decaging reactions.²⁷

To determine the nature of active species involved in the decaging reaction, we performed kinetic experiments with carbon disulfide (Figure 2e, Table S2). CS₂ acts as a catalyst poison for homogeneous and heterogeneous Pt(0) reactions, although Pt(II) species are unaffected. As seen in Figure 2e, the reaction rates are similar to those with or without CS₂. This result can be attributed to the noninvolvement of Pt(0) species in the reaction. However, the reaction rates were significantly affected by the addition of ethylenediamine tetraacetic acid (EDTA; Figure 2e), possibly due the participation of Pt(II) in the reaction.

We also performed computational studies to help understand the reaction mechanism (Figure 2f). These studies suggest that the most probable operating reaction pathway of substrate **4a** is a stepwise process involving the coordination of substrate molecule to Pt(II), followed by an intramolecular attack of the carbonyl oxygen of the Pt-coordinated substrate (CS₀) to the pentynoyl moiety, which gives five-membered ring intermediate CP. Different pathways to decomposition of CP were explored (Figure S20); the lowest energy one was the hydration of CP leading to formation of intermediate **Q₁**, which readily decomposes to liberate free amine **6a**. The metal complex is then recovered in a subsequent step by hydrolysis of **5** (Figure 2f). The complete calculation for the first reaction turnover of the main mechanism is depicted in Figure S21 and SI Movie. This mechanism is further supported by the identification of intermediate species CS₀ by LC-MS (Figures S22–S26). The main difference observed for the reaction with substrate **3a** relative to **4a** was the higher free energy of activation ($\Delta\Delta G^\ddagger = 2.75$ kcal mol⁻¹) for the intramolecular attack of the carbonyl oxygen at the pentynoyl moiety. However, both substrates share the same energy barrier for hydration of CP and release of **6a** (Figure S21).

Extending the Decaging Reaction to *N*-Propargyl Group. Following the discovery of a platinum-cleavable group, we hoped to extend the scope of handles that could be used for decaging. Metal-mediated decaging of *N*-propargyl handles has been widely explored to modulate the cytotoxic activity of antineoplastic drugs in a controlled manner.^{22,25} On this basis, we investigated the possibility of using *N*-propargyl groups introduced on drugs of interest for prodrug activation using platinum triggers. First, and similarly to the pentynoyl amide reaction, an *N*-propargyl group was used to protect a secondary amine on a naphthalimide derivative to generate fluorogenic probe **9** (Figure 2a). As described above, we tested the reactivity of K₂PtCl₄ and CisPt before and after formation of the aqua complexes (6 h incubation at 37 °C in DMF/water). Once again, dissociation of the chloride anions in water was found to be crucial for triggering the reactivity of platinum complexes. Indeed, we found that reactions with aqua complexes are faster according to the calculated half-time for the “fluorescent reactions” (from $t_{1/2} = 200 \pm 3$ min to $t_{1/2} = 27 \pm 3$ min for K₂PtCl₄ and from $t_{1/2} = 628 \pm 51$ min to $t_{1/2} = 303 \pm 34$ min for CisPt; Table S3). The fluorescence-based assay was also employed to calculate the second-order rate constant for the reaction. Accordingly, the calculated rate constant was 0.120 ± 0.001 M⁻¹ s⁻¹ for K₂PtCl₄ and 0.0160 ± 0.0004 M⁻¹ s⁻¹ for CisPt (Figure S27). These results show that *N*-propargyls decay slower than pentynoyl amides. As a reference, the same study was performed with palladium

complex Pd(OAc)₂, which behaved slightly better than the platinum salts, to promote formation of **10** with a second-order rate constant of 0.39 ± 0.015 M⁻¹ s⁻¹ (Figure S28). The reaction was also subjected to CS₂ and EDTA poisoning. CS₂ had no effect but EDTA completely inhibited the reaction, which indicates the participation of Pt(II) species (Figure S29 and Table S4). On the basis of these results and LC-MS analysis after 2 h of reaction between K₂PtCl₄ and probe **9** (Figure S30), we propose that the first turnover of the reaction proceeds as recently disclosed for palladium depropargylation,⁵⁹ i.e., (i) co-ordination of Pt(II) to alkyne moiety, (ii) attack of a H₂O molecule at the propargyl terminal carbon to form an enol, (iii) tautomerization to a more stable Pt-aldehyde complex, and (iv) C–N bond cleavage by either hydrolysis or β -N elimination followed by hydration of Pt-complex (Figure S31). Finally, we investigated the ability of platinum salts to remove the propargyl protecting group in cells (DMEM) and zebrafish (E3) media. The reaction with the fluorogenic probe was monitored for K₂PtCl₄ and CisPt for 14 h at 37 °C. Efficiencies in E3 media were generally high with the reaction complete in 60 and 150 min for K₂PtCl₄ and CisPt, respectively (Figure S32). In DMEM, cleavage was less efficient with conversion yields of 67% for K₂PtCl₄ (50 equiv) and 30% for CisPt (150 equiv) after 14 h at 37 °C (Figure S33).

Platinum-Mediated Decaging in Living Cells. To verify whether platinum-mediated depropargylation would function in cell culture, a pentynoyl amide derivative of antineoplastic drug MMAE was synthesized. MMAE is the drug present in the ADC brentuximab vedotin that is in clinical use to treat patients with relapsed Hodgkin lymphoma and systemic anaplastic large-cell lymphoma,⁶⁰ and remains the drug of choice for antibody-targeted therapies. In addition, a *N*-propargyl 5-fluorouracil (pFU) derivative was also tested, which was found to be efficiently decaged and activated with gold nanoparticles³¹ and palladium complexes.²⁵ When MMAE-am was treated in DMF/water (1:1) for 4 h with 10 equiv of K₂PtCl₄, complete consumption of MMAE-am was seen by LC-MS with 37% release of MMAE along with the formation of the intermediate **Q_s** (Figures S20 and S34). In a similar fashion, decaging of pFU proceeds with yields of $46\% \pm 2$ and $72\% \pm 2$ for K₂PtCl₄ and CisPt, after 14 h reaction with 2 equiv, at room temperature and 37 °C, respectively (Figures S35–S37). These prodrugs (MMAE-am **11** and pFU **12**, see the SI for synthetic details) were reacted with platinum salts in cell culture in the hope of observing a “turn-on” of toxicity. Unfortunately, the chemotherapeutic CisPt has a narrow window of nontoxic concentrations for efficient decaging in cells.⁶¹ Indeed, CisPt was demonstrated to be toxic in HeLa cells at concentrations as low as 2.5 μ M (Figure S38). On the contrary, platinum salts K₂PtCl₄ and K₂PtCl₆ did not significantly influence the viability of HeLa cells at concentrations below 50 μ M (Figure S38). With both prodrugs, an increase of about 2-fold in toxicity could be observed for some of the tested concentrations when reacted with K₂PtCl₄ over 3 days in cell culture (Figure 3a and 3b; e.g., 1 nM of MMAE-am and 50 μ M of pFU). In contrast, no decrease of cytotoxicity was observed in cells treated independently with cFU **13**, a non-decaging control derivative, or in combination with K₂PtCl₄ (Figure 3b). These control studies indicate that 5-FU was not generated because the alkyl handle does not undergo decaging by K₂PtCl₄.

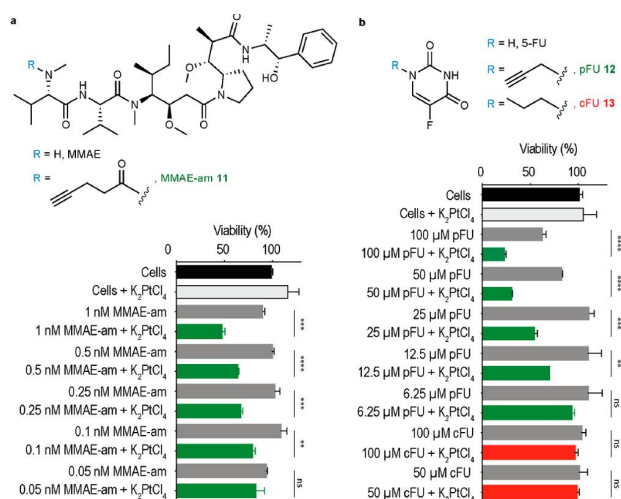


Figure 3. Platinum-mediated decaging in cells. HeLa cells were incubated with different concentrations of MMAE-am 11a or pFU 12b for 3 days with or without K₂PtCl₄ (20 μM, twice a day). Compound 13, a nondecaging alkyl-FU derivative, was used as a negative control. Toxicity was determined by AlamarBlue assay. Error bars represent \pm s.d. ($n = 3$). Each experiment was repeated three times. The statistical significance of the differences between groups was evaluated with the unpaired t test. Statistical results: ns > 0.05, ** $P \leq 0.01$, *** $P \leq 0.001$ and **** $P \leq 0.0001$.

It is important to note that for both prodrugs the addition of K₂PtCl₄ did not restore their toxicity to the level observed for unmodified MMAE and 5-FU drugs (Figures S39 and S40). Although a 2-fold increase in toxicity for the prodrug activation may look modest, it is important to mention that this is considered relevant given the slow reaction rates possible at the low concentration of K₂PtCl₄ complex tolerated by cells. Indeed, this low reagent concentration was necessary to ensure the platinum complex remained nontoxic. On top of this, in vitro studies with probes 7 and 9 revealed that the presence of nucleophiles (e.g., glutathione) ends in lower conversions into the corresponding decaged products. It should be noted, however, that even in the presence of high concentrations of glutathione (e.g., 1.5 mM) the reaction still proceeds with moderate rates ($t_{1/2} = 197$ min for 7 + K₂PtCl₄; $t_{1/2} = 246$ min for 9 + K₂PtCl₄; Table S5). Regarding CisPt, we found that the reaction is more susceptible to the presence of nucleophiles (e.g., $t_{1/2} = 921$ min for 7 + CisPt in the presence of 0.5 mM of glutathione; Table S6). This deactivation of the metals in the presence of nucleophiles is in line with the modest decaging yields observed in the cell studies. This is an issue that could be further improved, for example, by using platinum-based nanoparticles known to have reduced toxicity and higher payload concentrations or by using platinum complexes stabilized with different organic ligands in a way to optimize the metal reactivity.⁶² Our data, however, demonstrate that decaging reactions with platinum complexes are possible in cell culture and could achieve release of sufficient amounts of the active drug in cells to induce cell death.

Platinum Decaging of ADC. Next, we decided to extend the tertiary amide caging group for chemically controlled drug-release from an ADC. The caging group of MMAE-am 11 was adapted for this purpose because MMAE is a common payload in ADC design.⁵⁰ Ideally a CisPt-cleavable ADC would be stable to cleavage by endogenous extra- or intracellular

conditions. For this reason, we decided to use a carbonyl acrylic bioconjugation handle^{63,64} coupled to MMAE for antibody modification (Figure 4a; SI for synthesis).

To test the susceptibility of the conjugating linker to platinum decaging, compound 14 and K₂PtCl₄ (10 equiv) were incubated in DMF/water (1:1) at 37 °C for 18 h and analyzed by LC–MS (Figure S41). Release of MMAE was observed with complete consumption of 14 along with two potential

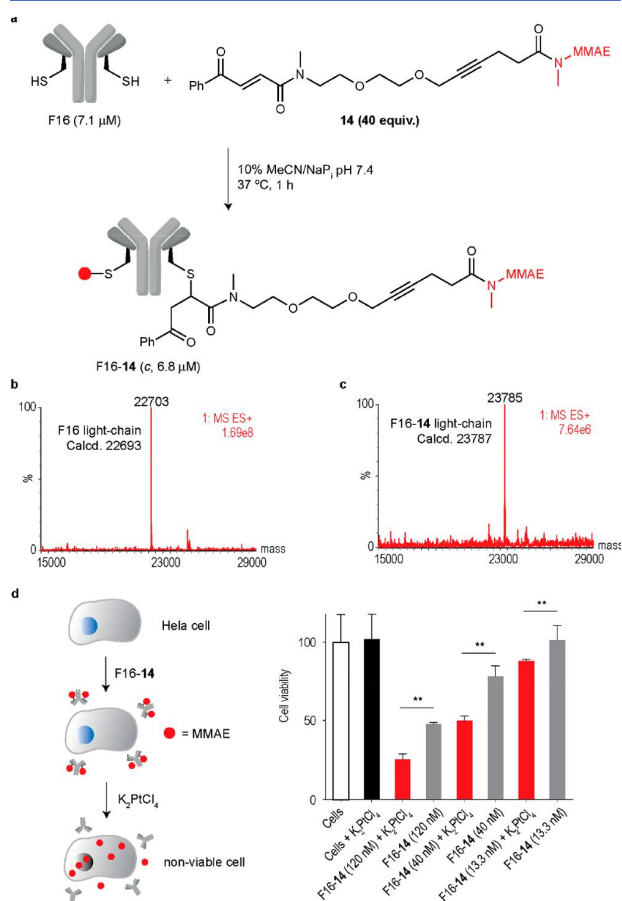


Figure 4. Platinum-mediated drug decaging from a noninternalizing ADC. a. Cysteine-selective and irreversible modification of the noninternalizing antibody F16 (anti tenascin-C) in IgG format with MMAE conjugating linker 14. IgG(F16) contains a single reactive cysteine at the C-terminal extremity of the light chain ideal for cysteine-specific modification. Briefly, a solution of F16 (7.1 μM) in sodium phosphate buffer (NaP_i) pH 7.4 was treated with 14 (40 equiv) in MeCN to a final concentration of 10% v/v. The reaction was heated to 37 °C for 1 h, and reaction progress was monitored by LC–MS. The ADC was purified by dialysis into fresh NaP_i buffer pH 7.4 with a 10 kDa MWCO overnight. b. Deconvoluted ESI–MS mass spectrum of the light-chain of F16. c. Deconvoluted ESI–MS mass spectrum of the light-chain of F16-14 that shows an exact drug-to-light-chain ratio of 1. d. Schematic of the platinum-mediated decaging of MMAE from a noninternalizing ADC. e. Cell viability of HeLa cells after treatment with F16-14 and subsequent decaging efficiency upon treatment with 20 μM K₂PtCl₄, twice daily. Cell viability was measured at day 3 by using AlamarBlue reagent. The statistical significance of the differences between groups was evaluated by using the unpaired t test. A p value < 0.05 (***) was considered statistically significant. Error bars represent \pm s.d. ($n = 3$). Experiments were performed three times.

intermediates (Figure S41). We then went on and selected the noninternalizing F16 antibody for modification, which is specific to the alternatively spliced A1 domain of tenascin-C, found overexpressed in most solid tumors.⁶⁵ A noninternalizing ADC ensures that as little ADC as possible will be metabolized by the cells and that the maximum possible drug release is due to extracellular decaging with platinum complexes. Site-selective conjugation is expected to occur at the engineered cysteine residues in each light-chain of F16 enabling the construction of a chemically defined ADC. Furthermore, the newly formed C–S bond between the linker and the antibody is stable and does not undergo thiol-exchange reactions as in the case of frequently used maleimides.^{63,64} Complete conversion to a homogeneous ADC was achieved after reaction of F16 for 1 h at 37 °C with the carbonyl acrylic MMAE drug linker 14 in sodium phosphate buffer pH 7.4 as assessed by LC–MS (Figure 4b,c). Importantly, the heavy chain remained unmodified as expected considering the absence of reactive cysteines in the structure (Figures S42 and S43). Next, we performed the decaging in cells to release MMAE from the ADC (Figure 4d). With a cancer cell line (HeLa cells) as a model, we found F16–14 to be more toxic to cells at submicromolar concentrations in the presence of nontoxic amounts of the platinum complex K₂PtCl₄ (Figure 4d). This tertiary amide decaging reaction should stimulate platinum-mediated MMAE delivery from antibodies in the context of targeted cancer therapeutics. Furthermore, a small model protein (ubiquitin-K63C) engineered with a single cysteine residue⁶⁶ was modified with linker 14 for ease of analysis by LC–MS. When attempting decaging in vitro with CisPt, loss of MMAE followed by further degradation of the linker could be observed by LC–MS, which provides further evidence for the efficient release of the secondary amine drug from the protected tertiary amide protected conjugate (Figures S44–S47).

Cisplatin-Mediated Prodrug Decaging in Vivo. To test the in vivo efficacy of pFU and its combinatorial effect with CisPt, we used the zebrafish larvae xenograft model.⁶⁷ This model is a fast in vivo platform with resolution to analyze crucial hallmarks of cancer, such as metastatic and angiogenic potentials but it is also highly sensitive to discriminate differential anticancer therapy responses with single-cell resolution.^{68–71} We first attempted to visualize the CisPt reaction by decaging fluorogenic probe 9 in larval zebrafish (Figure 5). This probe shows an increase in fluorescence of 22-fold upon removal of the propargyl group (Figure S48). For in vivo imaging, a set of zebrafish larvae were incubated with probe 9 for 24 h, washed for 1 h in embryonic medium and

then further incubated with dimethyl sulfoxide (DMSO) or CisPt for 24 h (Figure 5a). Probe 9 and CisPt were used at the highest nontoxic concentration to the zebrafish embryos (9, 1 μM; CisPt, 34 μM; Figure S49). As shown in Figure 5b, the control group displays nearly no background fluorescence, but the CisPt-treated group showed an increased fluorescence (Figure 5c). This implies that probe 9 and CisPt are tissue-permeable and capable of reacting in vivo.

Before measuring efficacy of CisPt deprotection, we assessed the maximum tolerated concentration for each compound: pFU 12, cFU 13, CisPt, pFU + CisPt, and cFU + CisPt in nontumor zebrafish larvae (Figure S49). Next, colorectal cancer (CRC) HCT116 zebrafish xenografts were generated as previously described.⁶⁷ Briefly, 24 h post injection (hpi), xenografts were randomly distributed into different treatments: DMSO (control), pFU (1.65 mM), cFU (1.65 mM), CisPt (0.034 mM), pFU + CisPt (1.65 mM + 0.034 mM), and cFU + CisPt (1.65 mM + 0.034 mM). Xenografts were analyzed at 4, 6, and 7 days post injection (dpi), i.e., 3, 5, and 6 days post treatment (dpt), respectively (Figure 6). At 3dpt (4dpi) (Figure 6 I), in the single treatments with pFU or CisPt, we could not observe any significant reduction of mitotic index (Figure 6 I, m), induction of apoptosis (activated caspase 3, Figure 6 I, n) or reduction of tumor size (Figure 6 I, o). In contrast, the combinatorial treatment—pFU + CisPt—induced a significant antitumoral synergistic effect manifested by a ~2 fold increase in apoptosis (Figure 6 I, n; DMSO versus pFU + CisPt ***P* = 0.0033; pFU versus pFU + CisPt ****P* = 0.0006) accompanied by 25% reduction of tumor size (Figure 6 I, o; DMSO versus pFU + CisPt **P* = 0.0279; Figure 6 I, a versus d). However, if the duration of the treatment is increased 2 (Figure 6 II) or 3 (Figure 6 III) additional days, then we could detect some toxicity in single treatment (Figure 6 II, p–r; Figure 6 III, s–u). Nevertheless, the combination of pFU with CisPt induced a clear pronounced antitumor synergistic effect. At 5 dpt (6 dpi), the combinatorial treatment led to a reduction of proliferation (Figure 6 II, p; DMSO versus pFU + CisPt *****P* < 0.0001; pFU versus pFU + CisPt **P* = 0.0104), a ~4 fold increase in cell death by apoptosis (Figure 6 II, q; DMSO versus pFU + CisPt *****P* < 0.0001; pFU versus pFU + CisPt *****P* < 0.0001) and a ~38% reduction of tumor size (Figure 6 II, r; DMSO versus pFU + CisPt *****P* < 0.0001; Figure 6 II, e versus h). Finally, the 6 days of treatment (7 dpi) culminates in a ~45% tumor shrinkage (Figure 6 III, u; DMSO versus pFU + CisPt ***P* = 0.0010; Figure 6 III, i versus l).

Importantly, by comparing the combined treatment of the nondecaging compound cFU with CisPt to the prodrug pFU with CisPt, it is clear that pFU was able to induce a more significant cytostatic (block proliferation) and cytotoxic effect (apoptosis and reduction of tumor size) than the control cFU at both 5 dpf (6 dpi) and 6 dpt (7 dpi; Figures S50 and S51). Also, the combined effect of pFU + CisPt was more pronounced than the combination of 5-FU + CisPt, regarding proliferation (DMSO versus pFU + CisPt *****P* < 0.0001; DMSO versus FU + CisPt **P* = 0.0104; Figure S50i) and tumor size (DMSO versus pFU + CisPt *****P* < 0.0001; DMSO versus FU + CisPt **P* = 0.0273; Figure S50k). This might be related with the increased permeability of pFU (versus FU), which results in a more efficient intracellular delivery of FU after Pt decaging. In conclusion, our results show the efficient activation of the anticancer pFU in the

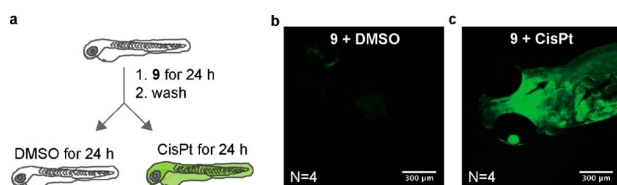


Figure 5. CisPt Decages the Fluorogenic Probe 9 in vivo. Zebrafish larvae were exposed to 9 diluted in embryonic medium for 24 h, followed by a 1 h wash in embryonic medium. Larvae were randomly distributed into two conditions: DMSO or CisPt for 24 h (a). Confocal image of zebrafish larvae exposed to 9 + DMSO (b) and 9 + CisPt (c).

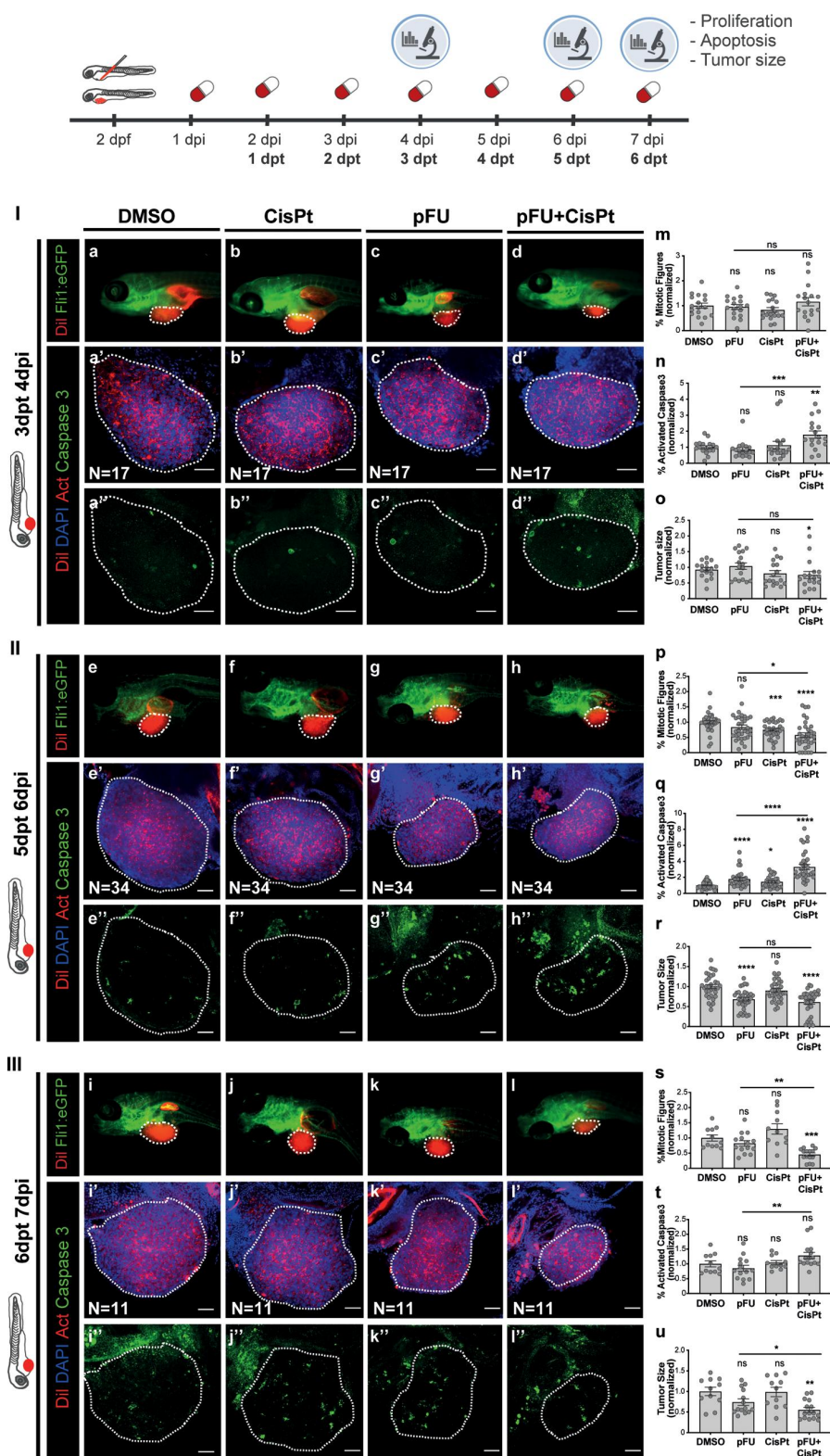


Figure 6. CisPt-mediated prodrug decaying in zebrafish xenografts. HCT116 human CRC cells were fluorescently labeled with lipophilic CM-Dii1 (shown in red) and injected into the perivitelline space (PVS) 2 days post fertilization (dpf) *Tg(Fli1:eGFP)* zebrafish larvae. Zebrafish xenografts were randomly distributed into treatment groups, daily treated with DMSO, CisPt, pFU, and pFU+CisPt and analyzed at 4, 6, or 7dpi for proliferation, apoptosis and tumor size. At 4 dpi, 6 dpi, and 7dpi, zebrafish xenografts were imaged by stereoscope (a–l) and by confocal microscopy (a'–l' DAPI plus DiI, a''–l'' maximum projection of activated caspase 3). Proliferation (mitotic figures: m; p, * $P = 0.0104$, *** $P = 0.0004$, **** $P < 0.0001$; s, ** $P = 0.0023$, *** $P = 0.0002$), apoptosis (activated caspase 3: n, ** $P = 0.0033$, *** $P = 0.0006$; q, * $P = 0.0126$, **** $P < 0.0001$; t, ** $P = 0.0068$) and tumor size (n° of tumor cells: o, * $P = 0.0279$; r, **** $P < 0.0001$; u, * $P = 0.0411$, ** $P = 0.0010$) were analyzed and

Figure 6. continued

quantified. Graphs represent fold induction (normalized values to controls) of $\text{Avg} \pm \text{SEM}$. The number of xenografts analyzed is indicated in the representative images and each dot represents one zebrafish xenograft. Statistical analysis was performed using an unpaired test. Statistical results: ns > 0.05, * $P \leq 0.05$, ** $P \leq 0.01$, *** $P \leq 0.001$, and **** $P \leq 0.0001$. All images are anterior to the left, posterior to right, dorsal up, and ventral down. Scale bar 50 μm .

presence of nontherapeutic amounts of the anticancer drug CisPt in an in vivo setting.

CONCLUSIONS

In summary, we present a new decaging reaction of alkynes with platinum complexes for the release of secondary amines from otherwise stable tertiary amides, both in mammalian cell culture and in living organisms. This reaction was shown to proceed by platinum-mediated intramolecular cyclization mechanism. Our data suggest that water, a necessary solvent in chemical biology applications, is working as a metal-activating agent. Molecular electronic structure calculations further corroborated the mechanism of the reaction which was also supported by LC–MS characterization of the intermediates. The reaction can proceed catalytically under certain conditions and was later extended to *N*-propargyl groups with comparable efficacies to that of palladium-mediated depropargylation. The caging group was adapted for the synthesis of a noninternalizing ADC, which results in drug release upon treatment with platinum complexes in cancer cells. The reaction was also adapted and demonstrated to function in a colorectal cancer zebrafish xenograft model with nontoxic amounts of CisPt to activate a prodrug of anticancer agent 5-FU, which led to a significant tumor reduction in vivo.

The work disclosed here represents a significant addition to the toolbox of decaging strategies for chemical biology applications. Indeed, the platinum-mediated cleavable reaction can be accomplished in aqueous systems having high concentrations of salts with high yields and reaction rates, similar to those observed for the standard palladium decaging metal. The reaction is, however, susceptible to the presence of nucleophiles resulting in slower rates (~6–15 times slower). We further demonstrate the compatibility of the reaction in cellular environments. Although the reaction is suitable for drug activation on cells inducing cytotoxicity, the presence of a range of biomolecules/nucleophiles significantly reduces the overall yield. These results are suggestive of instability of the Pt complexes, probably by formation of bioinorganic complexes. Although the active aqua Pt species have a limited lifetime in cell media, they persist long enough to be partially effective.

Our work was conceived on the hypothesis that platinum complexes could be used for prodrug activation on tumors during CisPt chemotherapy. The instability of the platinum complexes in physiological/biological conditions preclude the application envisioned. Further studies are needed to obtain Pt complexes compatible for such in vivo applications, but these results set the stage for future developments on platinum-mediated decaging reactions.

ASSOCIATED CONTENT

Supporting Information

The Supporting Information is available free of charge at <https://pubs.acs.org/doi/10.1021/jacs.0c01622>.

Detailed methods, characterization data and additional figures (PDF)

Movie with metadynamics calculations (MOV)

AUTHOR INFORMATION

Corresponding Authors

Gonçalo J. L. Bernardes — Department of Chemistry, University of Cambridge, Cambridge CB2 1EW, United Kingdom; Instituto de Medicina Molecular, Faculdade de Medicina, Universidade de Lisboa, 1649-028 Lisboa, Portugal; orcid.org/0000-0001-6594-8917; Email: gb453@cam.ac.uk

Rita Fior — Champalimaud Centre for the Unknown, Champalimaud Foundation, 1400-038 Lisboa, Portugal; Email: rita.fior@research.fchampalimaud.org

Bruno L. Oliveira — Department of Chemistry, University of Cambridge, Cambridge CB2 1EW, United Kingdom; Instituto de Medicina Molecular, Faculdade de Medicina, Universidade de Lisboa, 1649-028 Lisboa, Portugal; Email: bruno.oliveira@medicina.ulisboa.pt

Authors

Benjamin J. Stenton — Department of Chemistry, University of Cambridge, Cambridge CB2 1EW, United Kingdom

V. B. Unnikrishnan — Department of Chemistry, University of Cambridge, Cambridge CB2 1EW, United Kingdom

Cátia Rebelo de Almeida — Champalimaud Centre for the Unknown, Champalimaud Foundation, 1400-038 Lisboa, Portugal

João Conde — Instituto de Medicina Molecular, Faculdade de Medicina, Universidade de Lisboa, 1649-028 Lisboa, Portugal; orcid.org/0000-0001-8422-6792

Magda Negrão — Champalimaud Centre for the Unknown, Champalimaud Foundation, 1400-038 Lisboa, Portugal

Felipe S. S. Schneider — Department of Chemistry, Federal University of Santa Catarina—UFSC, Florianópolis, Santa Catarina 88040-900, Brazil; orcid.org/0000-0001-8090-2976

Carlos Cordeiro — Laboratório de FT-ICR e Espectrometria de Massa Estrutural, Faculdade de Ciências da Universidade de Lisboa, Campo-Grande 1749-016, Lisboa, Portugal

Miguel Godinho Ferreira — Champalimaud Centre for the Unknown, Champalimaud Foundation, 1400-038 Lisboa, Portugal; Institute for Research on Cancer and Aging of Nice (IRCAN), Université Côte d'Azur, UMR7284 U1081 UNS, 06107 Nice, France

Giovanni F. Caramori — Department of Chemistry, Federal University of Santa Catarina—UFSC, Florianópolis, Santa Catarina 88040-900, Brazil; orcid.org/0000-0002-6455-7831

Josiel B. Domingos — Department of Chemistry, Federal University of Santa Catarina—UFSC, Florianópolis, Santa Catarina 88040-900, Brazil; orcid.org/0000-0002-6001-4522

Complete contact information is available at <https://pubs.acs.org/10.1021/jacs.0c01622>

Author Contributions

[†]These authors contributed equally to this work.

Notes

The authors declare no competing financial interest.

ACKNOWLEDGMENTS

This project has received funding from the European Union's Horizon 2020 research and innovation programme under the Marie Skłodowska-Curie grant agreement Nos 675007 and 702574. We also thank the EPSRC (doctoral studentship to B.S.), FCT Portugal (FCT Investigator to G.J.L.B., IF/00624/2015; FCT Stimulus to B.L.O., CEECIND/02335/2017; LISBOA-01-0145-FEDER-022170 and FCT-PTDC/MEC-ONC/31627/2017 to R.F.), CNPq (PhD scholarship to F.S.S.S., 140485/2017-1; research grant to G.F.C., 311963/2017-0), the Champalimaud Foundation and Congento (R.F.), H2020 (EU_FT-ICR_MS, GA 731077, C.C.) and CAPES (Print call 88887.310560-00 to J.B.D. and G.J.L.B.) for funding. We also thank Prof. Dario Neri's laboratory for the generous gift of F16 antibody, Dr Ester Jiménez-Moreno for providing ubiquitin, the Champalimaud Fish and Rodents Facility for their excellent animal care, the Portuguese Mass Spectrometry Network (LISBOA-01-0145- FEDER-022125), SeTIC/UFSC, special staff members (Bruno Amattos, Guilherme Arthur Geronimo and Stephanie Andreon) for supercomputing resources, infrastructure and assistance, and Dr Vikki Cantrill for her help with the editing of this manuscript. G.J.L.B. is a Royal Society University Research Fellow (URF\R\180019) and the recipient of a European Research Council Starting Grant (TagIt, GA 676832).

REFERENCES

- (1) Hanahan, D.; Weinberg, R. A. Hallmarks of cancer: the next generation. *Cell* **2011**, *144* (5), 646–674.
- (2) Beck, A.; Goetsch, L.; Dumontet, C.; Corvaia, N. Strategies and challenges for the next generation of antibody-drug conjugates. *Nat. Rev. Drug Discovery* **2017**, *16* (5), 315–337.
- (3) Chudasama, V.; Maruani, A.; Caddick, S. Recent advances in the construction of antibody-drug conjugates. *Nat. Chem.* **2016**, *8* (2), 114–119.
- (4) Caculitan, N. G.; dela Cruz Chuh, J.; Ma, Y.; Zhang, D.; Kozak, K. R.; Liu, Y.; Pillow, T. H.; Sadowsky, J.; Cheung, T. K.; Phung, Q.; Haley, B.; Lee, B.-C.; Akita, R. W.; Sliwkowski, M. X.; Polson, A. G. Cathepsin B Is Dispensable for Cellular Processing of Cathepsin B-Cleavable Antibody-Drug Conjugates. *Cancer Res.* **2017**, *77* (24), 7027–7037.
- (5) Dorywalska, M.; Dushin, R.; Moine, L.; Farias, S. E.; Zhou, D.; Navaratnam, T.; Lui, V.; Hasa-Moreno, A.; Casas, M. G.; Tran, T.-T.; et al. Molecular Basis of Valine-Citrulline-PABC Linker Instability in Site-Specific ADCs and Its Mitigation by Linker Design. *Mol. Cancer Ther.* **2016**, *15* (5), 958–970.
- (6) Rodrigues, T.; Bernardes, G. J. L. Development of Antibody-Directed Therapies: Quo Vadis? *Angew. Chem., Int. Ed.* **2018**, *57* (8), 2032–2034.
- (7) Bargh, J. D.; Isidro-Llobet, A.; Parker, J. S.; Spring, D. R. Cleavable linkers in antibody-drug conjugates. *Chem. Soc. Rev.* **2019**, *48* (16), 4361–4374.
- (8) Li, J.; Chen, P. R. Development and application of bond cleavage reactions in bioorthogonal chemistry. *Nat. Chem. Biol.* **2016**, *12* (3), 129–137.
- (9) Rossin, R.; van Duijnhoven, S. M.; Ten Hoeve, W.; Janssen, H. M.; Kleijn, L. H.; Hoeben, F. J.; Versteegen, R. M.; Robillard, M. S. Triggered Drug Release from an Antibody-Drug Conjugate Using Fast "Click-to-Release" Chemistry in Mice. *Bioconjugate Chem.* **2016**, *27* (7), 1697–1706.

- (10) Rossin, R.; Versteegen, R. M.; Wu, J.; Khasanov, A.; Wessels, H. J.; Steenberg, E. J.; Ten Hoeve, W.; Janssen, H. M.; van Onzen, A.; Hudson, P. J.; et al. Chemically triggered drug release from an antibody-drug conjugate leads to potent antitumour activity in mice. *Nat. Commun.* **2018**, *9* (1), 1484.
- (11) Oliveira, B. L.; Guo, Z.; Bernardes, G. J. L. Inverse electron demand Diels-Alder reactions in chemical biology. *Chem. Soc. Rev.* **2017**, *46* (16), 4895–4950.
- (12) Mondal, M.; Liao, R.; Xiao, L.; Eno, T.; Guo, J. Highly Multiplexed Single-Cell In Situ Protein Analysis with Cleavable Fluorescent Antibodies. *Angew. Chem., Int. Ed.* **2017**, *56* (10), 2636–2639.
- (13) Nani, R. R.; Gorka, A. P.; Nagaya, T.; Kobayashi, H.; Schnermann, M. J. Near-IR Light-Mediated Cleavage of Antibody-Drug Conjugates Using Cyanine Photocages. *Angew. Chem., Int. Ed.* **2015**, *54* (46), 13635–13638.
- (14) Ji, X.; Pan, Z.; Yu, B.; De La Cruz, L. K.; Zheng, Y.; Ke, B.; Wang, B. Click and release: bioorthogonal approaches to "on-demand" activation of prodrugs. *Chem. Soc. Rev.* **2019**, *48* (4), 1077–1094.
- (15) Davies, S.; Stenton, B. J.; Bernardes, G. J. L. Bioorthogonal Decaging Reactions for Targeted Drug Activation. *Chimia* **2018**, *72* (11), 771–776.
- (16) Zhang, D. A.-O.; Dragovich, P. S.; Yu, S. F.; Ma, Y.; Pillow, T. H.; Sadowsky, J. D.; Su, D.; Wang, W.; Polson, A.; Khojasteh, S. C.; Hop, C. Exposure-Efficacy Analysis of Antibody-Drug Conjugates Delivering an Excessive Level of Payload to Tissues. *Drug Metab. Dispos.* **2019**, *47* (10), 1146–1155.
- (17) Durbin, K. R.; Phipps, C.; Liao, X. Mechanistic Modeling of Antibody-Drug Conjugate Internalization at the Cellular Level Reveals Inefficient Processing Steps. *Mol. Cancer Ther.* **2018**, *17* (6), 1341–1351.
- (18) Yang, M.; Li, J.; Chen, P. R. Transition metal-mediated bioorthogonal protein chemistry in living cells. *Chem. Soc. Rev.* **2014**, *43* (18), 6511–6526.
- (19) Soldevila-Barreda, J. J.; Metzler-Nolte, N. Intracellular Catalysis with Selected Metal Complexes and Metallic Nanoparticles: Advances toward the Development of Catalytic Metallodrugs. *Chem. Rev.* **2019**, *119* (2), 829–869.
- (20) Völker, T.; Meggers, E. Transition-metal-mediated uncaging in living human cells—an emerging alternative to photolabile protecting groups. *Curr. Opin. Chem. Biol.* **2015**, *25*, 48–54.
- (21) Miller, M. A.; Askevold, B.; Mikula, H.; Kohler, R. H.; Pirovich, D.; Weissleder, R. Nano-palladium is a cellular catalyst for in vivo chemistry. *Nat. Commun.* **2017**, *8* (1), 15906.
- (22) Yusop, R. M.; Unciti-Broceta, A.; Johansson, E. M.; Sanchez-Martin, R. M.; Bradley, M. Palladium-mediated intracellular chemistry. *Nat. Chem.* **2011**, *3* (3), 239–243.
- (23) Martinez-Calvo, M.; Couceiro, J. R.; Destito, P.; Rodriguez, J.; Mosquera, J.; Mascarenas, J. L. Intracellular Deprotection Reactions Mediated by Palladium Complexes Equipped with Designed Phosphine Ligands. *ACS Catal.* **2018**, *8* (7), 6055–6061.
- (24) Bray, T. L.; Salji, M.; Brombin, A.; Perez-Lopez, A. M.; Rubio-Ruiz, B.; Galbraith, L. C. A.; Patton, E. E.; Leung, H. Y.; Unciti-Broceta, A. Bright insights into palladium-triggered local chemotherapy. *Chem. Sci.* **2018**, *9* (37), 7354–7361.
- (25) Weiss, J. T.; Dawson, J. C.; Macleod, K. G.; Rybski, W.; Fraser, C.; Torres-Sanchez, C.; Patton, E. E.; Bradley, M.; Carragher, N. O.; Unciti-Broceta, A. Extracellular palladium-catalysed dealkylation of 5-fluoro-1-propargyl-uracil as a bioorthogonally activated prodrug approach. *Nat. Commun.* **2014**, *5*, 3277.
- (26) Weiss, J. T.; Carragher, N. O.; Unciti-Broceta, A. Palladium-mediated dealkylation of N-propargyl-floxuridine as a bioorthogonal oxygen-independent prodrug strategy. *Sci. Rep.* **2015**, *5* (1), 9329.
- (27) Stenton, B. J.; Oliveira, B. L.; Matos, M. J.; Sinatra, L.; Bernardes, G. J. L. A thioether-directed palladium-cleavable linker for targeted bioorthogonal drug decaging. *Chem. Sci.* **2018**, *9* (17), 4185–4189.

- (28) Streu, C.; Meggers, E. Ruthenium-induced allylcarbamate cleavage in living cells. *Angew. Chem., Int. Ed.* **2006**, *45* (34), 5645–5648.
- (29) Volker, T.; Dempwolff, F.; Graumann, P. L.; Meggers, E. Progress towards bioorthogonal catalysis with organometallic compounds. *Angew. Chem., Int. Ed.* **2014**, *53* (39), 10536–10540.
- (30) Tomas-Gamasa, M.; Martinez-Calvo, M.; Couceiro, J. R.; Mascarenas, J. L. Transition metal catalysis in the mitochondria of living cells. *Nat. Commun.* **2016**, *7* (1), 12538.
- (31) Perez-Lopez, A. M.; Rubio-Ruiz, B.; Sebastian, V.; Hamilton, L.; Adam, C.; Bray, T. L.; Irusta, S.; Brennan, P. M.; Lloyd-Jones, G. C.; Sieger, D.; Santamaria, J.; Unciti-Broceta, A. Gold-Triggered Uncaging Chemistry in Living Systems. *Angew. Chem., Int. Ed.* **2017**, *56* (41), 12548–12552.
- (32) Tsubokura, K.; Vong, K. K.; Pradipta, A. R.; Ogura, A.; Urano, S.; Tahara, T.; Nozaki, S.; Onoe, H.; Nakao, Y.; Sibgatullina, R.; Kurbangalieva, A.; Watanabe, Y.; Tanaka, K. In Vivo Gold Complex Catalysis within Live Mice. *Angew. Chem., Int. Ed.* **2017**, *56* (13), 3579–3584.
- (33) Wang, X.; Liu, Y.; Fan, X.; Wang, J.; Ngai, W. S. C.; Zhang, H.; Li, J.; Zhang, G.; Lin, J.; Chen, P. R. Copper-Triggered Bioorthogonal Cleavage Reactions for Reversible Protein and Cell Surface Modifications. *J. Am. Chem. Soc.* **2019**, *141* (43), 17133–17141.
- (34) Labinger, J. A. Platinum-Catalyzed C–H Functionalization. *Chem. Rev.* **2017**, *117* (13), 8483–8496.
- (35) Basu, U.; Banik, B.; Wen, R.; Pathak, R. K.; Dhar, S. The Platinum series: activation, targeting, and delivery. *Dalton Trans.* **2016**, *45* (33), 12992–13004.
- (36) Johnstone, T. C.; Suntharalingam, K.; Lippard, S. J. The Next Generation of Platinum Drugs: Targeted Pt(II) Agents, Nanoparticle Delivery, and Pt(IV) Prodrugs. *Chem. Rev.* **2016**, *116* (5), 3436–3486.
- (37) Ivanov, A. I.; Christodoulou, J.; Parkinson, J. A.; Barnham, K. J.; Tucker, A.; Woodrow, J.; Sadler, P. J. Cisplatin binding sites on human albumin. *J. Biol. Chem.* **1998**, *273* (24), 14721–14730.
- (38) Florea, A.-M.; Büsselberg, D. Cisplatin as an anti-tumor drug: cellular mechanisms of activity, drug resistance and induced side effects. *Cancers* **2011**, *3* (1), 1351–1371.
- (39) Kenny, R. G.; Marmion, C. J. Toward Multi-Targeted Platinum and Ruthenium Drugs—A New Paradigm in Cancer Drug Treatment Regimens? *Chem. Rev.* **2019**, *119* (2), 1058–1137.
- (40) Dasari, S.; Tchounwou, P. B. Cisplatin in cancer therapy: molecular mechanisms of action. *Eur. J. Pharmacol.* **2014**, *740*, 364–378.
- (41) Stewart, D. J.; Molepo, J. M.; Green, R. M.; Montpetit, V. A.; Hugenholtz, H.; Lamothe, A.; Mikhael, N. Z.; Redmond, M. D.; Gadia, M.; Goel, R. Factors affecting platinum concentrations in human surgical tumour specimens after cisplatin. *Br. J. Cancer* **1995**, *71* (3), 598–604.
- (42) van Hennik, M. B.; van der Vijgh, W. J.; Klein, I.; Elferink, F.; Vermorken, J. B.; Winograd, B.; Pinedo, H. M. Comparative pharmacokinetics of cisplatin and three analogues in mice and humans. *Cancer Res.* **1987**, *47* (23), 6297–6301.
- (43) Jacobs, S.; McCully, C. L.; Murphy, R. F.; Bacher, J.; Balis, F. M.; Fox, E. Extracellular fluid concentrations of cisplatin, carboplatin, and oxaliplatin in brain, muscle, and blood measured using microdialysis in nonhuman primates. *Cancer Chemother. Pharmacol.* **2010**, *65* (5), 817–824.
- (44) Klein, A. V.; Hambley, T. W. Platinum Drug Distribution in Cancer Cells and Tumors. *Chem. Rev.* **2009**, *109* (10), 4911–4920.
- (45) Holding, J. D.; Lindup, W. E.; Bowdler, D. A.; Siodlak, M. Z.; Stell, P. M. Disposition and tumour concentrations of platinum in hypoalbuminaemic patients after treatment with cisplatin for cancer of the head and neck. *Br. J. Clin. Pharmacol.* **1991**, *32* (2), 173–179.
- (46) Pujol, J. L.; Cupissol, D.; Gestin-Boyer, C.; Bres, J.; Serrou, B.; Michel, F. B. Tumor-tissue and plasma concentrations of platinum during chemotherapy of non-small-cell lung cancer patients. *Cancer Chemother. Pharmacol.* **1990**, *27* (1), 72–75.
- (47) Del Monte, U. Does the cell number 10(9) still really fit one gram of tumor tissue? *Cell Cycle* **2009**, *8* (3), 505–506.
- (48) Abu Sohel, S. M.; Liu, R.-S. Carbocyclisation of alkynes with external nucleophiles catalysed by gold, platinum and other electrophilic metals. *Chem. Soc. Rev.* **2009**, *38* (8), 2269–2281.
- (49) Tomás-Mendivil, E.; Toullec, P. Y.; Díez, J.; Conejero, S.; Michelet, V.; Cadierno, V. Cycloisomerization versus Hydration Reactions in Aqueous Media: A Au(III)-NHC Catalyst That Makes the Difference. *Org. Lett.* **2012**, *14* (10), 2520–2523.
- (50) Belger, K.; Krause, N. Smaller, faster, better: modular synthesis of unsymmetrical ammonium salt-tagged NHC–gold(i) complexes and their application as recyclable catalysts in water. *Org. Biomol. Chem.* **2015**, *13* (31), 8556–8560.
- (51) Alemán, J.; del Solar, V.; Navarro-Ranninger, C. Anticancer platinum complexes as non-innocent compounds for catalysis in aqueous media. *Chem. Commun.* **2010**, *46* (3), 454–456.
- (52) Ghosh, A. K.; Brindisi, M. Organic Carbamates in Drug Design and Medicinal Chemistry. *J. Med. Chem.* **2015**, *58* (7), 2895–2940.
- (53) Tu, J.; Xu, M.; Parvez, S.; Peterson, R. T.; Franzini, R. M. Bioorthogonal Removal of 3-Isocyanopropyl Groups Enables the Controlled Release of Fluorophores and Drugs in Vivo. *J. Am. Chem. Soc.* **2018**, *140* (27), 8410–8414.
- (54) Morihito, K.; Ankenbruck, N.; Lukasak, B.; Deiters, A. Small Molecule Release and Activation through DNA Computing. *J. Am. Chem. Soc.* **2017**, *139* (39), 13909–13915.
- (55) Corinti, D.; Coletti, C.; Re, N.; Piccirillo, S.; Giampà, M.; Crestoni, M. E.; Fornarini, S. Hydrolysis of cis- and transplatin: structure and reactivity of the aqua complexes in a solvent free environment. *RSC Adv.* **2017**, *7* (26), 15877–15884.
- (56) Berners-Price, S. J.; Appleton, T. G. The Chemistry of Cisplatin in Aqueous Solution. In *Platinum-Based Drugs in Cancer Therapy*; Kelland, L. R., Farrell, N. P., Eds.; Humana Press: Totowa, NJ, 2000; pp 3–35.
- (57) Dolezel, P.; Kuban, V. Mass spectrometric study of platinum complexes based on cisplatin. *Chem. Zvesti* **2002**, *56* (4), 236–240.
- (58) Vidal, C.; Tomás-Gamasa, M.; Destito, P.; López, F.; Mascareñas, J. L. Concurrent and orthogonal gold(I) and ruthenium(II) catalysis inside living cells. *Nat. Commun.* **2018**, *9* (1), 1913.
- (59) Coelho, S. E.; Schneider, F. S. S.; de Oliveira, D. C.; Tripodi, G. L.; Eberlin, M. N.; Caramori, G. F.; de Souza, B.; Domingos, J. B. Mechanism of Palladium(II)-Mediated Uncaging Reactions of Propargylic Substrates. *ACS Catal.* **2019**, *9* (5), 3792–3799.
- (60) Senter, P. D.; Sievers, E. L. The discovery and development of brentuximab vedotin for use in relapsed Hodgkin lymphoma and systemic anaplastic large cell lymphoma. *Nat. Biotechnol.* **2012**, *30* (7), 631–637.
- (61) Kelland, L. R.; Abel, G.; McKeage, M. J.; Jones, M.; Goddard, P. M.; Valenti, M.; Murrer, B. A.; Harrap, K. R. Preclinical Antitumor Evaluation of Bis-acetato-amine-dichloro-cyclohexylamine Platinum(IV): an Orally Active Platinum Drug. *Cancer Res.* **1993**, *53* (11), 2581–2586.
- (62) Cheng, Q.; Liu, Y. Multifunctional platinum-based nanoparticles for biomedical applications. *Wiley Interdiscip. Rev. Nanomed. Nanobiotechnol.* **2017**, *9* (2), No. e1410.
- (63) Bernardim, B.; Cal, P. M. S. D.; Matos, M. J.; Oliveira, B. L.; Martínez-Sáez, N.; Albuquerque, I. S.; Perkins, E.; Corzana, F.; Burtoloso, A. C. B.; Jiménez-Osés, G.; et al. Stoichiometric and irreversible cysteine-selective protein modification using carbonylacrylic reagents. *Nat. Commun.* **2016**, *7* (1), 13128.
- (64) Bernardim, B.; Matos, M. J.; Ferhati, X.; Compañón, I.; Guerreiro, A.; Akkapeddi, P.; Burtoloso, A. C. B.; Jiménez-Osés, G.; Corzana, F.; Bernardes, G. J. L. Efficient and irreversible antibody–cysteine bioconjugation using carbonylacrylic reagents. *Nat. Protoc.* **2019**, *14* (1), 86–99.
- (65) Gébleux, R.; Stringhini, M.; Casanova, R.; Soltermann, A.; Neri, D. Non-internalizing antibody–drug conjugates display potent anticancer activity upon proteolytic release of monomethyl auristatin E in the subendothelial extracellular matrix. *Int. J. Cancer* **2017**, *140* (7), 1670–1679.

(66) Lee, B.; Sun, S.; Jiménez-Moreno, E.; Neves, A. A.; Bernardes, G. J. L. Site-selective installation of an electrophilic handle on proteins for bioconjugation. *Bioorg. Med. Chem.* **2018**, *26* (11), 3060–3064.

(67) Fior, R.; Póvoa, V.; Mendes, R. V.; Carvalho, T.; Gomes, A.; Figueiredo, N.; Ferreira, M. G. Single-cell functional and chemosensitive profiling of combinatorial colorectal therapy in zebrafish xenografts. *Proc. Natl. Acad. Sci. U. S. A.* **2017**, *114* (39), No. E8234.

(68) Fazio, M.; Ablain, J.; Chuan, Y.; Langenau, D. M. Zebrafish patient avatars in cancer biology and precision cancer therapy. *Nat. Rev. Cancer* **2020**, *20* (9), 263–273.

(69) Fazio, M.; Zon, L. I. Fishing for answers in precision cancer medicine. *Proc. Natl. Acad. Sci. U. S. A.* **2017**, *114* (39), 10306.

(70) Yan, C.; Brunson, D. C.; Tang, Q.; Do, D.; Iftimia, N. A.; Moore, J. C.; Hayes, M. N.; Welker, A. M.; Garcia, E. G.; Dubash, T. D.; et al. Visualizing Engrafted Human Cancer and Therapy Responses in Immunodeficient Zebrafish. *Cell* **2019**, *177* (7), 1903–1914.

(71) Costa, B.; Ferreira, S.; Póvoa, V.; Cardoso, M. J.; Vieira, S.; Stroom, J.; Fidalgo, P.; Rio-Tinto, R.; Figueiredo, N.; Parés, O.; Greco, C.; Ferreira, M. G.; Fior, R. Developments in zebrafish avatars as radiotherapy sensitivity reporters — towards personalized medicine. *EBioMedicine* **2020**, *51*, 102578.

5 Paper III: Overreact, an *in silico* lab: automative quantum chemical microkinetic simulations for complex chemical reactions

SCHNEIDER, F. S. S.; CARAMORI, G. F. Overreact, an *in silico* lab: Automative quantum chemical microkinetic simulations for complex chemical reactions. **Journal of Computational Chemistry**, Wiley, Apr. 2022. ISSN 1096-987x. DOI: [10.1002/jcc.26861](https://doi.org/10.1002/jcc.26861). Available from: <http://dx.doi.org/10.1002/jcc.26861>

In order to overcome the challenges of this century, such as producing fuels and chemicals from biomass and greenhouse gases, and developing greener synthetic protocols, it is necessary to improve the understanding of reaction mechanisms. One way of accomplishing this is through the use of computational modelling tools and methodologies, which have become more efficient and accurate due to the growth of computing resources and methodological developments. However, these calculations must take into account as much of the relevant physics of the problem as possible, such as pre-equilibration and concentration, dispersion corrections, solvation, molecular symmetry [106], proper treatment of Gibbs energy contributions, standard state corrections, quantum tunnelling, and others.

First-principle calculations have been used to calculate binding free energies and reaction rate constants that are close to what is observed in experiments. It is thus viable to use calculations from computational chemistry to determine parameters of reactions, then simulate a microkinetic model for the process. A clear advantage of this approach is that it is possible to take the concentrations of the reactants into account. Microkinetic models can be used to analyze and test hypotheses in catalysis and chemical kinetics. This makes it possible to use first-principles microkinetic simulations to understand complex reactions over time. However, there is currently no general solution for first-principles microkinetic modelling that can do all of the necessary calculations and generate an equation system automatically.

This work introduces a novel Python package, named `overreact`. It is a user-friendly, open-source program that can be used to automatically perform microkinetic modelling of complex chemical reactions in solution or gas-phase using data from first-principles quantum chemical calculations. All it requires is a description of the hypothe-



Figure 4 – Logo of the `overreact` Python package, an open-source program that can be used to automatically perform microkinetic modelling of complex chemical reactions in solution or gas-phase using data from first-principles quantum chemical calculations.

sized reactions, the corresponding computational chemistry output files, initial concentrations, and reaction conditions such as temperature. It is compatible with 14 widely available computational chemistry packages (by making use of the `cclib` library [97]) and can be used to simulate reactions in both neat and buffered conditions. `overreact` supports a variety of quantum chemistry methods, from density functional theory to wavefunction methods, as well as composite models (e.g., DLPNO-CCSD(T)/cc-pVTZ//PBE0-D4/def2-TZVP), as long as the data is parseable by `cclib` [97]. It also allows the user to correct systematic errors in first-principle absolute Gibbs energy errors by the use of a single tunable parameter. This is important for bimolecular reactions, and a correction can be easily obtained by fitting systematic deviations in first-principles reaction schemes by using available experimental data, for instance.

The software is useful to inspect steady-state conditions (in the sense of *quasi-equilibria*), search for predominant species under catalytic conditions, computationally estimate the overall turn-over frequency and understand selectivity of a catalyst towards particular products. It allows rapid rational design and investigation in those areas where understanding how reactions work is important, and provides insight into concentration dependencies and comparison with experiment, since it performs microkinetic simulations and thus produces kinetic profiles. Kinetic models can be progressively constructed, with given pathways, thereby increasing human efficiency.

Some reaction examples were performed in the work, all using the default settings. For instance, the estimated autoisomerization rate of ethane from staggered to eclipsed and back to staggered was found to agree with experimental value. The reaction rate constant for the umbrella inversion of ammonia was estimated to agree with the experimental value of $4 \times 10^{10} \text{ s}^{-1}$.

In the context of gas-phase reactions, we modelled the degradation of methane degradation by chlorine radicals, an important atmospheric chemistry reaction. `overreact` provided reaction rate constants consistent with both experimental values ($1.0 \times 10^{-13} \text{ cm}^3 \cdot \text{molecule}^{-1} \text{ s}^{-1}$ [145]) and computational calculations by Tanaka; Xiao; Lasaga [146].

In the context of solvated-phase, M06-2X-D3(0)/6-311++G(d,p)/SMD was used to estimate the rate constant for $\text{NH}_{3(\text{w})} + \text{OH} \cdot_{(\text{w})} \longrightarrow \text{NH}_2 \cdot_{(\text{w})} + \text{H}_2\text{O}_{(\text{w})}$. at high pH, with values agreeing with experimental results. We also reproduced the results by Pérez-Soto; Besora; Maseras, who applied computer-aided analysis to study an imine formation reaction, taking into consideration the catalytic effect of small amounts of water in the milieu, either as contamination from residuals in the solvent or due to its formation as a by-product. Such systems can be complex and require microkinetics or other techniques to properly explain them, as direct consideration of concentrations through time is required. In total, the system simulates 25 simultaneous reactions and 17 species.

We investigated the mechanism of intramolecular amide hydrolysis, with three proposed mechanisms replicated. Since it is known that the reaction is strongly dependent on pH, we used the experimentally derived pK_a of acetic acid to correct all acid-base equilibria. From simulations at different pH values, it was also found that the reaction rate is strongly affected by the pH, and that it stops happening around pH 5, as expected from experimental results.

In fact, by simulating the system for an hour at different pH values and observing the concentrations of different intermediates over time, we could reproduce the experimental fact that the reaction only takes place in acidic environments. Furthermore, it was observed that the reaction rate increases significantly when a single water molecule actively participates as a proton shuttle, as proton transfer in a four-membered ring transition state is rate-determining.

To conclude, we discussed a software for obtaining reaction kinetic profiles from first-principle calculations. The package is automated and makes it easy for computational discoveries in the elucidation of reaction mechanisms to be compared with experimentally obtained results, which is crucial for studying chemical reactions. The open-source package presented in this article is available to explore and analyze reaction mechanisms. The software is suitable for predicting catalysts performance at scale, which is crucial for the emergent need for rapid and precise chemical modelling.

5.1 Full text

The `overreact` software was developed at the Department of Chemistry at the Federal University of Santa Catarina (UFSC). It can be regarded as a second iteration

on a previous attempt to build a chemical kinetics simulator [147]. The code is released under the permissive MIT open-source license [148].

This research was funded by the Brazilian Council for Scientific and Technological Development (CNPq), grant/award numbers 140485/2017–1 and 311132/2020–0.

The publication can be read in full next. Reprinted with permission from SCHNEIDER, F. S. S.; CARAMORI, G. F. Overreact, an *in silico* lab: Automotive quantum chemical microkinetic simulations for complex chemical reactions. **Journal of Computational Chemistry**, Wiley, Apr. 2022. ISSN 1096-987x. DOI: [10.1002/jcc.26861](https://doi.org/10.1002/jcc.26861). Available from: <<http://dx.doi.org/10.1002/jcc.26861>>. Copyright 2022 John Wiley & Sons, Inc.

SOFTWARE NOTE

Overreact, an in silico lab: Automative quantum chemical microkinetic simulations for complex chemical reactions

Felipe S. S. Schneider  | Giovanni F. Caramori 

Department of Chemistry, Federal University of Santa Catarina, Florianópolis, Santa Catarina, Brazil

Correspondence

Giovanni F. Caramori, Department of Chemistry, Federal University of Santa Catarina, Florianópolis, SC 88040-900, Brazil.
Email: giovanni.caramori@ufsc.br

Funding information

National Council for Scientific and Technological Development, Grant/Award Numbers: 140485/2017-1, 311132/2020-0

Abstract

Today's demand for precisely predicting chemical reactions from first principles requires research to go beyond Gibbs' free energy diagrams and consider other effects such as concentrations and quantum tunneling. The present work introduces overreact, a novel Python package for propagating chemical reactions over time using data from computational chemistry only. The overreact code infers all differential equations and parameters from a simple input that consists of a set of chemical equations and quantum chemistry package outputs for each chemical species. We evaluate some applications from the literature: gas-phase eclipsed-staggered isomerization of ethane, gas-phase umbrella inversion of ammonia, gas-phase degradation of methane by chlorine radical, and three solvation-phase reactions. Furthermore, we comment on a simple solvation-phase acid–base equilibrium. We show how it is possible to achieve reaction profiles and information matching experiments.

KEYWORDS

chemical reactions, concentration effects, in silico experiments, microkinetic modeling, overreact, Python3

1 | INTRODUCTION

Many of the challenges of this century, such as producing fuels and chemicals from biomass^{1–4} and greenhouse gases,^{5–8} as well as developing greener synthetic protocols,^{9–12} encompass problems related with both chemical kinetics and catalysis. Improving the understanding of reaction mechanisms is mandatory to meet the demand in designing efficient catalysts and molecular machines of increasingly complex behavior, needed to overcome such challenges in a sustainable and efficient manner.^{4,13–15}

The demand for rational design of reactions, catalysts, and chemical devices is leading our community towards the development of accurate and efficient computational modeling tools and methodologies.^{13,16–18} Despite the challenges in predicting observed reaction rate constants correctly, by using first principle calculations, the recent growth¹⁹ of computing resources and methodological developments have made the calculation of complex reaction mechanisms almost routine.^{16,18,20–26} This has uniquely aided both the elucidation of experiments and the comprehension of complex chemical phenomena.^{13,16}

Notwithstanding, feasible mechanistic propositions must be calculated with adequate levels of theory²⁷ and take into account all the relevant physics of the problem. The computational modeling of chemical reactions is a complex topic due to the overwhelming set of physical considerations that are required,²⁸ and the quest for mechanistic understandings actually requires a significant amount of automation,^{16,18} being therefore necessary to consider effects such as pre-equilibrium and concentration,²³ dispersion corrections,^{29,30} solvation,^{30–32} molecular symmetry,³⁰ proper treatment of Gibbs energy contributions,^{29,30,32,33} standard state corrections,^{30–32} tunneling and others.^{28,30}

Even so, most of the modeling of chemical reactions based on first-principles calculations is done using reaction rate constants alone, which is oftentimes not enough. Comparison with the experiment requires reaction rates, which depend on concentrations. For instance, the outcome and selectivity of two competing second-order reactions such as $R + A \rightarrow P_A$ and $R + B \rightarrow P_B$, whose kinetic equations are given by $d[P_A]/dt = k_1 [R][A]$ and $d[P_B]/dt = k_2 [R][B]$, are undoubtedly dependent not only on the rate constants k_1 and k_2 , but also on the concentrations $[A]$ and $[B]$.²³ Furthermore, it is well known that a

TABLE 1 Comparison of programs in the literature for theoretical chemical kinetics. Partially adapted from Dzib et al.³⁸ (only available software indicated).

Program	Theory	Molecularity	Phase	Tunnel effect	Language
overreact	TST	Any	Gas, solution	Wigner, Eckart	Python
Eyringpy	TST, MT, CKT	Uni/bi	Gas, solution	Wigner, Eckart	Python
Polyrate	TST, VTST, RRKM	Uni/bi	Gas, solid, gas–solid	ZCT, SCT, LCT	Fortran
MultiWell	ME, RRKM	Uni	Gas	–	Fortran
TAMkin	TST	Uni/bi	Gas	Wigner, Eckart	Python
MESMER	ME, RRKM	Uni/bi	Gas, solution	Eckart	C++
KiSThelp	TST, VTST, RRKM	Uni/bi	Gas	Wigner, Eckart	Java
RMG	TST, CKT	Uni/bi	Gas, solution	Wigner, Eckart	Python
APUAMA	TST	Uni/bi	Gas	Wigner, Eckart, SCT	C++
Pilgrim ⁵⁹	TST, VTST, CVT	Uni/bi	Gas	SCT	Python

Abbreviations: CKT, Collins–Kimbal Theory; CVT, canonical variational transition state theory; LCT, large curvature tunneling; ME, master equation; MT, Marcus theory; RRKM, Rise–Ramsperger–Kassel–Marcus; SCT, small curvature tunneling; VTST, variational transition state theory; ZCT, zero curvature tunneling.

single reaction step may not be enough to determine a whole chemical reaction path or catalytic cycle,^{34–36} bringing ambiguity in the general concept of “rate-determining step.”³⁵ The reasoning becomes still more entangled when a single observed reaction rate law is taken into consideration, such as when two steps with similar barriers within a single mechanism exist or when concurrent mechanisms coexist with an equal probability of occurring. Those problems have led to the development of new analytical tools, broadening the interpretation of reactions and, in particular, catalytic processes.^{34,36,37}

A useful solution to these issues is to simulate reaction models whose parameters are taken from computational chemistry calculations. For instance, modeling reactions using microkinetic simulations has become increasingly important, especially when it is essential to take concentration effects into account.²³ First-principle calculations have allowed us to calculate binding free energies³⁰ and reaction rate constants³⁸ reasonably close to experimental values, as long as the correct physical phenomena are appropriately addressed. This idea is not new in the experimental laboratory: Blackmond have advocated using full-blown kinetics simulations to elucidate experimentally observed reaction mechanisms through model exploration.^{34,36} This analysis protocol has been shown to be crucial for elucidating many mechanisms of industrial importance. Similarly, microkinetic models provide time-resolved kinetic analysis that allows one to consolidate, analyze and test hypotheses in catalysis and chemical kinetics in general,^{34,36} and it has extensively used in computational heterogeneous catalysis,^{15,39–55} experimental biology⁵⁶ and mechanism validation.⁵⁷ It is thus possible to accurately perform first-principles microkinetic simulations on rather complex reaction phenomena over time, which allows one to better comprehend tricky aspects not revealed by more simplistic models.^{34,36} Even with possible systematic errors brought by first-principle calculations, insights are warranted.^{35,37,58}

Unfortunately, there is currently no general solution for first-principles microkinetic modeling that, simultaneously, (1) calculates all the required thermochemical quantities and corrections from first-principles, (2) automatically calculates reaction rate constants, including

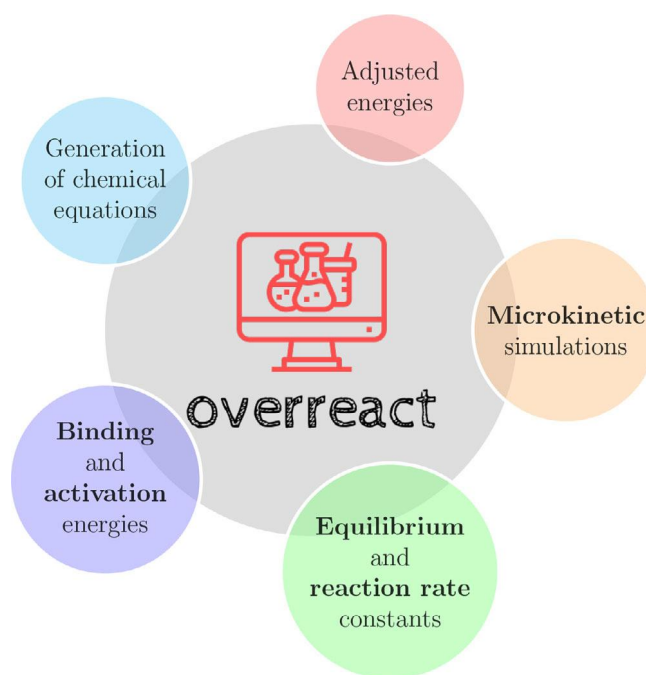
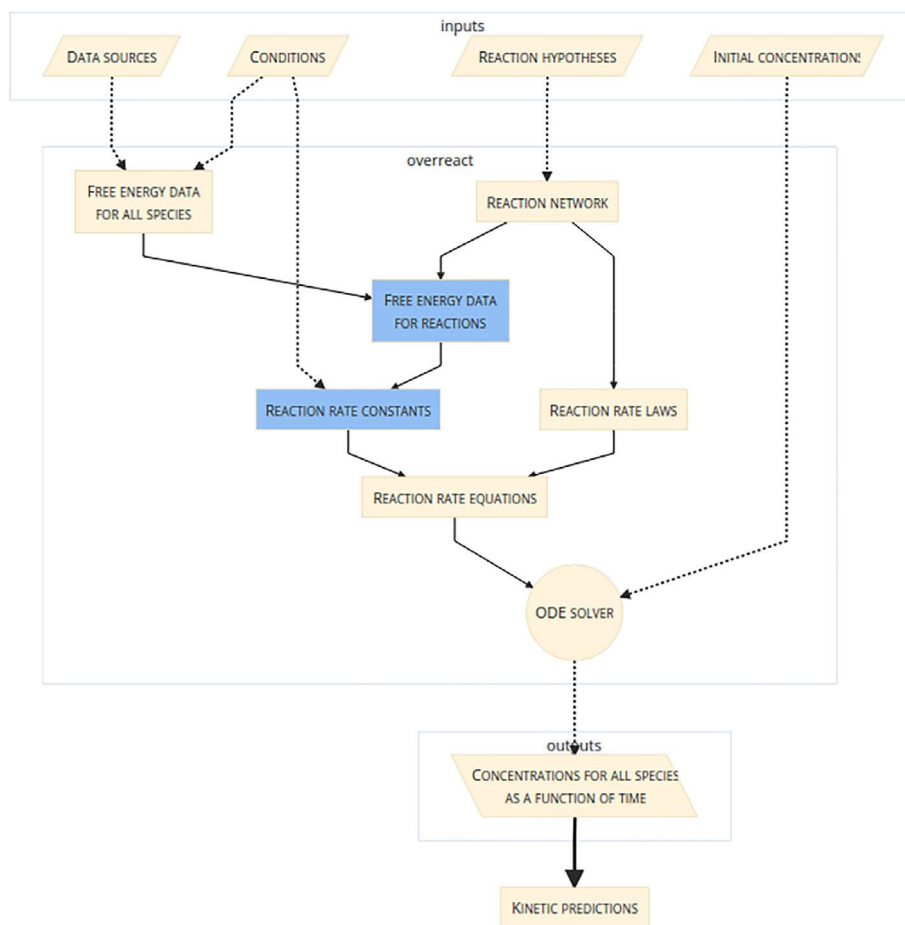


FIGURE 1 Visual depiction of some of the capabilities of overreact, a Python library and command-line tool for building and analyzing homogeneous microkinetic models from first-principles calculations. Instructions on how to install and use can be found at <https://geem-lab.github.io/overreact-guide>

quantum tunneling approximations, for all reactions, (3) generates an (usually non-linear) ordinary differential equation (ODE) system from an arbitrary reaction scheme automatically, (4) produces a Jacobian for the ODE system using automatic differentiation for improved accuracy and performance, and (5) propagates the chemical kinetic processes generating concentrations for all compounds as a function of time and initial concentrations. Table 1 compares the capabilities of overreact with some other known microkinetic software in the literature.

FIGURE 2 A simplified diagram featuring the overreact dataflow. Computational chemistry logfiles are taken as data sources. Together with temperature conditions, a chemical reaction network and initial concentrations, overreact calculates Gibbs' free energies for all species. From this information, reaction rate constants and a system of ordinary differential equations (ODEs) are devised. This ODE system is solved, yielding concentrations for all species over time. Further details can be found in the supporting information



The present work presents a simple yet robust software that treats all the five points listed above in an automated way, starting from the outputs of ab initio calculations of numerous levels of theory (Density Functional Theory, Hartree-Fock, post-Hartree-Fock or any other where Hessian calculations are available).⁶⁰ It is able to solve any chemical reaction network, including parallel and concurrent reactions, from elementary steps at constant temperature in the well-stirred approximation. The key features of the proposed code, called overreact, are highlighted in Figure 1. It has been developed as a user-friendly, open-source (MIT license) Python program and library that does simple and automatic microkinetic modeling of complex reaction networks in solution and gas-phase using only the user description of the reactions to be considered in the model, the corresponding computational chemistry output files, initial concentrations, and a set of reaction conditions such as temperature. Only the converged geometries, electronic energies, and vibrational frequencies of each species in the model are required from the outputs. Overreact is freely available, simple to install and use, well tested, well documented, and encompasses an easy-to-use command-line application (<https://geem-lab.github.io/overreact-guide/>). Although only thoroughly tested with ORCA⁶¹ and Gaussian 09⁶² output files at the moment, it employs the Python library cclib⁶³ for parsing computational chemistry outputs, which is actually known to work with 14 different computational chemistry packages. Overreact not only

generates and solves arbitrary chemical kinetic ODE problems, but also allows the user to fix the concentration of one or more compounds, which is useful for simulating reactions in neat or buffered conditions. Furthermore, the user can adjust systematic first-principle absolute Gibbs energy errors by comparison with experiments automatically, which are expected to be up to 4 kcal mol⁻¹ even when suitable density functional are employed.^{26,64-67}

2 | METHODOLOGY

The overreact code attempts to make the process of building precise chemical microkinetic models from first principle calculations as automatic as possible. It takes data from computational chemistry logfiles and uses them to calculate thermodynamic and kinetic properties, as shown in the dataflow diagram in Figure 2. This information gives rise to reaction rate constants and a system of ordinary differential equations, which, together with initial concentrations, yields concentrations of all species over time.

The dataflow diagram of Figure 2 is simplification of the whole process, not a complete description of the system. A detailed description of the library's core functionalities can be found in the Supporting Information, where automated procedures, methodologies and capabilities implemented in overreact are highlighted.

3 | RESULTS AND DISCUSSION

Representative results of overreact usage are available in the following subsections. Defaults are used when not otherwise specified.

3.1 | Examples in the gas phase

3.1.1 | Simple gas-phase autoisomerizations

In order to demonstrate that overreact can estimate precise reaction rate constants from ab initio calculations, we first consider some simple gas-phase autoisomerization reactions.

Ethane

We estimated the rate of autoisomerization of the ethane from staggered to eclipsed back to staggered again. At B97-3c,⁶⁸ the rate calculated was found to be $8.2 \times 10^{10} \text{ s}^{-1}$ (including tunneling coefficient of 1.11). Higher levels of theory gave similar results (4.8×10^{10} and $6.3 \times 10^{10} \text{ s}^{-1}$, including tunneling coefficients of 1.13 and 1.12, for 6-311G(d,p) and UMP2/6-311G(3df,3pd), respectively). There is overall good agreement with the experimental estimate of $8.3 \times 10^{10} \text{ s}^{-1}$.⁶⁹

Ammonia

The reaction rate constant for the umbrella inversion of ammonia was estimated to be $1.3 \times 10^{10} \text{ s}^{-1}$ at MP2/ma-def2-TZVP (tunneling coefficient $\kappa = 2.00$), which agrees with the experimental value of $4 \times 10^{10} \text{ s}^{-1}$.⁷⁰ On the other hand, the barrier at MP2/ma-def2-TZVP was found to be $4.1 \text{ kcal mol}^{-1}$, lower than the experimental one ($5.8 \text{ kcal mol}^{-1}$).⁷⁰ A calculation at CCSD(T)/cc-pVTZ better agrees with the thermodynamical barrier ($6.0 \text{ kcal mol}^{-1}$), but degrades the reaction rate constant ($5.9 \times 10^8 \text{ s}^{-1}$, with $\kappa = 2.37$). Similar results were found using DFT ($\Delta G^\ddagger = 5.4 \text{ kcal mol}^{-1}$ and $k = 3.6 \times 10^9 \text{ s}^{-1}$ with $\kappa = 4.88$ at ω B97X-D4-gCP/def2-TZVP), suggesting that the Eckart approximation is not enough to get quantitative results in this particular case, as one of the key assumptions of the model is that the reaction takes place through a linear path in the potential energy surface.

3.1.2 | $\text{CH}_4 + \text{Cl} \rightarrow \text{CH}_3 + \text{HCl}$

Tanaka et al. studied the degradation of methane by chlorine radical gas in the context of the global methane cycle in the atmosphere.⁷¹ In line with the results reported by Dzib et al.,³⁸ we obtained a reaction rate constant of $9.3 \times 10^{-14} \text{ cm}^3 \text{ molecule}^{-1} \text{ s}^{-1}$ ($\kappa = 3.64$) at UMP2/cc-pVTZ for this bimolecular reaction, in line with previous computational results of Tanaka et al.⁷¹ ($2.2 \times 10^{-13} \text{ cm}^3 \text{ molecule}^{-1} \text{ s}^{-1}$) and the current recommended experimental value of $1.0 \times 10^{-13} \text{ cm}^3 \text{ molecule}^{-1} \text{ s}^{-1}$.⁷² Overall, the calculated reaction rate constants using the Eckart tunneling approximation fall in the lower range of the experimental 95% confidence interval in the range 181–300 K (Figure 3A), in excellent agreement with experimental results in that range ($r^2 = 0.9984$, Figure 3B). Furthermore, a one-second

microkinetic modeling of this fast gas-phase reaction example (using as initial concentrations 250, 100, and 25 nM for CH_4 , Cl , and HCl , respectively) is shown in Figure 3c, where the concentrations of all species are obtained as a function of time.

3.2 | Examples in solution

3.2.1 | Constrained equilibria: acetic acid-acetate equilibrium concentrations versus pH

overreact is able to calculate simple equilibrium systems without knowledge of reaction rate constants by producing them such that equilibrium constants are satisfied. When used together in a reaction network, the algorithm ensures that the fictitious, calculated forward and backwards reaction rate constants are larger than any other reaction rate constant in the system by a factor of eight. Although it makes equations stiffer, this allows investigating systems containing both equilibria and fast reactions together, as is indicated in the following sections.

On the other hand, pure equilibria can still be useful. Even though it is not possible to obtain *quantitative* kinetic profiles with equilibria alone, it is perfectly reasonable to obtain final Boltzmann populations from them. In fact, together with a simple constraint optimizer implemented in overreact, it is possible to fix the concentrations of any part of the system and check how this would affect the final populations.

In order to assess the correctness of pure equilibria calculations in overreact, as well as the concentration constraining feature, we estimated the final concentrations in solution of the acetic acid-acetate, acid-base equilibrium system. For that, we employed a combination of ab initio calculations and experimental pK_a values to account for systematic errors.^{31,73} Different values of pH were fixed by constraining the H^+ concentration.

Optimizations and frequencies for the $\text{AcOH}(\text{aq}) \rightleftharpoons \text{AcO}^-(\text{aq}) + \text{H}^+(\text{aq})$ system were performed at UM06-2X/6-311++G(d,p)/SMD(water).^{31,74,75} All data for H^+ was inserted directly in the overreact input. For comparison, two distinct energies for the proton solvation energy were separately employed: $-265.9 \text{ kcal mol}^{-1}$, as used in the parameterization process of SMD,³¹ and $-277.2 \text{ kcal mol}^{-1}$, which is the value that correctly predicts the experimental pK_a of 4.756 for this system.⁷⁶ The final calculated concentrations as a function of pH for both proton solvation energies can be seen in Figure 4. As can be seen, although errors are very sensitive to the energy values provided, overreact produces the expected result if precise energy values are provided.

3.2.2 | Hickel (1992)

We compared the applicability of overreact for reactions in solvation using the well-known radical reaction $\text{NH}_{3(\text{w})} + \text{OH}_{(\text{w})} \rightarrow \text{NH}_{2(\text{w})} + \text{H}_2\text{O}_{(\text{w})}$ at M06-2X-D3(0)/6-311++G(d,p)/SMD(water)^{31,74,75} (using ORCA 4.2.1⁶¹). The calculated reaction rate constant can be seen in Figure 5, together with a comparison with experimental and theoretical results available in the literature (exact figures are available in

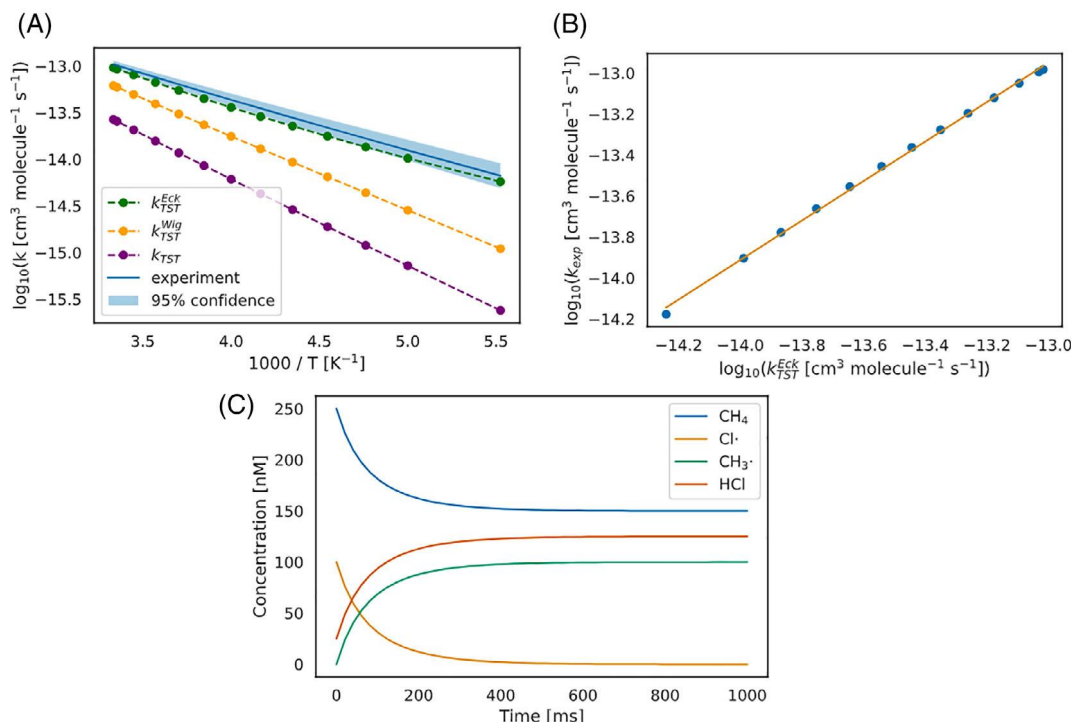


FIGURE 3 Computed chemical kinetics of $\text{CH}_4 + \text{Cl} \rightarrow \text{CH}_3 + \text{HCl}$ in the gas phase. (A) Arrhenius plots in the range 181–300 K with different tunneling approximations compared against the recommended experimental fit of Burkholder et al. and its 95% confidence interval.⁷² Compare to Figures 1 and 2 of Dzib et al.³⁸ and Tanaka et al.,⁷¹ respectively. (B) Linear regression between the calculated, Eckart-corrected reaction rate constants against the experimental results, in logarithmic scale ($\log_{10}(k_{TST}^{Eck}) = 0.9633 \times \log_{10}(k_{exp}) + 0.4256$, $r^2 = 0.9984$). (C) Microkinetic simulation of the gas-phase reaction $\text{CH}_4 + \text{Cl} \rightarrow \text{CH}_3 + \text{HCl}$ (using 250, 100, and 25 nM as initial concentrations of CH_4 , $\text{Cl}\cdot$, and HCl , respectively)

FIGURE 4 Computed acid–base equilibrium for $\text{AcOH}(\text{aq}) \rightleftharpoons \text{AcO}^-(\text{aq}) + \text{H}^+(\text{aq})$ at UM06-2X/6-311++G(d,p)/SMD(water)^{31,74,75} for a series of pH values

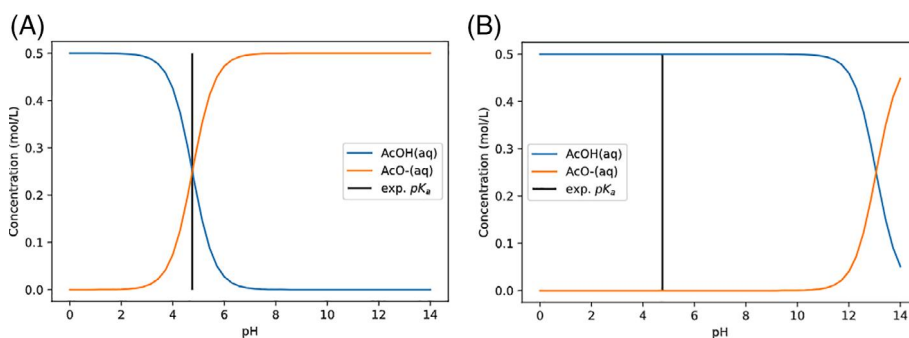


Table S1). The experimental results were all measured at high pH and, since the effect of the ammonia-ammonium equilibrium is negligible in those conditions,^{38,77} the phenomenon was not considered in this case for simplicity.

3.2.3 | Pérez-Soto (2020)

Pérez-Soto et al. have applied computer experiments to a well-studied imine formation reaction using techniques very similar to the ones in the present work.⁶⁷ Since those reactions encompass a proton transfer, they suffer from effects of residual water, as water can facilitate proton shuttling. Even though the reaction happens in dichloromethane, water is found as

an impurity in the commercially-available solvent and, most importantly, it is produced as a by-product in the second, dehydrating step.⁶⁷

Such cases are not uncommon and can hardly be properly rationalized by simple free energy diagrams, requiring microkinetics or other techniques that take into account changes of concentration throughout the reaction.^{24,25}

The work of Pérez-Soto et al. is particularly important due to their investigation on systematic errors in bimolecular reaction barriers.⁶⁷ This takes place due to the impossibility, for bimolecular reactions, of the common error cancellation found in monomolecular reactions. They not only showed the systematicity of such errors, but also that they could be reduced, for a given reaction, by properly adjusting all Gibbs' free energies with a single tunable parameter.⁶⁷

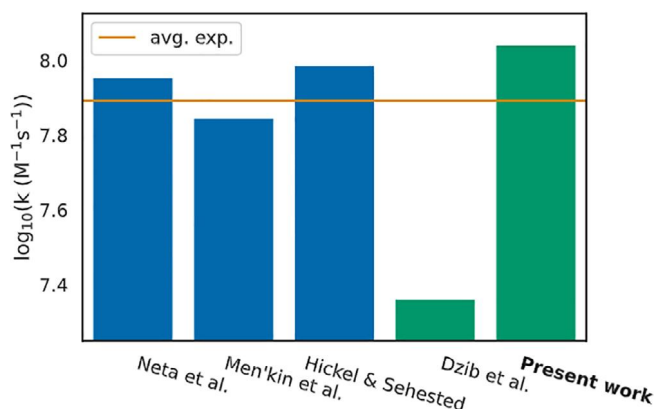


FIGURE 5 Comparison of experimental and computational results from the literature for the reaction rate constant of the reaction $\text{NH}_{3(\text{w})} + \text{OH}_{(\text{w})} \rightarrow \text{NH}_{2(\text{w})} + \text{H}_2\text{O}_{(\text{w})}$ at M06-2X-D3(O)/6-311++G(d,p)/SMD(water)^{31,74,75} (using ORCA 4.2.1⁶¹). All values indicated are in logarithmic scale. Blue and green bars represent experimental and computational results, respectively. The orange line is the log₁₀ value of the average of experimental values. The exact values can be found in Table S1

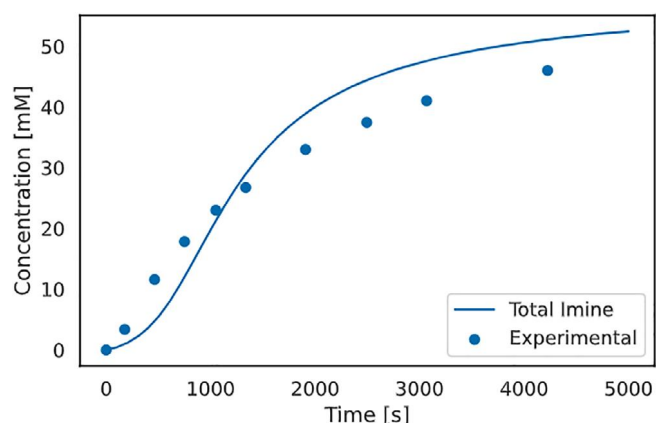


FIGURE 6 Predicted kinetic profile for the reaction of Pérez-Soto et al.⁶⁷ experimental data taken from the supporting information of Pérez-Soto et al.⁶⁷ is also shown. A systematic bias of 3.2 kcal mol⁻¹ was employed in agreement with the original work,⁶⁷ which translates to a root-mean-squared deviation (RMSD) of 4.97 mM. The summed concentration of the imine product is shown, as it is found in association with different amine and water quantities. A detailed profile with all relevant species can be found in Figure S3

In Figure 6 a reproduction of their work is shown and compared against experimental concentration data points. The exact same Gibb's free energy adjustment of 3.2 kcal mol⁻¹ as employed in the original work was used by us, which is equivalent to a root-mean-squared error of 4.97 mM when compared against the experimental data points. Apart from that, the present results differ from Pérez-Soto et al. in that we employed all additional approximations implemented in overreact: Eckart tunneling corrections for all reaction steps and the quasi-rigid rotor-harmonic approximation for both enthalpies and entropies. The fact that a systematic energy correction

was still required to attain experimental-grade quality suggests yet another source of error.

A systematic study on the effect of the tunable parameter can be seen in Figure S2, which shows a flat region around 2–3 kcal mol⁻¹. This suggests that, even though such energy adjustments might be seen as arbitrary, they may make little influence on the final result as long as the chosen value is reasonable. Due to DFT errors in general, fitting systematic deviations in first-principles reaction schemes seems to be warranted and, in the future, this could be performed automatically using available experimental data. Progress is currently being made in this respect in our laboratory.

3.2.4 | Intramolecular amide hydrolysis of N-alkyl maleamic acids

We have looked into intramolecular amide hydrolysis initially investigated by Kirby and Lancaster⁷⁸ and subsequently studied by others.^{79–81} We employed calculations using ω B97XD/6-311++G**/SMD(water)^{31,74,82} and used Gaussian 09 (Revision C.01).⁶² As before, the proton energy was adjusted in order to reproduce the experimental pK_a of 4.756 for acetic acid.⁷⁶ Three distinct mechanisms proposed in the literature can be seen in Figure 7. One thing that is worth of note in Figure 7 is the step going through I[‡], which presents a proton transfer in a four-membered ring transition state. While its bare barrier is around 28.8 kcal mol⁻¹, this can be reduced to 13.6 kcal mol⁻¹ by the use of a single-water-molecule proton shuttle. Furthermore, while the facilitated transfer shows only an 8% reaction rate constant increase due to tunneling (using the Eckart approximation), the bare reaction step shows a 960 times (!) increase, even at room temperature. Notwithstanding, the product M is not formed during simulation if the facilitated I[‡] step is removed from the system. All this, together with the indication that the tetrahedral intermediate J appears to be an important rest state, strongly suggests that the step passing through I[‡] is the rate-determining one, and that it includes active participation of the solvent.

One key feature of this reaction is its strong dependency on pH: as early shown by Kirby and Lancaster, the reaction takes place on acidity environments only.⁷⁸ In order to access its behavior in different acidic environments, we employed a series of short (0.5 s) simulations at different pH values, always starting with 0.1 M of the maleamic acid A (Figure 8A). We kept the concentration of H⁺ at a different value for each simulation (corresponding to pH 0–7), but we employed pseudo-first order conditions with respect to the solvent in each of them, constraining the water concentration to stay at 55.6 M. In total, the presented system encompasses 25 simultaneous and automatically simulated reactions and 17 distinct species. As can be seen in Figure 8A, the results corroborate with initial velocity essays worked by Kirby and Lancaster for closely-related systems,⁷⁸ where reaction ceases to happen around pH 5.

By simulating the whole system for an hour at pH 2, we could obtain the kinetic profile in Figure 8B. Observing the concentration over time of different intermediates leads us to conclude that, under

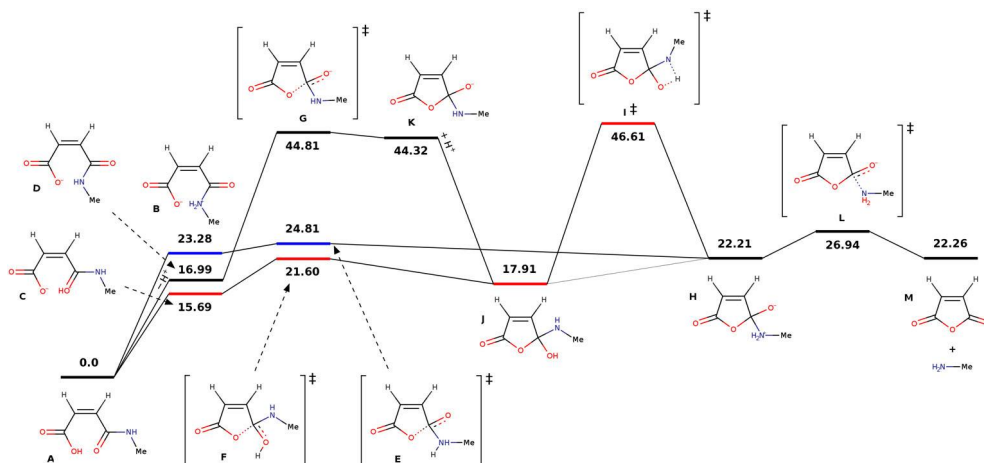
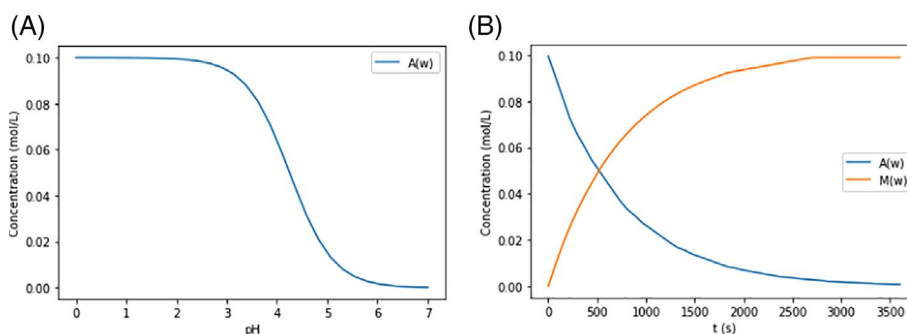


FIGURE 7 Proposed reaction mechanisms for the amide hydrolysis of N-alkyl maleamic acids, as previously proposed in the literature.^{78–81} Three possible mechanisms are indicated with distinct colors. The black bars denote the path starting with proton dissociation, followed by an intramolecular attack on the amide carbon. The red bars indicate a path where the attack happens concomitant to a proton transfer to the amide carbonyl. In addition, the blue bars indicate a similar path, but the proton is transferred to the amide nitrogen upon attack on the carbon. Subsequent dissociation of the product complex is worth $\Delta G^\circ = -4.74 \text{ kcal mol}^{-1}$. In the current work, we investigate the base case where $R_1 = -\text{CH}_3$ and $R_2 = R_3 = \text{H}$

FIGURE 8 (A) Short (0.5 s) simulations at different pH values (pH 0–7). (B) Kinetic profile for the reaction at pH 2, as simulated for an hour (3600 s). In all cases, pseudo-first order conditions with respect to water were maintained (55.6 M) and the initial concentration of the maleamic acid A (Figure 7) was 0.1 M. All reactions presented so far were included in the simulations (25 in total, see text and Figure 7)



these conditions, the reaction seems to happen mostly through equilibrium-state C and rest-state J: as J starts to build up, it gradually transitions, with the help of the solvent, to H, whose C–N bond has been elongated at this point. Finally, after the production of both M and the primary amine leaving group, actual separation further steers the reaction forward due to entropy ($\Delta S^\circ = 27 \text{ cal mol}^{-1} \text{ K}^{-1}$).

4 | SUMMARY AND OUTLOOK

We applied an automatic process for obtaining reaction kinetic profiles of increasingly complex reactions from first principles. The presented method allows for direct comparison with experimentally obtained results, which are often indispensable when studying chemical reactions.¹⁶ Known disparities can be systematically adjusted using energetic biases if the computational model is known to deliver systematic errors, which is particularly important in systems involving bimolecular reactions.

Although not a magic blackbox, overreact offers a hopefully complete but simple predictive computational environment for hypothesis

testing in first-principles homogeneous chemical kinetics and catalysis. In fact, from the calculated concentrated curves using microkinetic simulations, observed reaction rate constants can be inferred using the same mathematical techniques employed in common experimental data treatments.^{34,36}

The open-source package presented in this article is already available to explore and analyze reaction mechanisms. Detailed instructions on how to install and use can be found at <https://geem-lab.github.io/overreact-guide/>. In the future, we will investigate the applicability of overreact to more complex, catalytic systems,^{83,84} extend the present work to heterogeneous reactions, and attempt to fully predict the outcome of reactors by coupling computational fluid dynamics with first-principles microkinetic modeling.⁸⁵ All this would, in principle, allow us to design catalysts that work well in the scale they are meant to.

ACKNOWLEDGMENTS

The authors Felipe S. S. Schneider and Giovanni F. Caramori thank the National Council for Scientific and Technological Development, CNPq for their PhD (140485/2017-1) and research (311132/2020-0) grants, respectively.

DATA AVAILABILITY STATEMENT

Data that supports the findings of this study are available in the supplementary material of this article. A complete data set is openly available in <https://github.com/geem-lab/overreact-data>. The source code of overreact is also openly available at <https://github.com/geem-lab/overreact>. A user guide can be found at <https://geem-lab.github.io/overreact-guide/>.

ORCID

Felipe S. S. Schneider  <https://orcid.org/0000-0001-8090-2976>

Giovanni F. Caramori  <https://orcid.org/0000-0002-6455-7831>

REFERENCES

- [1] D. Klass, *Biomass for Renewable Energy, Fuels, and Chemicals*, Academic Press, Cambridge, Massachusetts **1998**.
- [2] A. Demirbaş, *Energy Convers. Manag.* **2001**, *42*, 1357.
- [3] J. B. Binder, R. T. Raines, *J. Am. Chem. Soc.* **2009**, *131*, 1979.
- [4] R. Šivic, M. Grilc, M. Huš, B. Likozar, *Ind. Eng. Chem. Res.* **2019**, *58*, 16018.
- [5] M. Auffhammer, V. Ramanathan, J. R. Vincent, *Proc. Natl. Acad. Sci.* **2006**, *103*, 19668.
- [6] H. V. M. Hamelers, O. Schaetzle, J. M. Paz-García, P. M. Biesheuvel, C. J. N. Buisman, *Environ. Sci. Technol. Lett.* **2013**, *1*, 31.
- [7] V. Barbarossa, G. Vanga, R. Viscardi, D. M. Gattia, *Energy Procedia* **2014**, *45*, 1325.
- [8] J. Fanchi, C. Fanchi, *Energy IN THE 21st Century*, 4th ed., World Scientific Publishing Company, Hackensack, NJ **2016**.
- [9] P. Raveendran, J. Fu, S. L. Wallen, *J. Am. Chem. Soc.* **2003**, *125*, 13940.
- [10] A. Arcadi, *Chem. Rev.* **2008**, *108*, 3266.
- [11] P. Anastas, N. Eghbali, *Chem. Soc. Rev.* **2010**, *39*, 301.
- [12] O. V. Kharissova, B. I. Kharisov, C. M. Oliva González, Y. P. Méndez, I. López, *R. Soc. Open Sci.* **2019**, *6*, 191378.
- [13] D. J. Tantillo, C. Jiangang, K. N. Houk, *Curr. Opin. Chem. Biol.* **1998**, *2*, 743.
- [14] K. N. Houk, F. Liu, *Acc. Chem. Res.* **2017**, *50*, 539.
- [15] Y. Wang, L. Xiao, Y. Qi, M. Mahmoodinia, X. Feng, J. Yang, Y.-A. Zhu, D. Chen, *Phys. Chem. Chem. Phys.* **2019**, *21*, 19269.
- [16] S. Ahn, M. Hong, M. Sundararajan, D. H. Ess, M.-H. Baik, *Chem. Rev.* **2019**, *119*, 6509.
- [17] J. W. Kim, Y. Kim, K. Y. Baek, K. Lee, W. Y. Kim, *Chem. A Eur. J.* **2019**, *123*, 4796.
- [18] I. Funes-Ardoiz, F. Schoenebeck, *Chem* **2020**, *6*, 1904.
- [19] M. S. Gordon, G. Barca, S. S. Leang, D. Poole, A. P. Rendell, J. L. Galvez Vallejo, B. Westheimer, *Chem. A Eur. J.* **2020**, *124*, 4557.
- [20] N. Nikbin, S. Caratzoulas, D. G. Vlachos, *ChemCatChem* **2012**, *4*, 504.
- [21] J. Jover, *Phys. Chem. Chem. Phys.* **2017**, *19*, 29344.
- [22] W. Guo, R. Kuniyil, J. E. Gómez, F. Maseras, A. W. Kleij, *J. Am. Chem. Soc.* **2018**, *140*, 3981.
- [23] M. Besora, F. Maseras, *Wiley Interdiscip. Rev.: Comput. Mol. Sci.* **2018**, *8*, e1372.
- [24] Y. Yu, Y. Zhu, M. N. Bhagat, A. Raghuraman, K. F. Hirsekorn, J. M. Notestein, S. T. Nguyen, L. J. Broadbelt, *ACS Catal.* **2018**, *8*, 11119.
- [25] M. Jaraiz, J. E. Rubio, L. Enríquez, R. Pinacho, J. L. López-Pérez, A. Lesarri, *ACS Catal.* **2019**, *9*, 4804.
- [26] A. Ishikawa, Y. Tateyama, *J. Comput. Chem.* **2019**, *40*, 1866.
- [27] P. Morgante, R. Peverati, *Int. J. Quantum Chem.* **2020**, *120*, e26332.
- [28] H. Ryu, J. Park, H. K. Kim, J. Y. Park, S.-T. Kim, M.-H. Baik, *Organometallics* **2018**, *37*, 3228.
- [29] S. Grimme, *Chem. Eur. J.* **2012**, *18*, 9955.
- [30] J. H. Jensen, *Phys. Chem. Chem. Phys.* **2015**, *17*, 12441.
- [31] A. V. Marenich, C. J. Cramer, D. G. Truhlar, *J. Phys. Chem. B* **2009**, *113*, 6378.
- [32] R. F. Ribeiro, A. V. Marenich, C. J. Cramer, D. G. Truhlar, *J. Phys. Chem. B* **2011**, *115*, 14556.
- [33] Y.-P. Li, J. Gomes, S. Mallikarjun Sharada, A. T. Bell, M. Head-Gordon, *J. Phys. Chem. C* **2015**, *119*, 1840.
- [34] D. G. Blackmond, *Angew. Chem. Int. Ed.* **2005**, *44*, 4302.
- [35] S. Kozuch, J. M. L. Martin, *ChemPhysChem* **2011**, *12*, 1413.
- [36] D. G. Blackmond, *J. Am. Chem. Soc.* **2015**, *137*, 10852.
- [37] E. Solel, N. Tarannam, S. Kozuch, *Chem. Commun.* **2019**, *55*, 5306.
- [38] E. Dzib, J. L. Cabellos, F. Ortíz-Chi, S. Pan, A. Galano, G. Merino, *Int. J. Quantum Chem.* **2018**, *119*, e25686.
- [39] J. A. Dumesic, D. F. Rudd, D. F. Rudd, L. M. Aparicio, J. E. Rekoske, A. A. Trevino, *The microkinetics of heterogeneous catalysis*, American Chemical Society, **1993**.
- [40] A. van de Runstraat, J. van Grondelle, R. A. van Santen, *Ind. Eng. Chem. Res.* **1997**, *36*, 3116.
- [41] M. Neurock, E. W. Hansen, *Comput. Chem. Eng.* **1998**, *22*, S1045.
- [42] A. B. Mhadeshwar, H. Wang, D. G. Vlachos, *J. Phys. Chem. B* **2003**, *107*, 12721.
- [43] A. Bhan, S. Hsu, G. Blau, J. Caruthers, V. Venkatasubramanian, W. Delgass, *J. Catal.* **2005**, *235*, 35.
- [44] L. C. Grabow, A. A. Gokhale, S. T. Evans, J. A. Dumesic, M. Mavrikakis, *J. Phys. Chem. C* **2008**, *112*, 4608.
- [45] G. Novell-Leruth, J. M. Ricart, J. Pérez-Ramírez, *J. Phys. Chem. C* **2008**, *112*, 13554.
- [46] S. C. Ammal, A. Heyden, *J. Phys. Chem. Lett.* **2012**, *3*, 2767.
- [47] R. A. van Santen, A. J. Markvoort, I. A. W. Filot, M. M. Ghouri, E. J. M. Hensen, *Phys. Chem. Chem. Phys.* **2013**, *15*, 17038.
- [48] A. J. Medford, C. Shi, M. J. Hoffmann, A. C. Lausche, S. R. Fitzgibbon, T. Bliigaard, J. K. Nørskov, *Catal. Lett.* **2015**, *145*, 794.
- [49] C. F. Goldsmith, R. H. West, *J. Phys. Chem. C* **2017**, *121*, 9970.
- [50] Y. Mao, H. Wang, P. Hu, *WIREs* **2017**, *7*, e1321.
- [51] Z. Chen, H. Wang, N. Q. Su, S. Duan, T. Shen, X. Xu, *ACS Catal.* **2018**, *8*, 5816.
- [52] L. Foppa, K. Larmier, A. Comas-Vives, *CHIMIA Int. J. Chem.* **2019**, *73*, 239.
- [53] J. Park, J. Cho, Y. Lee, M.-J. Park, W. B. Lee, *Ind. Eng. Chem. Res.* **2019**, *58*, 8663.
- [54] H. Liu, J. Liu, B. Yang, *Phys. Chem. Chem. Phys.* **2019**, *21*, 9876.
- [55] M. Huš, M. Grilc, A. Pavlišič, B. Likozar, A. Hellman, *Catal. Today* **2019**, *338*, 128.
- [56] A. L. Slusarczyk, A. Lin, R. Weiss, *Nat. Rev. Genet.* **2012**, *13*, 406.
- [57] M. O. Miranda, Y. DePorre, H. Vazquez-Lima, M. A. Johnson, D. J. Marell, C. J. Cramer, W. B. Tolman, *Inorg. Chem.* **2013**, *52*, 13692.
- [58] R. Christensen, H. A. Hansen, T. Vegge, *Cat. Sci. Technol.* **2015**, *5*, 4946.
- [59] Ferro-Costas, D.; Truhlar, D. G.; Fernández-Ramos, A. Pilgrim: A thermal rate constant calculator and kinetics Monte Carlo Simulator (version 1.0). <https://github.com/daferro/Pilgrim>, **2019**; Accessed: March 2022.
- [60] Schneider, F. S. S. *geem-lab/overreact: v1.0.2*. **2021**; <https://zenodo.org/record/5730603>.
- [61] F. Neese, *WIREs Comput. Mol. Sci.* **2017**, *8*, e1327.
- [62] M. J. Frisch, G. W. Trucks, H. B. Schlegel, G. E. Scuseria, M. A. Robb, J. R. Cheeseman, G. Scalmani, V. Barone, G. A. Petersson, H. Nakatsuji, X. Li, M. Caricato, A. V. Marenich, J. Bloino, B. G. Janesko, R. Gomperts, B. Mennucci, H. P. Hratchian, J. V. Ortiz, A. F. Izmaylov, J. L. Sonnenberg, D. Williams-Young, F. Ding, F. Lipparini, F. Egidi, J. Goings, B. Peng, A. Petrone, T. Henderson, D. Ranasinghe, V. G. Zakrzewski, J. Gao, N. Rega, G. Zheng, W. Liang, M. Hada, M. Ehara, K. Toyota, R. Fukuda, J. Hasegawa, M. Ishida, T. Nakajima, Y. Honda, O. Kitao, H. Nakai, T. Vreven, K. Throssell, J. A. Montgomery Jr., J. E. Peralta, F. Ogliaro, M. J. Bearpark, J. J. Heyd, E. N. Brothers, K. N. Kudin, V. N. Staroverov, T. A. Keith, R. Kobayashi, J. Normand, K. Raghavachari, A. P. Rendell, J. C. Burant, S. S. Iyengar, J. Tomasi, M. Cossi, J. M. Millam, M. Klene, C. Adamo, R. Cammi, J. W. Ochterski,

- R. L. Martin, K. Morokuma, O. Farkas, J. B. Foresman, D. J. Fox, *Gaussian ~09 Revision C.01*, Gaussian Inc., Wallingford, CT **2010**.
- [63] N. M. O'boyle, A. L. Tenderholt, K. M. Langner, *J. Comput. Chem.* **2008**, *29*, 839.
- [64] L. Goerigk, S. Grimme, *Phys. Chem. Chem. Phys.* **2011**, *13*, 6670.
- [65] N. Mardirossian, M. Head-Gordon, *Mol. Phys.* **2017**, *115*, 2315.
- [66] L. Goerigk, A. Hansen, C. Bauer, S. Ehrlich, A. Najibi, S. Grimme, *Phys. Chem. Chem. Phys.* **2017**, *19*, 32184.
- [67] R. Pérez-Soto, M. Besora, F. Maseras, *Org. Lett.* **2020**, *22*, 2873.
- [68] J. G. Brandenburg, C. Bannwarth, A. Hansen, S. Grimme, *J. Chem. Phys.* **2018**, *148*, 064104.
- [69] J. Zheng, *Science* **2006**, *313*, 1951.
- [70] J. M. Lehn, *Dynamic Stereochemistry*, Springer, Berlin, Heidelberg **1970**, p. 311.
- [71] N. Tanaka, Y. Xiao, A. C. Lasaga, *J. Atmos. Chem.* **1996**, *23*, 37.
- [72] J. Burkholder, S. Sander, J. Abbatt, J. Barker, C. Cappa, J. Crouse, T. Dibble, R. Huie, C. Kolb, M. Kurylo, V. L. Orkin, *Chemical kinetics and photochemical data for use in atmospheric studies; evaluation number, 19*, JPL Publication, Jet Propulsion Laboratory, Pasadena **2020**.
- [73] P. Pracht, S. Grimme, *Chem. A Eur. J.* **2021**, *125*, 5681.
- [74] R. Krishnan, J. S. Binkley, R. Seeger, J. A. Pople, *J. Chem. Phys.* **1980**, *72*, 650.
- [75] Y. Zhao, D. G. Truhlar, *Theor. Chem. Acc.* **2007**, *120*, 215.
- [76] R. N. Goldberg, N. Kishore, R. M. Lennen, *J. Phys. Chem. Ref. Data* **2002**, *31*, 231.
- [77] P. Neta, P. Maruthamuthu, P. M. Carton, R. W. Fessenden, *J. Phys. Chem.* **1978**, *82*, 1875.
- [78] A. J. Kirby, P. W. Lancaster, *J. Chem. Soc., Perkin Trans. 2* **1972**, 1206.
- [79] R. Karaman, *Comput. Theor. Chem.* **2011**, *974*, 133.
- [80] B. S. Souza, J. R. Mora, E. H. Wanderlind, R. M. Clementin, J. C. Gesser, H. D. Fiedler, F. Nome, F. M. Menger, *Angew. Chem. Int. Ed.* **2017**, *56*, 5345.
- [81] S. Su, F.-S. Du, Z.-C. Li, *Org. Biomol. Chem.* **2017**, *15*, 8384.
- [82] J.-D. Chai, M. Head-Gordon, *Phys. Chem. Chem. Phys.* **2008**, *10*, 6615.
- [83] S. E. Coelho, F. S. S. Schneider, D. C. de Oliveira, G. L. Tripodi, M. N. Eberlin, G. F. Caramori, B. de Souza, J. B. Domingos, *ACS Catal.* **2019**, *9*, 3792.
- [84] B. L. Oliveira, B. J. Stenton, V. B. Unnikrishnan, C. R. de Almeida, J. Conde, M. Negrão, F. S. S. Schneider, C. Cordeiro, M. G. Ferreira, G. F. Caramori, J. B. Domingos, R. Fior, G. J. L. Bernardes, *J. Am. Chem. Soc.* **2020**, *142*, 10869.
- [85] B. Partopour, A. G. Dixon, *Ind. Eng. Chem. Res.* **2019**, *58*, 5733.

SUPPORTING INFORMATION

Additional supporting information may be found in the online version of the article at the publisher's website.

How to cite this article: F. S. S. Schneider, G. F. Caramori, *J. Comput. Chem.* **2022**, *1*. <https://doi.org/10.1002/jcc.26861>

6 Concluding remarks and closing

The most important contributions presented in the present thesis, from the scientific and technological points of view, can be summarized as follows:

- **Electronic structure calculations of the transition state (TS) and/or intermediates have been applied in the elucidation of chemical reactions [1, 2].**

Approaches to reaction mechanism elucidation were described in general. Computational-experimental collaborative elucidation of two specific reaction mechanisms was described more explicitly, using density functional theory (DFT) calculations [1, 2].

- **The `overreact` software package has been developed for predicting chemical reaction kinetics and simulating microkinetics automatically from first principles [3].**

A third purely computational publication has been included, reporting the development of an open-source library and command-line application for automating the investigation of reaction mechanisms. The package was then applied to a series of different reactions in gas and solvated phases [3].

We hope that the original scientific articles published from the work done during the present thesis provided interesting and noteworthy insights in the elucidation of chemical reaction mechanisms, bridging the gap between classical mechanism elucidation and modern electronic structure calculations using a variety of methodologies, including the production of a software package for semiautonomous generation of kinetic profiles [3]. The implications of such contributions are twofold: • the potential to facilitate the elucidation of chemical reaction mechanisms in the future, and • ways of strongly automating such elucidations.

In terms of limitations, observations should be made regarding • effects that have not been taken into account in none of the reactions here, such as free-volume solvation entropies, conformational entropies, and others, • screening and explorative bias towards intuitive and well-known reaction motifs, as all pathways were conceived by the authors' chemical intuition, and • imprecisions due to methodological errors, such as potential deficiencies in density functional theory, whose implications can were lightly touched on in the `overreact` article [3], • limitations of classical transition state theory *per se*, which could in principle be overcome by other theories such as variational transition

state theory, although with an increased computational cost, • limitations of the applied classical transition state theory corrections, such as quantum tunnelling approximations and the *quasi*-rigid rotor-harmonic oscillator approximation.

The contributions posed here put in motion a new generation of models for the elucidation of complex route and emergent reaction mechanisms based on atomistic simulations and electronic structure calculations, which in future advancements may introduce the consideration of other effects into the picture while reducing the limitations listed above. There is a consensus that such methodological limitations need to be considered if the outcome of calculations is to be further explored and their limitations and consequences are to be correctly investigated. Future work is proposed to include and tackle the following issues:

- the inclusion of free-volume solvation entropies, for instance by implementing the approach in Garza [149], and conformational entropies, by using results provided by a fast method such as xTB [66],
- automatic screening and exploration of chemical reaction pathways by means of machine learning algorithms that have no or minimal inherent human bias,
- development of methods for estimating the systematic methodological errors in energies by direct comparison with experimental data, so that a correction be made for similar reactions of interest,
- incorporate the numerical calculation of rate constants using different theories, in particular, ones that broaden the applicability of the software, such as Marcus' theory [150–152], necessary in the modelling of reactions such as electron [150] and hydride [152] transfers,
- adjustment of reaction rate constants for diffusion-controlled regimes,
- use of improved quantum tunnelling corrections based on the shape of the calculated potential energy surface.

Finally, two further features are envisioned for addition in *overreact*, but don't necessarily mitigate the issues described above. The first is the automatic calculation of kinetic isotope effects in general. The other is the extension of the symmetry module to more complicated host-guest complexes in order to account for their individual symmetries: we currently detect point-group [106] and reaction symmetries but not internal symmetries of weakly bound complexes [108].

References

- 1 COELHO, S. E. et al. Mechanism of Palladium(II)-Mediated Uncaging Reactions of Propargylic Substrates. **ACS Catalysis**, American Chemical Society (ACS), v. 9, n. 5, p. 3792–3799, Mar. 2019. ISSN 2155-5435. DOI: [10.1021/acscatal.9b00210](https://doi.org/10.1021/acscatal.9b00210). Available from: <http://dx.doi.org/10.1021/acscatal.9b00210>>. Cit. on pp. 11, 13, 15, 20, 21, 44–47, 57, 87, 114.
- 2 OLIVEIRA, B. L. et al. Platinum-Triggered Bond-Cleavage of Pentynoyl Amide and N-Propargyl Handles for Drug-Activation. **Journal of the American Chemical Society**, American Chemical Society (ACS), v. 142, n. 24, p. 10869–10880, May 2020. ISSN 1520-5126. DOI: [10.1021/jacs.0c01622](https://doi.org/10.1021/jacs.0c01622). Available from: <http://dx.doi.org/10.1021/jacs.0c01622>>. Cit. on pp. 11, 14, 15, 20, 21, 44, 57–59, 87, 115.
- 3 SCHNEIDER, F. S. S.; CARAMORI, G. F. Overreact, an *in silico* lab: Automative quantum chemical microkinetic simulations for complex chemical reactions. **Journal of Computational Chemistry**, Wiley, Apr. 2022. ISSN 1096-987x. DOI: [10.1002/jcc.26861](https://doi.org/10.1002/jcc.26861). Available from: <http://dx.doi.org/10.1002/jcc.26861>>. Cit. on pp. 11, 14, 15, 20, 21, 37, 44, 73, 76, 87, 114, 115.
- 4 THE Nobel Prize in Chemistry 1918. [S.l.: s.n.], 1918. <https://www.nobelprize.org/prizes/chemistry/1918/summary/>. Accessed: 2022-12-05. Available from: <https://www.nobelprize.org/prizes/chemistry/1918/summary/>>. Cit. on p. 19.
- 5 ERISMAN, J. W. et al. How a century of ammonia synthesis changed the world. **Nature Geoscience**, Springer Science and Business Media LLC, v. 1, n. 10, p. 636–639, Sept. 2008. ISSN 1752-0908. DOI: [10.1038/ngeo325](https://doi.org/10.1038/ngeo325). Available from: <http://dx.doi.org/10.1038/ngeo325>>. Cit. on p. 19.
- 6 LEWIS, S. L.; MASLIN, M. A. Defining the Anthropocene. **Nature**, Springer Science and Business Media LLC, v. 519, n. 7542, p. 171–180, Mar. 2015. ISSN 1476-4687. DOI: [10.1038/nature14258](https://doi.org/10.1038/nature14258). Available from: <http://dx.doi.org/10.1038/nature14258>>. Cit. on p. 19.
- 7 THE Nobel Prize in Chemistry 1931. [S.l.: s.n.], 1931. <https://www.nobelprize.org/prizes/chemistry/1931/summary/>. Accessed: 2022-12-05. Available from:

- <<https://www.nobelprize.org/prizes/chemistry/1931/summary/>>. Cit. on p. 19.
- 8 SMIL, V. Detonator of the population explosion. **Nature**, Springer Science and Business Media LLC, v. 400, n. 6743, p. 415–415, July 1999. ISSN 1476-4687. DOI: [10.1038/22672](https://doi.org/10.1038/22672). Available from: <<http://dx.doi.org/10.1038/22672>>. Cit. on p. 19.
- 9 CANFIELD, D. E.; GLAZER, A. N.; FALKOWSKI, P. G. The Evolution and Future of Earth's Nitrogen Cycle. **Science**, American Association for the Advancement of Science (AAAS), v. 330, n. 6001, p. 192–196, Oct. 2010. ISSN 1095-9203. DOI: [10.1126/science.1186120](https://doi.org/10.1126/science.1186120). Available from: <<http://dx.doi.org/10.1126/science.1186120>>. Cit. on p. 19.
- 10 BERTOZZI, C. R. et al. Grand Challenges in Chemistry for 2016 and Beyond. **ACS Central Science**, American Chemical Society (ACS), v. 2, n. 1, p. 1–3, Jan. 2016. ISSN 2374-7951. DOI: [10.1021/acscentsci.6b00010](https://doi.org/10.1021/acscentsci.6b00010). Available from: <<http://dx.doi.org/10.1021/acscentsci.6b00010>>. Cit. on p. 19.
- 11 RECOGNIZING the Best in Innovation: Breakthrough Catalyst. [S.l.: s.n.], Sept. 2005. P. 20. R&D Magazine. Cit. on p. 19.
- 12 MARKET Report: Global Catalyst Market. Third. [S.l.]: Acmite Market Intelligence, Mar. 2015. P. 542. Cit. on p. 19.
- 13 KITCHIN, J. Preface: Trends in Computational Catalysis. **Topics in Catalysis**, Springer Science and Business Media LLC, v. 55, n. 5-6, p. 227–228, May 2012. ISSN 1572-9028. DOI: [10.1007/s11244-012-9808-0](https://doi.org/10.1007/s11244-012-9808-0). Available from: <<http://dx.doi.org/10.1007/s11244-012-9808-0>>. Cit. on pp. 19, 20.
- 14 HOUK, K. N.; LIU, P. Using Computational Chemistry to Understand & Discover Chemical Reactions. **Daedalus**, MIT Press — Journals, v. 143, n. 4, p. 49–66, Oct. 2014. ISSN 1548-6192. DOI: [10.1162/daed_a_00305](https://doi.org/10.1162/daed_a_00305). Available from: <http://dx.doi.org/10.1162/DAED%5C_a%5C_00305>. Cit. on p. 19.
- 15 CHEW, A. K. et al. Fast predictions of liquid-phase acid-catalyzed reaction rates using molecular dynamics simulations and convolutional neural networks. **Chemical Science**, Royal Society of Chemistry (RSC), v. 11, n. 46, p. 12464–12476, 2020. ISSN 2041-6539. DOI: [10.1039/d0sc03261a](https://doi.org/10.1039/d0sc03261a). Available from: <<http://dx.doi.org/10.1039/D0SC03261A>>. Cit. on p. 19.
- 16 CHIN, Y. P. et al. Computational discoveries of reaction mechanisms: recent highlights and emerging challenges. **Organic & Biomolecular Chemistry**, Royal Society of Chemistry (RSC), v. 20, n. 10, p. 2028–2042, 2022. ISSN 1477-0539. DOI: [10.1039/d1ob02139g](https://doi.org/10.1039/d1ob02139g). Available from: <<http://dx.doi.org/10.1039/D1OB02139G>>. Cit. on p. 19.

- 17 CAO, Y. et al. Reinforcement learning supercharges redox flow batteries. **Nature Machine Intelligence**, Springer Science and Business Media LLC, Aug. 2022. ISSN 2522-5839. DOI: [10.1038/s42256-022-00523-2](https://doi.org/10.1038/s42256-022-00523-2). Available from: <http://dx.doi.org/10.1038/s42256-022-00523-2>. Cit. on p. 19.
- 18 MAEDA, S.; MOROKUMA, K. Finding Reaction Pathways of Type $A + B \rightarrow X$: Toward Systematic Prediction of Reaction Mechanisms. **Journal of Chemical Theory and Computation**, American Chemical Society (ACS), v. 7, n. 8, p. 2335–2345, July 2011. ISSN 1549-9626. DOI: [10.1021/ct200290m](https://doi.org/10.1021/ct200290m). Available from: <http://dx.doi.org/10.1021/ct200290m>. Cit. on p. 20.
- 19 SIMM, G. N.; REIHER, M. Context-Driven Exploration of Complex Chemical Reaction Networks. **Journal of Chemical Theory and Computation**, American Chemical Society (ACS), v. 13, n. 12, p. 6108–6119, Nov. 2017. ISSN 1549-9626. DOI: [10.1021/acs.jctc.7b00945](https://doi.org/10.1021/acs.jctc.7b00945). Available from: <http://dx.doi.org/10.1021/acs.jctc.7b00945>. Cit. on p. 20.
- 20 RAPPOPORT, D.; ASPURU-GUZIK, A. Predicting Feasible Organic Reaction Pathways Using Heuristically Aided Quantum Chemistry. **Journal of Chemical Theory and Computation**, American Chemical Society (ACS), v. 15, n. 7, p. 4099–4112, June 2019. ISSN 1549-9626. DOI: [10.1021/acs.jctc.9b00126](https://doi.org/10.1021/acs.jctc.9b00126). Available from: <http://dx.doi.org/10.1021/acs.jctc.9b00126>. Cit. on p. 20.
- 21 PLATA, R. E.; SINGLETON, D. A. A Case Study of the Mechanism of Alcohol-Mediated Morita Baylis-Hillman Reactions. The Importance of Experimental Observations. **Journal of the American Chemical Society**, American Chemical Society (ACS), v. 137, n. 11, p. 3811–3826, Mar. 2015. ISSN 1520-5126. DOI: [10.1021/ja5111392](https://doi.org/10.1021/ja5111392). Available from: <http://dx.doi.org/10.1021/ja5111392>. Cit. on p. 20.
- 22 SANTORO, S. et al. Elucidation of Mechanisms and Selectivities of Metal-Catalyzed Reactions using Quantum Chemical Methodology. **Accounts of Chemical Research**, American Chemical Society (ACS), v. 49, n. 5, p. 1006–1018, Apr. 2016. ISSN 1520-4898. DOI: [10.1021/acs.accounts.6b00050](https://doi.org/10.1021/acs.accounts.6b00050). Available from: <http://dx.doi.org/10.1021/acs.accounts.6b00050>. Cit. on p. 20.
- 23 KOMP, E.; JANULAITIS, N.; VALLEAU, S. Progress towards machine learning reaction rate constants. **Physical Chemistry Chemical Physics**, Royal Society of Chemistry (RSC), v. 24, n. 5, p. 2692–2705, 2022. ISSN 1463-9084. DOI: [10.1039/d1cp04422b](https://doi.org/10.1039/d1cp04422b). Available from: <http://dx.doi.org/10.1039/d1cp04422b>. Cit. on p. 20.

- 24 TU, Z.; STUYVER, T.; COLEY, C. W. Predictive chemistry: machine learning for reaction deployment, reaction development, and reaction discovery. **Chemical Science**, Royal Society of Chemistry (RSC), 2022. ISSN 2041-6539. DOI: [10.1039/d2sc05089g](https://doi.org/10.1039/d2sc05089g). Available from: <http://dx.doi.org/10.1039/D2SC05089G>. Cit. on p. 20.
- 25 WANG, L.-P. et al. Discovering chemistry with an ab initio nanoreactor. **Nature Chemistry**, Springer Science and Business Media LLC, v. 6, n. 12, p. 1044–1048, Nov. 2014. ISSN 1755-4349. DOI: [10.1038/nchem.2099](https://doi.org/10.1038/nchem.2099). Available from: <http://dx.doi.org/10.1038/nchem.2099>. Cit. on p. 20.
- 26 PENG, Q.; DUARTE, F.; PATON, R. S. Computing organic stereoselectivity — from concepts to quantitative calculations and predictions. **Chemical Society Reviews**, Royal Society of Chemistry (RSC), v. 45, n. 22, p. 6093–6107, 2016. ISSN 1460-4744. DOI: [10.1039/c6cs00573j](https://doi.org/10.1039/c6cs00573j). Available from: <http://dx.doi.org/10.1039/C6CS00573J>. Cit. on p. 20.
- 27 JENCKS, W. P. **Catalysis in Chemistry and Enzymology**. [S.l.]: Dover Publications, 1987. ISBN 0486654605. Cit. on p. 20.
- 28 BESORA, M.; MASERAS, F. Microkinetic modelling in homogeneous catalysis. **Wiley Interdisciplinary Reviews: Computational Molecular Science**, Wiley, v. 8, n. 6, e1372, June 2018. ISSN 1759-0876. DOI: [10.1002/wcms.1372](https://doi.org/10.1002/wcms.1372). Available from: <http://dx.doi.org/10.1002/wcms.1372>. Cit. on p. 20.
- 29 SCHNEIDER, F. S. S. **geem-lab/overreact: overreact v1.0.2**. [S.l.]: Zenodo, Nov. 2021. <https://doi.org/10.5281/ZENODO.5730603>. Accessed: 2022-07-29. DOI: [10.5281/zenodo.5730603](https://doi.org/10.5281/zenodo.5730603). Available from: <https://zenodo.org/record/5730603>. Cit. on pp. 21, 44, 114, 115.
- 30 BORN, M.; OPPENHEIMER, R. Zur Quantentheorie der Molekeln. **Annalen der Physik**, Wiley, v. 389, n. 20, p. 457–484, 1927. ISSN 1521-3889. DOI: [10.1002/andp.19273892002](https://doi.org/10.1002/andp.19273892002). Available from: <http://dx.doi.org/10.1002/andp.19273892002>. Cit. on p. 25.
- 31 BANERJEE, A. et al. Search for stationary points on surfaces. **The Journal of Physical Chemistry**, American Chemical Society (ACS), v. 89, n. 1, p. 52–57, Jan. 1985. ISSN 1541-5740. DOI: [10.1021/j100247a015](https://doi.org/10.1021/j100247a015). Available from: <http://dx.doi.org/10.1021/j100247a015>. Cit. on pp. 25, 26.
- 32 ZIMMERMAN, P. M. Growing string method with interpolation and optimization in internal coordinates: Method and examples. **The Journal of Chemical Physics**, AIP Publishing, v. 138, n. 18, p. 184102, May 2013. ISSN 1089-7690. DOI: [10.1063/1.4804162](https://doi.org/10.1063/1.4804162). Available from: <http://dx.doi.org/10.1063/1.4804162>. Cit. on pp. 25, 26.

- 33 ZIMMERMAN, P. Reliable Transition State Searches Integrated with the Growing String Method. **Journal of Chemical Theory and Computation**, American Chemical Society (ACS), v. 9, n. 7, p. 3043–3050, June 2013. ISSN 1549-9626. DOI: [10.1021/ct400319w](https://doi.org/10.1021/ct400319w). Available from: <http://dx.doi.org/10.1021/ct400319w>. Cit. on pp. 25, 26.
- 34 ZIMMERMAN, P. M. Single-ended transition state finding with the growing string method. **Journal of Computational Chemistry**, Wiley, v. 36, n. 9, p. 601–611, Jan. 2015. ISSN 0192-8651. DOI: [10.1002/jcc.23833](https://doi.org/10.1002/jcc.23833). Available from: <http://dx.doi.org/10.1002/jcc.23833>. Cit. on pp. 25, 26.
- 35 JAFARI, M.; ZIMMERMAN, P. M. Reliable and efficient reaction path and transition state finding for surface reactions with the growing string method. **Journal of Computational Chemistry**, Wiley, v. 38, n. 10, p. 645–658, Jan. 2017. ISSN 0192-8651. DOI: [10.1002/jcc.24720](https://doi.org/10.1002/jcc.24720). Available from: <http://dx.doi.org/10.1002/jcc.24720>. Cit. on pp. 25, 26.
- 36 SCHLEGEL, H. B. Optimization of Equilibrium Geometries and Transition Structures. In: *AB Initio Methods in Quantum Chemistry, Part 1 (Advances in Chemical Physics)*. [S.l.]: Wiley-Interscience, Mar. 1987. P. 249–286. ISBN 9780471909002. DOI: [10.1002/9780470142936.ch4](https://doi.org/10.1002/9780470142936.ch4). Available from: <http://dx.doi.org/10.1002/9780470142936.ch4>. Cit. on pp. 25, 26.
- 37 PENG, C.; BERNHARD SCHLEGEL, H. Combining Synchronous Transit and Quasi-Newton Methods to Find Transition States. **Israel Journal of Chemistry**, Wiley-Blackwell, v. 33, n. 4, p. 449–454, 1993. ISSN 0021-2148. DOI: [10.1002/ijch.199300051](https://doi.org/10.1002/ijch.199300051). Available from: <http://dx.doi.org/10.1002/ijch.199300051>. Cit. on pp. 25, 26.
- 38 PENG, C. et al. Using redundant internal coordinates to optimize equilibrium geometries and transition states. **Journal of Computational Chemistry**, Wiley-Blackwell, v. 17, n. 1, p. 49–56, Jan. 1996. ISSN 1096-987x. DOI: [10.1002/\(sici\)1096-987x\(19960115\)17:1<49::aid-jcc5>3.0.co;2-0](https://doi.org/10.1002/(sici)1096-987x(19960115)17:1<49::aid-jcc5>3.0.co;2-0). Available from: [http://dx.doi.org/10.1002/\(SICI\)1096-987X\(19960115\)17:1%3C49::AID-JCC5%3E3.0.CO;2-0](http://dx.doi.org/10.1002/(SICI)1096-987X(19960115)17:1%3C49::AID-JCC5%3E3.0.CO;2-0). Cit. on pp. 25, 26.
- 39 HENKELMAN, G.; UBERUAGA, B. P.; JÓNSSON, H. A climbing image nudged elastic band method for finding saddle points and minimum energy paths. **The Journal of Chemical Physics**, AIP Publishing, v. 113, n. 22, p. 9901–9904, Dec. 2000. ISSN 1089-7690. DOI: [10.1063/1.1329672](https://doi.org/10.1063/1.1329672). Available from: <http://dx.doi.org/10.1063/1.1329672>. Cit. on pp. 25, 26.
- 40 HENKELMAN, G.; JÓNSSON, H. Improved tangent estimate in the nudged elastic band method for finding minimum energy paths and saddle points. **The Journal of Chemical Physics**, AIP Publishing, v. 113, n. 22, p. 9978–9985, Dec.

2000. ISSN 1089-7690. DOI: [10.1063/1.1323224](https://doi.org/10.1063/1.1323224). Available from: <http://dx.doi.org/10.1063/1.1323224>>. Cit. on pp. 25, 26.
- 41 HENKELMAN, G.; JÓHANNESON, G.; JÓNSSON, H. Methods for Finding Saddle Points and Minimum Energy Paths. **Progress in Theoretical Chemistry and Physics**, Kluwer Academic Publishers, p. 269–302, 2002. DOI: [10.1007/0-306-46949-9_10](https://doi.org/10.1007/0-306-46949-9_10). Available from: http://dx.doi.org/10.1007/0-306-46949-9_10>. Cit. on pp. 25, 26.
- 42 MAURO, J. C.; LOUCKS, R. J.; BALAKRISHNAN, J. A Simplified Eigenvector-Following Technique for Locating Transition Points in an Energy Landscape. **The Journal of Physical Chemistry A**, American Chemical Society (ACS), v. 109, n. 42, p. 9578–9583, Oct. 2005. ISSN 1520-5215. DOI: [10.1021/jp053581t](https://doi.org/10.1021/jp053581t). Available from: <http://dx.doi.org/10.1021/jp053581t>>. Cit. on pp. 25, 26.
- 43 SHEPPARD, D.; TERRELL, R.; HENKELMAN, G. Optimization methods for finding minimum energy paths. **The Journal of Chemical Physics**, AIP Publishing, v. 128, n. 13, p. 134106, Apr. 2008. ISSN 1089-7690. DOI: [10.1063/1.2841941](https://doi.org/10.1063/1.2841941). Available from: <http://dx.doi.org/10.1063/1.2841941>>. Cit. on pp. 25, 26.
- 44 PERDEW, J. P. Jacob's ladder of density functional approximations for the exchange-correlation energy. **AIP Conference Proceedings**, Aip, 2001. ISSN 0094-243x. DOI: [10.1063/1.1390175](https://doi.org/10.1063/1.1390175). Available from: <http://dx.doi.org/10.1063/1.1390175>>. Cit. on p. 26.
- 45 HOHENBERG, P.; KOHN, W. Inhomogeneous Electron Gas. **Physical Review**, American Physical Society (APS), v. 136, 3b, b864–b871, Nov. 1964. ISSN 0031-899x. DOI: [10.1103/physrev.136.b864](https://doi.org/10.1103/physrev.136.b864). Available from: <http://dx.doi.org/10.1103/PhysRev.136.B864>>. Cit. on p. 26.
- 46 ARAGÓ, J. et al. Ab Initio Modelling of Donor-Acceptor Interactions and Charge-Transfer Excitations in Molecular Complexes: The Case of Terthiophene-Tetracyanoquinodimethane. **Journal of Chemical Theory and Computation**, American Chemical Society (ACS), v. 7, n. 7, p. 2068–2077, July 2011. ISSN 1549-9626. DOI: [10.1021/ct200203k](https://doi.org/10.1021/ct200203k). Available from: <http://dx.doi.org/10.1021/ct200203k>>. Cit. on p. 26.
- 47 SALZNER, U.; AYDIN, A. Improved Prediction of Properties of π -Conjugated Oligomers with Range-Separated Hybrid Density Functionals. **Journal of Chemical Theory and Computation**, American Chemical Society (ACS), v. 7, n. 8, p. 2568–2583, Aug. 2011. ISSN 1549-9626. DOI: [10.1021/ct2003447](https://doi.org/10.1021/ct2003447). Available from: <http://dx.doi.org/10.1021/ct2003447>>. Cit. on p. 26.

- 48 BURNS, L. A. et al. Density-functional approaches to noncovalent interactions: A comparison of dispersion corrections (DFT-D), exchange-hole dipole moment (XDM) theory, and specialized functionals. **The Journal of Chemical Physics**, AIP Publishing, v. 134, n. 8, p. 084107, Feb. 2011. ISSN 1089-7690. DOI: [10.1063/1.3545971](https://doi.org/10.1063/1.3545971). Available from: <http://dx.doi.org/10.1063/1.3545971>. Cit. on p. 26.
- 49 MINENKOV, Y. et al. The accuracy of DFT-optimized geometries of functional transition metal compounds: a validation study of catalysts for olefin metathesis and other reactions in the homogeneous phase. **Dalton Transactions**, Royal Society of Chemistry (RSC), v. 41, n. 18, p. 5526, 2012. ISSN 1477-9234. DOI: [10.1039/c2dt12232d](https://doi.org/10.1039/c2dt12232d). Available from: <http://dx.doi.org/10.1039/C2DT12232D>. Cit. on pp. 26, 27.
- 50 PERDEW, J. P. et al. Gedanken densities and exact constraints in density functional theory. **The Journal of Chemical Physics**, AIP Publishing, v. 140, n. 18, 18a533, May 2014. ISSN 1089-7690. DOI: [10.1063/1.4870763](https://doi.org/10.1063/1.4870763). Available from: <http://dx.doi.org/10.1063/1.4870763>. Cit. on p. 26.
- 51 KRYACHKO, E. S.; LUDEÑA, E. V. Density functional theory: Foundations reviewed. **Physics Reports**, Elsevier BV, v. 544, n. 2, p. 123–239, Nov. 2014. ISSN 0370-1573. DOI: [10.1016/j.physrep.2014.06.002](https://doi.org/10.1016/j.physrep.2014.06.002). Available from: <http://dx.doi.org/10.1016/j.physrep.2014.06.002>. Cit. on p. 26.
- 52 YU, H. S.; LI, S. L.; TRUHLAR, D. G. Perspective: Kohn-Sham density functional theory descending a staircase. **The Journal of Chemical Physics**, AIP Publishing, v. 145, n. 13, p. 130901, Oct. 2016. ISSN 1089-7690. DOI: [10.1063/1.4963168](https://doi.org/10.1063/1.4963168). Available from: <http://dx.doi.org/10.1063/1.4963168>. Cit. on p. 26.
- 53 SWART, M.; BICKELHAUPT, F. M.; DURAN, M. **DFT2016 poll**. [S.l.: s.n.], 2016. <http://www.marcelswart.eu/dft-poll/news2016.pdf>. Accessed: 2017-06-10. Available from: <http://www.marcelswart.eu/dft-poll/news2016.pdf>. Cit. on p. 26.
- 54 KOHN, W.; SHAM, L. J. Self-Consistent Equations Including Exchange and Correlation Effects. **Physical Review**, American Physical Society (APS), v. 140, 4a, a1133–a1138, Nov. 1965. ISSN 0031-899x. DOI: [10.1103/physrev.140.a1133](https://doi.org/10.1103/physrev.140.a1133). Available from: <http://dx.doi.org/10.1103/PhysRev.140.A1133>. Cit. on p. 26.
- 55 PERDEW, J. P.; BURKE, K.; ERNZERHOF, M. Generalized Gradient Approximation Made Simple. **Physical Review Letters**, American Physical Society (APS), v. 77, n. 18, p. 3865–3868, Oct. 1996. ISSN 1079-7114. DOI:

- [10.1103/physrevlett.77.3865](https://doi.org/10.1103/physrevlett.77.3865). Available from:
<<http://dx.doi.org/10.1103/PhysRevLett.77.3865>>. Cit. on p. 26.
- 56 PERDEW, J. P.; BURKE, K.; ERNZERHOF, M. Generalized Gradient Approximation Made Simple [Phys. Rev. Lett. 77, 3865 (1996)]. **Physical Review Letters**, American Physical Society (APS), v. 78, n. 7, p. 1396–1396, Feb. 1997. ISSN 1079-7114. DOI: [10.1103/physrevlett.78.1396](https://doi.org/10.1103/physrevlett.78.1396). Available from: <<http://dx.doi.org/10.1103/PhysRevLett.78.1396>>. Cit. on p. 26.
- 57 ERNZERHOF, M.; SCUSERIA, G. E. Assessment of the Perdew-Burke-Ernzerhof exchange-correlation functional. **The Journal of Chemical Physics**, AIP Publishing, v. 110, n. 11, p. 5029–5036, Mar. 1999. ISSN 1089-7690. DOI: [10.1063/1.478401](https://doi.org/10.1063/1.478401). Available from: <<http://dx.doi.org/10.1063/1.478401>>. Cit. on p. 26.
- 58 ADAMO, C.; BARONE, V. Toward reliable density functional methods without adjustable parameters: The PBE0 model. **The Journal of Chemical Physics**, AIP Publishing, v. 110, n. 13, p. 6158–6170, Apr. 1999. ISSN 1089-7690. DOI: [10.1063/1.478522](https://doi.org/10.1063/1.478522). Available from: <<http://dx.doi.org/10.1063/1.478522>>. Cit. on p. 26.
- 59 CHAI, J.-D.; HEAD-GORDON, M. Systematic optimization of long-range corrected hybrid density functionals. **The Journal of Chemical Physics**, AIP Publishing, v. 128, n. 8, p. 084106, Feb. 2008. ISSN 1089-7690. DOI: [10.1063/1.2834918](https://doi.org/10.1063/1.2834918). Available from: <<http://dx.doi.org/10.1063/1.2834918>>. Cit. on p. 26.
- 60 _____. Long-range corrected hybrid density functionals with damped atom-atom dispersion corrections. **Physical Chemistry Chemical Physics**, Royal Society of Chemistry (RSC), v. 10, n. 44, p. 6615, 2008. ISSN 1463-9084. DOI: [10.1039/b810189b](https://doi.org/10.1039/b810189b). Available from: <<http://dx.doi.org/10.1039/B810189B>>. Cit. on p. 26.
- 61 GOERIGK, L.; GRIMME, S. A thorough benchmark of density functional methods for general main group thermochemistry, kinetics, and noncovalent interactions. **Physical Chemistry Chemical Physics**, Royal Society of Chemistry (RSC), v. 13, n. 14, p. 6670, 2011. ISSN 1463-9084. DOI: [10.1039/c0cp02984j](https://doi.org/10.1039/c0cp02984j). Available from: <<http://dx.doi.org/10.1039/c0cp02984j>>. Cit. on pp. 26, 27.
- 62 SZABO, A.; OSTLUND, N. S. **Modern Quantum Chemistry: Introduction to Advanced Electronic Structure Theory (Dover Books on Chemistry)**. [S.l.]: Dover Publications, 1996. ISBN 0486691861. Cit. on p. 26.

- 63 RIPLINGER, C. et al. Natural triple excitations in local coupled cluster calculations with pair natural orbitals. **The Journal of Chemical Physics**, AIP Publishing, v. 139, n. 13, p. 134101, Oct. 2013. ISSN 1089-7690. DOI: [10.1063/1.4821834](https://doi.org/10.1063/1.4821834). Available from: <http://dx.doi.org/10.1063/1.4821834>>. Cit. on pp. 26, 28.
- 64 RIPLINGER, C. et al. Sparse maps—A systematic infrastructure for reduced-scaling electronic structure methods. II. Linear scaling domain based pair natural orbital coupled cluster theory. **The Journal of Chemical Physics**, AIP Publishing, v. 144, n. 2, p. 024109, Jan. 2016. ISSN 1089-7690. DOI: [10.1063/1.4939030](https://doi.org/10.1063/1.4939030). Available from: <http://dx.doi.org/10.1063/1.4939030>>. Cit. on pp. 26, 28.
- 65 STEWART, J. J. P. **Mopac2016**. [S.l.: s.n.], 2016. <http://openmopac.net/>. Stewart Computational Chemistry, Colorado Springs, CO, USA. Accessed: 2018-04-19. Available from: <http://openmopac.net/>>. Cit. on p. 26.
- 66 BANNWARTH, C. et al. Extended tight-binding quantum chemistry methods. **WIREs Computational Molecular Science**, Wiley, v. 11, n. 2, Aug. 2020. ISSN 1759-0884. DOI: [10.1002/wcms.1493](https://doi.org/10.1002/wcms.1493). Available from: <http://dx.doi.org/10.1002/wcms.1493>>. Cit. on pp. 26, 88.
- 67 MARENICH, A. V.; CRAMER, C. J.; TRUHLAR, D. G. Universal Solvation Model Based on Solute Electron Density and on a Continuum Model of the Solvent Defined by the Bulk Dielectric Constant and Atomic Surface Tensions. **The Journal of Physical Chemistry B**, American Chemical Society (ACS), v. 113, n. 18, p. 6378–6396, May 2009. ISSN 1520-5207. DOI: [10.1021/jp810292n](https://doi.org/10.1021/jp810292n). Available from: <http://dx.doi.org/10.1021/jp810292n>>. Cit. on pp. 26, 40.
- 68 MARENICH, A. V. et al. Resolution of a Challenge for Solvation Modelling: Calculation of Dicarboxylic Acid Dissociation Constants Using Mixed Discrete-Continuum Solvation Models. **The Journal of Physical Chemistry Letters**, American Chemical Society (ACS), v. 3, n. 11, p. 1437–1442, May 2012. ISSN 1948-7185. DOI: [10.1021/jz300416r](https://doi.org/10.1021/jz300416r). Available from: <http://dx.doi.org/10.1021/jz300416r>>. Cit. on p. 26.
- 69 DITCHFIELD, R.; HEHRE, W. J.; POPLER, J. A. Self-Consistent Molecular-Orbital Methods. IX. An Extended Gaussian-Type Basis for Molecular-Orbital Studies of Organic Molecules. **The Journal of Chemical Physics**, AIP Publishing, v. 54, n. 2, p. 724–728, Jan. 1971. ISSN 1089-7690. DOI: [10.1063/1.1674902](https://doi.org/10.1063/1.1674902). Available from: <http://dx.doi.org/10.1063/1.1674902>>. Cit. on p. 26.

- 70 HELGAKER, T. et al. The prediction of molecular equilibrium structures by the standard electronic wave functions. **The Journal of Chemical Physics**, AIP Publishing, v. 106, n. 15, p. 6430–6440, Apr. 1997. ISSN 1089-7690. DOI: [10.1063/1.473634](http://dx.doi.org/10.1063/1.473634). Available from: <http://dx.doi.org/10.1063/1.473634>. Cit. on p. 26.
- 71 BLAUDEAU, J.-P. et al. Extension of Gaussian-2 (G2) theory to molecules containing third-row atoms K and Ca. **The Journal of Chemical Physics**, AIP Publishing, v. 107, n. 13, p. 5016–5021, Oct. 1997. ISSN 1089-7690. DOI: [10.1063/1.474865](http://dx.doi.org/10.1063/1.474865). Available from: <http://dx.doi.org/10.1063/1.474865>. Cit. on p. 26.
- 72 RASSOLOV, V. A. et al. 6-31G*basis set for atoms K through Zn. **The Journal of Chemical Physics**, AIP Publishing, v. 109, n. 4, p. 1223–1229, July 1998. ISSN 1089-7690. DOI: [10.1063/1.476673](http://dx.doi.org/10.1063/1.476673). Available from: <http://dx.doi.org/10.1063/1.476673>. Cit. on p. 26.
- 73 RASSOLOV, V. A. et al. 6-31G*basis set for third-row atoms. **Journal of Computational Chemistry**, Wiley-Blackwell, v. 22, n. 9, p. 976–984, 2001. ISSN 1096-987x. DOI: [10.1002/jcc.1058](http://dx.doi.org/10.1002/jcc.1058). Available from: <http://dx.doi.org/10.1002/jcc.1058>. Cit. on p. 26.
- 74 JENSEN, F. Atomic orbital basis sets. **Wiley Interdisciplinary Reviews: Computational Molecular Science**, Wiley, v. 3, n. 3, p. 273–295, Oct. 2012. ISSN 1759-0876. DOI: [10.1002/wcms.1123](http://dx.doi.org/10.1002/wcms.1123). Available from: <http://dx.doi.org/10.1002/wcms.1123>. Cit. on p. 26.
- 75 HILL, J. G. Gaussian basis sets for molecular applications. **International Journal of Quantum Chemistry**, Wiley, v. 113, n. 1, p. 21–34, Oct. 2012. ISSN 0020-7608. DOI: [10.1002/qua.24355](http://dx.doi.org/10.1002/qua.24355). Available from: <http://dx.doi.org/10.1002/qua.24355>. Cit. on p. 26.
- 76 HEHRE, W. J.; DITCHFIELD, R.; POPLÉ, J. A. Self-Consistent Molecular Orbital Methods. XII. Further Extensions of Gaussian-Type Basis Sets for Use in Molecular Orbital Studies of Organic Molecules. **The Journal of Chemical Physics**, AIP Publishing, v. 56, n. 5, p. 2257–2261, Mar. 1972. ISSN 1089-7690. DOI: [10.1063/1.1677527](http://dx.doi.org/10.1063/1.1677527). Available from: <http://dx.doi.org/10.1063/1.1677527>. Cit. on p. 26.
- 77 HARIHARAN, P. C.; POPLÉ, J. A. The influence of polarization functions on molecular orbital hydrogenation energies. **Theoretica Chimica Acta**, Springer Nature, v. 28, n. 3, p. 213–222, 1973. ISSN 1432-2234. DOI: [10.1007/bf00533485](http://dx.doi.org/10.1007/bf00533485). Available from: <http://dx.doi.org/10.1007/BF00533485>. Cit. on p. 26.

- 78 _____. Accuracy of AHnequilibrium geometries by single determinant molecular orbital theory. **Molecular Physics**, Informa UK Limited, v. 27, n. 1, p. 209–214, Jan. 1974. ISSN 1362-3028. DOI: [10.1080/00268977400100171](https://doi.org/10.1080/00268977400100171). Available from: <http://dx.doi.org/10.1080/00268977400100171>>. Cit. on p. 26.
- 79 GORDON, M. S. The isomers of silacyclopropane. **Chemical Physics Letters**, Elsevier BV, v. 76, n. 1, p. 163–168, Nov. 1980. ISSN 0009-2614. DOI: [10.1016/0009-2614\(80\)80628-2](https://doi.org/10.1016/0009-2614(80)80628-2). Available from: [http://dx.doi.org/10.1016/0009-2614\(80\)80628-2](http://dx.doi.org/10.1016/0009-2614(80)80628-2)>. Cit. on p. 26.
- 80 FRANCL, M. M. et al. Self-consistent molecular orbital methods. XXIII. A polarization-type basis set for second-row elements. **The Journal of Chemical Physics**, AIP Publishing, v. 77, n. 7, p. 3654–3665, Oct. 1982. ISSN 1089-7690. DOI: [10.1063/1.444267](https://doi.org/10.1063/1.444267). Available from: <http://dx.doi.org/10.1063/1.444267>>. Cit. on p. 26.
- 81 CLARK, T. et al. Efficient diffuse function-augmented basis sets for anion calculations. III. The 3-21+G basis set for first-row elements, Li-F. **Journal of Computational Chemistry**, Wiley-Blackwell, v. 4, n. 3, p. 294–301, 1983. ISSN 1096-987x. DOI: [10.1002/jcc.540040303](https://doi.org/10.1002/jcc.540040303). Available from: <http://dx.doi.org/10.1002/jcc.540040303>>. Cit. on p. 26.
- 82 FRISCH, M. J.; POPLER, J. A.; BINKLEY, J. S. Self-consistent molecular orbital methods 25. Supplementary functions for Gaussian basis sets. **The Journal of Chemical Physics**, AIP Publishing, v. 80, n. 7, p. 3265–3269, Apr. 1984. ISSN 1089-7690. DOI: [10.1063/1.447079](https://doi.org/10.1063/1.447079). Available from: <http://dx.doi.org/10.1063/1.447079>>. Cit. on p. 26.
- 83 BINNING, R. C.; CURTISS, L. A. Compact contracted basis sets for third-row atoms: Ga-Kr. **Journal of Computational Chemistry**, Wiley-Blackwell, v. 11, n. 10, p. 1206–1216, Nov. 1990. ISSN 1096-987x. DOI: [10.1002/jcc.540111013](https://doi.org/10.1002/jcc.540111013). Available from: <http://dx.doi.org/10.1002/jcc.540111013>>. Cit. on p. 26.
- 84 FRISCH, M. J. et al. **Gaussian 09 Revision C.01**. [S.l.: s.n.], 2009. Gaussian Inc. Wallingford CT. Cit. on p. 26.
- 85 NEESE, F. Software update: the ORCA program system, version 4.0. **WIREs Computational Molecular Science**, Wiley, v. 8, n. 1, July 2017. ISSN 1759-0884. DOI: [10.1002/wcms.1327](https://doi.org/10.1002/wcms.1327). Available from: <http://dx.doi.org/10.1002/wcms.1327>>. Cit. on p. 26.
- 86 GOERIGK, L.; MEHTA, N. A Trip to the Density Functional Theory Zoo: Warnings and Recommendations for the User. **Australian Journal of Chemistry**, CSIRO Publishing, v. 72, n. 8, p. 563, 2019. ISSN 0004-9425. DOI:

- [10.1071/ch19023](http://dx.doi.org/10.1071/CH19023). Available from: <<http://dx.doi.org/10.1071/CH19023>>. Cit. on p. 26.
- 87 MARDIROSSIAN, N.; HEAD-GORDON, M. Thirty years of density functional theory in computational chemistry: an overview and extensive assessment of 200 density functionals. **Molecular Physics**, Informa UK Limited, v. 115, n. 19, p. 2315–2372, June 2017. ISSN 1362-3028. DOI: [10.1080/00268976.2017.1333644](http://dx.doi.org/10.1080/00268976.2017.1333644). Available from: <<http://dx.doi.org/10.1080/00268976.2017.1333644>>. Cit. on pp. 26, 27.
- 88 MORGANTE, P.; PEVERATI, R. The devil in the details: A tutorial review on some undervalued aspects of density functional theory calculations. **International Journal of Quantum Chemistry**, Wiley, v. 120, n. 18, June 2020. ISSN 1097-461x. DOI: [10.1002/qua.26332](http://dx.doi.org/10.1002/qua.26332). Available from: <<http://dx.doi.org/10.1002/qua.26332>>. Cit. on p. 26.
- 89 BURSCH, M. et al. Best-Practice DFT Protocols for Basic Molecular Computational Chemistry**. **Angewandte Chemie**, Wiley, v. 134, n. 42, Sept. 2022. ISSN 1521-3757. DOI: [10.1002/ange.202205735](http://dx.doi.org/10.1002/ange.202205735). Available from: <<http://dx.doi.org/10.1002/ange.202205735>>. Cit. on pp. 26–28.
- 90 BÜHL, M.; KABREDE, H. Geometries of Transition-Metal Complexes from Density-Functional Theory. **Journal of Chemical Theory and Computation**, American Chemical Society (ACS), v. 2, n. 5, p. 1282–1290, June 2006. ISSN 1549-9626. DOI: [10.1021/ct6001187](http://dx.doi.org/10.1021/ct6001187). Available from: <<http://dx.doi.org/10.1021/ct6001187>>. Cit. on p. 26.
- 91 SIRIANNI, D. A. et al. Assessment of Density Functional Methods for Geometry Optimization of Bimolecular van der Waals Complexes. **Journal of Chemical Theory and Computation**, American Chemical Society (ACS), v. 14, n. 6, p. 3004–3013, May 2018. ISSN 1549-9626. DOI: [10.1021/acs.jctc.8b00114](http://dx.doi.org/10.1021/acs.jctc.8b00114). Available from: <<http://dx.doi.org/10.1021/acs.jctc.8b00114>>. Cit. on p. 27.
- 92 KATARI, M. et al. Improved Infrared Spectra Prediction by DFT from a New Experimental Database. **Chemistry — A European Journal**, Wiley, v. 23, n. 35, p. 8414–8423, Apr. 2017. ISSN 0947-6539. DOI: [10.1002/chem.201700340](http://dx.doi.org/10.1002/chem.201700340). Available from: <<http://dx.doi.org/10.1002/chem.201700340>>. Cit. on p. 27.
- 93 HOWARD, J. C.; ENYARD, J. D.; TSCHUMPER, G. S. Assessing the accuracy of some popular DFT methods for computing harmonic vibrational frequencies of water clusters. **The Journal of Chemical Physics**, AIP Publishing, v. 143, n. 21, p. 214103, Dec. 2015. ISSN 1089-7690. DOI: [10.1063/1.4936654](http://dx.doi.org/10.1063/1.4936654). Available from: <<http://dx.doi.org/10.1063/1.4936654>>. Cit. on p. 27.

- 94 GRIMME, S. et al. Consistent structures and interactions by density functional theory with small atomic orbital basis sets. **The Journal of Chemical Physics**, AIP Publishing, v. 143, n. 5, p. 054107, Aug. 2015. ISSN 1089-7690. DOI: [10.1063/1.4927476](https://doi.org/10.1063/1.4927476). Available from: <http://dx.doi.org/10.1063/1.4927476>. Cit. on p. 28.
- 95 PAIVA, P.; RAMOS, M. J.; FERNANDES, P. A. Assessing the validity of DLPNO-CCSD(T) in the calculation of activation and reaction energies of ubiquitous enzymatic reactions. **Journal of Computational Chemistry**, Wiley, v. 41, n. 29, p. 2459–2468, Sept. 2020. ISSN 1096-987x. DOI: [10.1002/jcc.26401](https://doi.org/10.1002/jcc.26401). Available from: <http://dx.doi.org/10.1002/jcc.26401>. Cit. on p. 28.
- 96 SANDLER, I. et al. Accuracy of DLPNO-CCSD(T): Effect of Basis Set and System Size. **The Journal of Physical Chemistry A**, American Chemical Society (ACS), v. 125, n. 7, p. 1553–1563, Feb. 2021. ISSN 1520-5215. DOI: [10.1021/acs.jpca.0c11270](https://doi.org/10.1021/acs.jpca.0c11270). Available from: <http://dx.doi.org/10.1021/acs.jpca.0c11270>. Cit. on p. 28.
- 97 O'BOYLE, N. M.; TENDERHOLT, A. L.; LANGNER, K. M. ccLib: A library for package-independent computational chemistry algorithms. **Journal of Computational Chemistry**, Wiley, v. 29, n. 5, p. 839–845, 2008. ISSN 1096-987x. DOI: [10.1002/jcc.20823](https://doi.org/10.1002/jcc.20823). Available from: <http://dx.doi.org/10.1002/jcc.20823>. Cit. on pp. 28, 74.
- 98 RIBEIRO, R. F. et al. Use of Solution-Phase Vibrational Frequencies in Continuum Models for the Free Energy of Solvation. **The Journal of Physical Chemistry B**, American Chemical Society (ACS), v. 115, n. 49, p. 14556–14562, Dec. 2011. ISSN 1520-5207. DOI: [10.1021/jp205508z](https://doi.org/10.1021/jp205508z). Available from: <http://dx.doi.org/10.1021/jp205508z>. Cit. on pp. 29, 31.
- 99 MCQUARRIE, D. et al. **Physical Chemistry: A Molecular Approach**. [S.l.]: University Science Books, 1997. (G — Reference, Information and Interdisciplinary Subjects Series). ISBN 9780935702996. Available from: <https://books.google.com.br/books?id=f-bje0-DEYUC>. Cit. on p. 29.
- 100 JENSEN, J. H. Predicting accurate absolute binding energies in aqueous solution: thermodynamic considerations for electronic structure methods. **Physical Chemistry Chemical Physics**, Royal Society of Chemistry (RSC), v. 17, n. 19, p. 12441–12451, 2015. ISSN 1463-9084. DOI: [10.1039/c5cp00628g](https://doi.org/10.1039/c5cp00628g). Available from: <http://dx.doi.org/10.1039/c5cp00628g>. Cit. on pp. 30, 31, 35.
- 101 GRIMME, S. Supramolecular Binding Thermodynamics by Dispersion-Corrected Density Functional Theory. **Chemistry — A European Journal**, Wiley, v. 18, n. 32, p. 9955–9964, July 2012. ISSN 0947-6539. DOI: [10.1002/chem.201200497](https://doi.org/10.1002/chem.201200497).

- Available from: <<http://dx.doi.org/10.1002/chem.201200497>>. Cit. on pp. 31, 32.
- 102 RYU, H. et al. Pitfalls in Computational Modelling of Chemical Reactions and How To Avoid Them. **Organometallics**, American Chemical Society (ACS), v. 37, n. 19, p. 3228–3239, Sept. 2018. ISSN 1520-6041. DOI: [10.1021/acs.organomet.8b00456](https://doi.org/10.1021/acs.organomet.8b00456). Available from: <<http://dx.doi.org/10.1021/acs.organomet.8b00456>>. Cit. on pp. 31, 39.
- 103 CHAI, J.-D.; HEAD-GORDON, M. Long-range corrected hybrid density functionals with damped atom-atom dispersion corrections. **Physical Chemistry Chemical Physics**, Royal Society of Chemistry (RSC), v. 10, n. 44, p. 6615, 2008. ISSN 1463-9084. DOI: [10.1039/b810189b](https://doi.org/10.1039/b810189b). Available from: <<http://dx.doi.org/10.1039/B810189B>>. Cit. on p. 31.
- 104 LI, Y.-P. et al. Improved Force-Field Parameters for QM/MM Simulations of the Energies of Adsorption for Molecules in Zeolites and a Free Rotor Correction to the Rigid Rotor Harmonic Oscillator Model for Adsorption Enthalpies. **The Journal of Physical Chemistry C**, American Chemical Society (ACS), v. 119, n. 4, p. 1840–1850, Jan. 2015. ISSN 1932-7455. DOI: [10.1021/jp509921r](https://doi.org/10.1021/jp509921r). Available from: <<http://dx.doi.org/10.1021/jp509921r>>. Cit. on pp. 31, 32.
- 105 INPUT format reference — overreact documentation. [S.l.: s.n.], 2022. <https://geem-lab.github.io/overreact-guide/input.html>. Accessed: 2022-12-14. Available from: <<https://geem-lab.github.io/overreact-guide/input.html>>. Cit. on pp. 31, 32.
- 106 BERUSKI, O.; VIDAL, L. N. Algorithms for computer detection of symmetry elements in molecular systems. **Journal of Computational Chemistry**, Wiley, v. 35, n. 4, p. 290–299, Nov. 2013. ISSN 0192-8651. DOI: [10.1002/jcc.23493](https://doi.org/10.1002/jcc.23493). Available from: <<http://dx.doi.org/10.1002/jcc.23493>>. Cit. on pp. 31, 73, 88.
- 107 FERNÁNDEZ-RAMOS, A. et al. Symmetry numbers and chemical reaction rates. **Theoretical Chemistry Accounts**, Springer Science and Business Media LLC, v. 118, n. 4, p. 813–826, July 2007. ISSN 1432-2234. DOI: [10.1007/s00214-007-0328-0](https://doi.org/10.1007/s00214-007-0328-0). Available from: <<http://dx.doi.org/10.1007/s00214-007-0328-0>>. Cit. on pp. 32, 35.
- 108 GILSON, M. K.; IRIKURA, K. K. Symmetry Numbers for Rigid, Flexible, and Fluxional Molecules: Theory and Applications†. **The Journal of Physical Chemistry B**, American Chemical Society (ACS), v. 114, n. 49, p. 16304–16317, Dec. 2010. ISSN 1520-5207. DOI: [10.1021/jp110434s](https://doi.org/10.1021/jp110434s). Available from: <<http://dx.doi.org/10.1021/jp110434s>>. Cit. on pp. 32, 35, 88.

- 109 PÉREZ-SOTO, R.; BESORA, M.; MASERAS, F. The Challenge of Reproducing with Calculations Raw Experimental Kinetic Data for an Organic Reaction. **Organic Letters**, American Chemical Society (ACS), v. 22, n. 8, p. 2873–2877, Feb. 2020. ISSN 1523-7052. DOI: [10.1021/acs.orglett.0c00367](https://doi.org/10.1021/acs.orglett.0c00367). Available from: <http://dx.doi.org/10.1021/acs.orglett.0c00367>>. Cit. on pp. 33, 36, 37, 75.
- 110 KOZUCH, S.; SHAIK, S. A Combined Kinetic-Quantum Mechanical Model for Assessment of Catalytic Cycles: Application to Cross-Coupling and Heck Reactions. **Journal of the American Chemical Society**, American Chemical Society (ACS), v. 128, n. 10, p. 3355–3365, Mar. 2006. ISSN 1520-5126. DOI: [10.1021/ja0559146](https://doi.org/10.1021/ja0559146). Available from: <http://dx.doi.org/10.1021/ja0559146>>. Cit. on p. 34.
- 111 KOZUCH, S. Steady State Kinetics of Any Catalytic Network: Graph Theory, the Energy Span Model, the Analogy between Catalysis and Electrical Circuits, and the Meaning of “Mechanism”. **ACS Catalysis**, American Chemical Society (ACS), v. 5, n. 9, p. 5242–5255, Aug. 2015. ISSN 2155-5435. DOI: [10.1021/acscatal.5b00694](https://doi.org/10.1021/acscatal.5b00694). Available from: <http://dx.doi.org/10.1021/acscatal.5b00694>>. Cit. on p. 34.
- 112 SOLEL, E.; TARANNAM, N.; KOZUCH, S. Catalysis: energy is the measure of all things. **Chemical Communications**, Royal Society of Chemistry (RSC), v. 55, n. 37, p. 5306–5322, 2019. ISSN 1364-548x. DOI: [10.1039/c9cc00754g](https://doi.org/10.1039/c9cc00754g). Available from: <http://dx.doi.org/10.1039/c9cc00754g>>. Cit. on p. 34.
- 113 MICHAELIS, L.; MENTEN, M. L., et al. Die kinetik der invertinwirkung. **Biochem. z**, Berlin, v. 49, n. 333-369, p. 352, 1913. Cit. on p. 34.
- 114 JOHNSON, K. A.; GOODY, R. S. The Original Michaelis Constant: Translation of the 1913 Michaelis-Menten Paper. **Biochemistry**, American Chemical Society (ACS), v. 50, n. 39, p. 8264–8269, Sept. 2011. ISSN 1520-4995. DOI: [10.1021/bi201284u](https://doi.org/10.1021/bi201284u). Available from: <http://dx.doi.org/10.1021/bi201284u>>. Cit. on p. 34.
- 115 SRINIVASAN, B. Explicit Treatment of Non-Michaelis-Menten and Atypical Kinetics in Early Drug Discovery**. **ChemMedChem**, Wiley, v. 16, n. 6, p. 899–918, Dec. 2020. ISSN 1860-7187. DOI: [10.1002/cmdc.202000791](https://doi.org/10.1002/cmdc.202000791). Available from: <http://dx.doi.org/10.1002/cmdc.202000791>>. Cit. on p. 34.
- 116 _____. A guide to the Michaelis-Menten equation: steady state and beyond. **The FEBS Journal**, Wiley, v. 289, n. 20, p. 6086–6098, July 2021. ISSN 1742-4658. DOI: [10.1111/febs.16124](https://doi.org/10.1111/febs.16124). Available from: <http://dx.doi.org/10.1111/febs.16124>>. Cit. on p. 34.

- 117 EYRING, H. The Activated Complex in Chemical Reactions. **The Journal of Chemical Physics**, AIP Publishing, v. 3, n. 2, p. 107–115, Feb. 1935. ISSN 1089-7690. DOI: [10.1063/1.1749604](https://doi.org/10.1063/1.1749604). Available from: <http://dx.doi.org/10.1063/1.1749604>. Cit. on p. 35.
- 118 EVANS, M. G.; POLANYI, M. Some applications of the transition state method to the calculation of reaction velocities, especially in solution. **Transactions of the Faraday Society**, Royal Society of Chemistry (RSC), v. 31, p. 875, 1935. ISSN 0014-7672. DOI: [10.1039/tf9353100875](https://doi.org/10.1039/tf9353100875). Available from: <http://dx.doi.org/10.1039/TF9353100875>. Cit. on p. 35.
- 119 TRANSITION state theory. **IUPAC Compendium of Chemical Terminology**, Iupac, Feb. 2014. Accessed: 2017-05-27. DOI: [10.1351/goldbook.t06470](https://doi.org/10.1351/goldbook.t06470). Available from: <http://dx.doi.org/10.1351/goldbook.T06470>. Cit. on p. 35.
- 120 BECKE, A. D. Perspective: Fifty years of density-functional theory in chemical physics. **The Journal of Chemical Physics**, AIP Publishing, v. 140, n. 18, 18a301, May 2014. ISSN 1089-7690. DOI: [10.1063/1.4869598](https://doi.org/10.1063/1.4869598). Available from: <http://dx.doi.org/10.1063/1.4869598>. Cit. on p. 36.
- 121 BOGOJESKI, M. et al. Quantum chemical accuracy from density functional approximations *via* machine learning. **Nature Communications**, Springer Science and Business Media LLC, v. 11, n. 1, Oct. 2020. ISSN 2041-1723. DOI: [10.1038/s41467-020-19093-1](https://doi.org/10.1038/s41467-020-19093-1). Available from: <http://dx.doi.org/10.1038/s41467-020-19093-1>. Cit. on p. 36.
- 122 AHN, S. et al. Design and Optimization of Catalysts Based on Mechanistic Insights Derived from Quantum Chemical Reaction Modelling. **Chemical Reviews**, American Chemical Society (ACS), v. 119, n. 11, p. 6509–6560, May 2019. ISSN 1520-6890. DOI: [10.1021/acs.chemrev.9b00073](https://doi.org/10.1021/acs.chemrev.9b00073). Available from: <http://dx.doi.org/10.1021/acs.chemrev.9b00073>. Cit. on p. 37.
- 123 BIM, D. et al. Beyond the classical thermodynamic contributions to hydrogen atom abstraction reactivity. **Proceedings of the National Academy of Sciences**, Proceedings of the National Academy of Sciences, v. 115, n. 44, Sept. 2018. ISSN 1091-6490. DOI: [10.1073/pnas.1806399115](https://doi.org/10.1073/pnas.1806399115). Available from: <http://dx.doi.org/10.1073/pnas.1806399115>. Cit. on p. 37.
- 124 WIGNER, E. On the Quantum Correction For Thermodynamic Equilibrium. **Physical Review**, American Physical Society (APS), v. 40, n. 5, p. 749–759, June 1932. ISSN 0031-899x. DOI: [10.1103/physrev.40.749](https://doi.org/10.1103/physrev.40.749). Available from: <http://dx.doi.org/10.1103/PhysRev.40.749>. Cit. on p. 37.

- 125 ECKART, C. The Penetration of a Potential Barrier by Electrons. **Physical Review**, American Physical Society (APS), v. 35, n. 11, p. 1303–1309, June 1930. ISSN 0031-899x. DOI: [10.1103/physrev.35.1303](https://doi.org/10.1103/physrev.35.1303). Available from: <http://dx.doi.org/10.1103/PhysRev.35.1303>>. Cit. on p. 37.
- 126 THE command-line tool — overreact documentation. [S.l.: s.n.], 2022. <https://geem-lab.github.io/overreact-guide/cli.html>. Accessed: 2022-12-14. Available from: <https://geem-lab.github.io/overreact-guide/cli.html>>. Cit. on p. 38.
- 127 CURTISS, C. F.; HIRSCHFELDER, J. O. Integration of Stiff Equations. **Proceedings of the National Academy of Sciences**, Proceedings of the National Academy of Sciences, v. 38, n. 3, p. 235–243, Mar. 1952. ISSN 1091-6490. DOI: [10.1073/pnas.38.3.235](https://doi.org/10.1073/pnas.38.3.235). Available from: <http://dx.doi.org/10.1073/pnas.38.3.235>>. Cit. on p. 39.
- 128 HAIRER, E.; WANNER, G. Solving Ordinary Differential Equations II. **Springer Series in Computational Mathematics**, Springer Berlin Heidelberg, 1991. ISSN 0179-3632. DOI: [10.1007/978-3-662-09947-6](https://doi.org/10.1007/978-3-662-09947-6). Available from: <http://dx.doi.org/10.1007/978-3-662-09947-6>>. Cit. on p. 39.
- 129 PETZOLD, L. Automatic Selection of Methods for Solving Stiff and Nonstiff Systems of Ordinary Differential Equations. **SIAM Journal on Scientific and Statistical Computing**, Society for Industrial & Applied Mathematics (SIAM), v. 4, n. 1, p. 136–148, Mar. 1983. ISSN 2168-3417. DOI: [10.1137/0904010](https://doi.org/10.1137/0904010). Available from: <http://dx.doi.org/10.1137/0904010>>. Cit. on p. 39.
- 130 HAIRER, E.; WANNER, G. Solving Ordinary Differential Equations II. **Springer Series in Computational Mathematics**, Springer Berlin Heidelberg, 1996. ISSN 0179-3632. DOI: [10.1007/978-3-642-05221-7](https://doi.org/10.1007/978-3-642-05221-7). Available from: <http://dx.doi.org/10.1007/978-3-642-05221-7>>. Cit. on p. 39.
- 131 VIRTANEN, P. et al. SciPy 1.0: fundamental algorithms for scientific computing in Python. **Nature Methods**, Springer Science and Business Media LLC, v. 17, n. 3, p. 261–272, Feb. 2020. ISSN 1548-7105. DOI: [10.1038/s41592-019-0686-2](https://doi.org/10.1038/s41592-019-0686-2). Available from: <http://dx.doi.org/10.1038/s41592-019-0686-2>>. Cit. on p. 39.
- 132 BRADBURY, J. et al. **JAX: composable transformations of Python+NumPy programs**. [S.l.: s.n.], 2018. Available from: <http://github.com/google/jax>>. Cit. on p. 39.
- 133 DING, F.; SMITH, J. M.; WANG, H. First-Principles Calculation of pK_a Values for Organic Acids in Nonaqueous Solution. **The Journal of Organic Chemistry**, American Chemical Society (ACS), v. 74, n. 7, p. 2679–2691, Apr.

2009. ISSN 1520-6904. DOI: [10.1021/jo802641r](https://doi.org/10.1021/jo802641r). Available from: <http://dx.doi.org/10.1021/jo802641r>. Cit. on pp. 39, 40.
- 134 SUMON, K. Z.; HENNI, A.; EAST, A. L. L. Predicting pK_a of Amines for CO₂ Capture: Computer versus Pencil-and-Paper. **Industrial & Engineering Chemistry Research**, American Chemical Society (ACS), v. 51, n. 37, p. 11924–11930, Sept. 2012. ISSN 1520-5045. DOI: [10.1021/ie301033p](https://doi.org/10.1021/ie301033p). Available from: <http://dx.doi.org/10.1021/ie301033p>. Cit. on p. 39.
- 135 TISSANDIER, M. D. et al. The Proton's Absolute Aqueous Enthalpy and Gibbs Free Energy of Solvation from Cluster-Ion Solvation Data. **The Journal of Physical Chemistry A**, American Chemical Society (ACS), v. 102, n. 40, p. 7787–7794, Oct. 1998. ISSN 1520-5215. DOI: [10.1021/jp982638r](https://doi.org/10.1021/jp982638r). Available from: <http://dx.doi.org/10.1021/jp982638r>. Cit. on p. 40.
- 136 YANG, C. et al. Theoretical Study on the Acidities of Chiral Phosphoric Acids in Dimethyl Sulfoxide: Hints for Organocatalysis. **The Journal of Organic Chemistry**, American Chemical Society (ACS), v. 78, n. 14, p. 7076–7085, July 2013. ISSN 1520-6904. DOI: [10.1021/jo400915f](https://doi.org/10.1021/jo400915f). Available from: <http://dx.doi.org/10.1021/jo400915f>. Cit. on p. 40.
- 137 PLIEGO, J. R.; RIVEROS, J. M. Theoretical Calculation of pK_a Using the Cluster-Continuum Model. **The Journal of Physical Chemistry A**, American Chemical Society (ACS), v. 106, n. 32, p. 7434–7439, Aug. 2002. ISSN 1520-5215. DOI: [10.1021/jp025928n](https://doi.org/10.1021/jp025928n). Available from: <http://dx.doi.org/10.1021/jp025928n>. Cit. on p. 40.
- 138 GOLDBERG, R. N.; KISHORE, N.; LENNEN, R. M. Thermodynamic Quantities for the Ionization Reactions of Buffers. **Journal of Physical and Chemical Reference Data**, AIP Publishing, v. 31, n. 2, p. 231–370, June 2002. ISSN 1529-7845. DOI: [10.1063/1.1416902](https://doi.org/10.1063/1.1416902). Available from: <http://dx.doi.org/10.1063/1.1416902>. Cit. on p. 40.
- 139 GROSS, I. P. et al. Polylactic acid, maleic anhydride and dicumyl peroxide: NMR study of the free-radical melt reaction product. **Polymer Degradation and Stability**, Elsevier BV, v. 155, p. 1–8, Sept. 2018. ISSN 0141-3910. DOI: [10.1016/j.polyimdegstab.2018.06.016](https://doi.org/10.1016/j.polyimdegstab.2018.06.016). Available from: <http://dx.doi.org/10.1016/j.polyimdegstab.2018.06.016>. Cit. on pp. 43, 113.
- 140 SCHNEIDER, F. S. et al. A theoretical investigation on the aminolysis of pyromellitic and 1,4,5,8-naphthalenetetracarboxylic dianhydrides. **Computational and Theoretical Chemistry**, Elsevier BV, v. 1147, p. 13–19, Jan. 2019. ISSN 2210-271x. DOI: [10.1016/j.comptc.2018.11.008](https://doi.org/10.1016/j.comptc.2018.11.008). Available

- from: <<http://dx.doi.org/10.1016/j.comptc.2018.11.008>>. Cit. on pp. 43, 114.
- 141 ALMERINDO, G. I. et al. Kinetics and adsorption calculations: insights into the MgO-catalyzed detoxification of simulants of organophosphorus biocides. **Journal of Materials Chemistry A**, Royal Society of Chemistry (RSC), v. 8, n. 36, p. 19011–19021, 2020. ISSN 2050-7496. DOI: [10.1039/c9ta14028j](https://doi.org/10.1039/c9ta14028j). Available from: <<http://dx.doi.org/10.1039/C9TA14028J>>. Cit. on pp. 43, 115.
- 142 MILLER, M. A. et al. Nano-palladium is a cellular catalyst for *in vivo* chemistry. **Nature Communications**, Springer Science and Business Media LLC, v. 8, n. 1, July 2017. ISSN 2041-1723. DOI: [10.1038/ncomms15906](https://doi.org/10.1038/ncomms15906). Available from: <<http://dx.doi.org/10.1038/ncomms15906>>. Cit. on p. 57.
- 143 ACS AuthorChoice/Editors' Choice *via* Creative Commons CC-BY Usage Agreement. [S.l.: s.n.], 2014. https://pubs.acs.org/page/policy/authorchoice_ccby_termsofuse.html. Accessed: 2022-11-30. Available from: <https://pubs.acs.org/page/policy/authorchoice%5C_ccby%5C_termsofuse.html>. Cit. on pp. 58, 59.
- 144 NOTÍCIAS da UFSC: Artigo de professores da UFSC é capa da revista *Journal of the American Chemical Society*. [S.l.: s.n.], June 2020. <https://noticias.ufsc.br/2020/06/artigo-de-professores-da-ufsc-e-capda-revista-journal-of-the-american-chemical-society/>. Accessed: 2022-07-24. Available from: <<https://noticias.ufsc.br/2020/06/artigo-de-professores-da-ufsc-e-capda-revista-journal-of-the-american-chemical-society/>>. Cit. on p. 59.
- 145 BURKHOLDER, J. et al. **Chemical kinetics and photochemical data for use in atmospheric studies; evaluation number 19**. [S.l.], May 2020. Cit. on p. 75.
- 146 TANAKA, N.; XIAO, Y.; LASAGA, A. C. Ab initio study on carbon Kinetic Isotope Effect (KIE) in the reaction of CH₄+Cl? **Journal of Atmospheric Chemistry**, Springer Science and Business Media LLC, v. 23, n. 1, p. 37–49, Jan. 1996. ISSN 1573-0662. DOI: [10.1007/bf00058703](https://doi.org/10.1007/bf00058703). Available from: <<http://dx.doi.org/10.1007/BF00058703>>. Cit. on p. 75.
- 147 SCHNEIDER, F. S. S. **schneiderfelipe/pyrrole: pyrrole 0.2.1**. [S.l.]: Zenodo, June 2019. <https://doi.org/10.5281/zenodo.3242195>. Accessed: 2022-07-29. DOI: [10.5281/zenodo.3242195](https://doi.org/10.5281/zenodo.3242195). Available from: <<https://zenodo.org/record/3242196>>. Cit. on pp. 76, 114.

- 148 MIT License: Software Package Data Exchange (SPDX). [S.l.: s.n.], 1987.
<https://spdx.org/licenses/MIT.html>. Accessed: 2022-12-07. Available from:
<<https://spdx.org/licenses/MIT.html>>. Cit. on p. 76.
- 149 GARZA, A. J. Solvation Entropy Made Simple. **Journal of Chemical Theory and Computation**, American Chemical Society (ACS), v. 15, n. 5, p. 3204–3214, Mar. 2019. ISSN 1549-9626. DOI: [10.1021/acs.jctc.9b00214](https://doi.org/10.1021/acs.jctc.9b00214). Available from:
<<http://dx.doi.org/10.1021/acs.jctc.9b00214>>. Cit. on p. 88.
- 150 MILLER, J. R.; CALCATERRA, L. T.; CLOSS, G. L. Intramolecular long-distance electron transfer in radical anions. The effects of free energy and solvent on the reaction rates. **Journal of the American Chemical Society**, American Chemical Society (ACS), v. 106, n. 10, p. 3047–3049, May 1984. ISSN 1520-5126. DOI: [10.1021/ja00322a058](https://doi.org/10.1021/ja00322a058). Available from:
<<http://dx.doi.org/10.1021/ja00322a058>>. Cit. on p. 88.
- 151 THE Nobel Prize in Chemistry 1992. [S.l.: s.n.], 1992.
<https://www.nobelprize.org/prizes/chemistry/1992/summary/>. Accessed: 2022-12-06. Available from:
<<https://www.nobelprize.org/prizes/chemistry/1992/summary/>>. Cit. on p. 88.
- 152 NIKBIN, N.; CARATZOULAS, S.; VLACHOS, D. G. A First Principles-Based Microkinetic Model for the Conversion of Fructose to 5-Hydroxymethylfurfural. **ChemCatChem**, Wiley, v. 4, n. 4, p. 504–511, Feb. 2012. ISSN 1867-3880. DOI: [10.1002/cctc.201100444](https://doi.org/10.1002/cctc.201100444). Available from:
<<http://dx.doi.org/10.1002/cctc.201100444>>. Cit. on p. 88.
- 153 KAR, T. et al. Solvation Enhances the Distinction between Carboxylated Armchair and Zigzag Single-Wall Carbon Nanotubes (SWNT-COOH). **The Journal of Physical Chemistry C**, American Chemical Society (ACS), v. 121, n. 17, p. 9516–9527, Apr. 2017. ISSN 1932-7455. DOI: [10.1021/acs.jpcc.6b10676](https://doi.org/10.1021/acs.jpcc.6b10676). Available from:
<<http://dx.doi.org/10.1021/acs.jpcc.6b10676>>. Cit. on p. 113.
- 154 SCHNEIDER, F. S. S. et al. Bond Analysis in Dihalogen-Halide and Dihalogen-Dimethylchalcogenide Systems. **European Journal of Inorganic Chemistry**, Wiley, v. 2018, n. 8, p. 1007–1015, Feb. 2018. ISSN 1099-0682. DOI: [10.1002/ejic.201701337](https://doi.org/10.1002/ejic.201701337). Available from:
<<http://dx.doi.org/10.1002/ejic.201701337>>. Cit. on p. 113.
- 155 ØSTRØM, I. et al. Quest for Insight into Ultrashort C-H··· π Proximities in Molecular “Iron Maidens”. **The Journal of Organic Chemistry**, American Chemical Society (ACS), v. 83, n. 9, p. 5114–5122, Apr. 2018. ISSN 1520-6904.

- DOI: [10.1021/acs.joc.8b00461](https://doi.org/10.1021/acs.joc.8b00461). Available from:
<<http://dx.doi.org/10.1021/acs.joc.8b00461>>. Cit. on p. 113.
- 156 SCHNEIDER, F. S. S. et al. How Do Secondary Phosphine Oxides Interact with Silver Nanoclusters? Insights from Computation. **The Journal of Physical Chemistry C**, American Chemical Society (ACS), v. 122, n. 37, p. 21449–21461, Aug. 2018. ISSN 1932-7455. DOI: [10.1021/acs.jpcc.8b06244](https://doi.org/10.1021/acs.jpcc.8b06244). Available from:
<<http://dx.doi.org/10.1021/acs.jpcc.8b06244>>. Cit. on p. 113.
- 157 SCHNEIDER, F. S. S. **schneiderfelipe/pnictogen: Lightweight generation of input files**. [S.l.]: Zenodo, Aug. 2019.
<https://doi.org/10.5281/zenodo.3380593>. Accessed: 2022-07-29. DOI:
[10.5281/zenodo.3380593](https://doi.org/10.5281/zenodo.3380593). Available from:
<<https://zenodo.org/record/3380594>>. Cit. on p. 114.
- 158 MELO, C. E. de et al. Solvatochromism of new substituted 4-[(E)-(4-nitrophenyl)diazanyl]phenolate dyes. **Journal of Molecular Liquids**, Elsevier BV, v. 301, p. 112330, Mar. 2020. ISSN 0167-7322. DOI:
[10.1016/j.molliq.2019.112330](https://doi.org/10.1016/j.molliq.2019.112330). Available from:
<<http://dx.doi.org/10.1016/j.molliq.2019.112330>>. Cit. on p. 114.
- 159 ORENHA, R. P. et al. On the recognition of chloride, bromide and nitrate anions by anthracene-squaramide conjugated compounds: a computational perspective. **New Journal of Chemistry**, Royal Society of Chemistry (RSC), v. 44, n. 41, p. 17831–17839, 2020. ISSN 1369-9261. DOI: [10.1039/d0nj03685d](https://doi.org/10.1039/d0nj03685d). Available from:
<<http://dx.doi.org/10.1039/D0NJ03685D>>. Cit. on p. 114.
- 160 SCHNEIDER, F. S. S. **schneiderfelipe/doi2bib: doi2bib v1.1**. [S.l.]: Zenodo, Mar. 2021. <https://doi.org/10.5281/ZENODO.4625655>. Accessed: 2022-07-29. DOI: [10.5281/zenodo.4625655](https://doi.org/10.5281/zenodo.4625655). Available from:
<<https://zenodo.org/record/4625655>>. Cit. on p. 115.

Appendices

Appendix A – List of Works

The following list presents all the papers that I have co-authored and published during my PhD (March 2017–December 2022), together with open-source software that I have developed or contributed to. The ones relevant to the current topic are highlighted and referenced to the relevant chapters¹.

2017

- KAR, T. et al. Solvation Enhances the Distinction between Carboxylated Armchair and Zigzag Single-Wall Carbon Nanotubes (SWNT-COOH). **The Journal of Physical Chemistry C**, American Chemical Society (ACS), v. 121, n. 17, p. 9516–9527, Apr. 2017. ISSN 1932-7455. DOI: [10.1021/acs.jpcc.6b10676](https://doi.org/10.1021/acs.jpcc.6b10676). Available from: <http://dx.doi.org/10.1021/acs.jpcc.6b10676>
- SCHNEIDER, F. S. S. et al. Bond Analysis in Dihalogen-Halide and Dihalogen-Dimethylchalcogenide Systems. **European Journal of Inorganic Chemistry**, Wiley, v. 2018, n. 8, p. 1007–1015, Feb. 2018. ISSN 1099-0682. DOI: [10.1002/ejic.201701337](https://doi.org/10.1002/ejic.201701337). Available from: <http://dx.doi.org/10.1002/ejic.201701337>

2018

- ØSTRØM, I. et al. Quest for Insight into Ultrashort C-H... π Proximities in Molecular “Iron Maidens”. **The Journal of Organic Chemistry**, American Chemical Society (ACS), v. 83, n. 9, p. 5114–5122, Apr. 2018. ISSN 1520-6904. DOI: [10.1021/acs.joc.8b00461](https://doi.org/10.1021/acs.joc.8b00461). Available from: <http://dx.doi.org/10.1021/acs.joc.8b00461>
- GROSS, I. P. et al. Polylactic acid, maleic anhydride and dicumyl peroxide: NMR study of the free-radical melt reaction product. **Polymer Degradation and Stability**, Elsevier BV, v. 155, p. 1–8, Sept. 2018. ISSN 0141-3910. DOI: [10.1016/j.polymdegradstab.2018.06.016](https://doi.org/10.1016/j.polymdegradstab.2018.06.016). Available from: <http://dx.doi.org/10.1016/j.polymdegradstab.2018.06.016> (**Minor contribution**, see Section 2.1.)
- SCHNEIDER, F. S. S. et al. How Do Secondary Phosphine Oxides Interact with Silver Nanoclusters? Insights from Computation. **The Journal of Physical Chem-**

¹ “Minor contributions” are publications tangentially relevant to this thesis’ topic, while “major contributions” encompass publications described in the present work.

istry C, American Chemical Society (ACS), v. 122, n. 37, p. 21449–21461, Aug. 2018. ISSN 1932-7455. DOI: [10.1021/acs.jpcc.8b06244](https://doi.org/10.1021/acs.jpcc.8b06244). Available from: <http://dx.doi.org/10.1021/acs.jpcc.8b06244>

2019

- SCHNEIDER, F. S. et al. A theoretical investigation on the aminolysis of pyromellitic and 1,4,5,8-naphthalenetetracarboxylic dianhydrides. **Computational and Theoretical Chemistry**, Elsevier BV, v. 1147, p. 13–19, Jan. 2019. ISSN 2210-271x. DOI: [10.1016/j.comptc.2018.11.008](https://doi.org/10.1016/j.comptc.2018.11.008). Available from: <http://dx.doi.org/10.1016/j.comptc.2018.11.008> (**Minor contribution**, see Section 2.1.)
- COELHO, S. E. et al. Mechanism of Palladium(II)-Mediated Uncaging Reactions of Propargylic Substrates. **ACS Catalysis**, American Chemical Society (ACS), v. 9, n. 5, p. 3792–3799, Mar. 2019. ISSN 2155-5435. DOI: [10.1021/acscatal.9b00210](https://doi.org/10.1021/acscatal.9b00210). Available from: <http://dx.doi.org/10.1021/acscatal.9b00210> (**Major contribution**, see Section 2.2 and Chapter 3.)

Software

- SCHNEIDER, F. S. S. **schneiderfelipe/pyrrole: pyrrole 0.2.1**. [S.l.]: Zenodo, June 2019. <https://doi.org/10.5281/zenodo.3242195>. Accessed: 2022-07-29. DOI: [10.5281/zenodo.3242195](https://doi.org/10.5281/zenodo.3242195). Available from: <https://zenodo.org/record/3242196> (A first iteration on overreact [3, 29], see Section 2.2 and Chapter 5.)
- SCHNEIDER, F. S. S. **schneiderfelipe/pnictogen: Lightweight generation of input files**. [S.l.]: Zenodo, Aug. 2019. <https://doi.org/10.5281/zenodo.3380593>. Accessed: 2022-07-29. DOI: [10.5281/zenodo.3380593](https://doi.org/10.5281/zenodo.3380593). Available from: <https://zenodo.org/record/3380594>

2020

- MELO, C. E. de et al. Solvatochromism of new substituted 4-[(E)-(4-nitrophenyl)diazenyl]phenolate dyes. **Journal of Molecular Liquids**, Elsevier BV, v. 301, p. 112330, Mar. 2020. ISSN 0167-7322. DOI: [10.1016/j.molliq.2019.112330](https://doi.org/10.1016/j.molliq.2019.112330). Available from: <http://dx.doi.org/10.1016/j.molliq.2019.112330>
- ORENHA, R. P. et al. On the recognition of chloride, bromide and nitrate anions by anthracene-squaramide conjugated compounds: a computational perspective. **New**

Journal of Chemistry, Royal Society of Chemistry (RSC), v. 44, n. 41, p. 17831–17839, 2020. ISSN 1369-9261. DOI: [10.1039/d0nj03685d](https://doi.org/10.1039/d0nj03685d). Available from: <http://dx.doi.org/10.1039/D0NJ03685D>

- ALMERINDO, G. I. et al. Kinetics and adsorption calculations: insights into the MgO-catalyzed detoxification of simulants of organophosphorus biocides. **Journal of Materials Chemistry A**, Royal Society of Chemistry (RSC), v. 8, n. 36, p. 19011–19021, 2020. ISSN 2050-7496. DOI: [10.1039/c9ta14028j](https://doi.org/10.1039/c9ta14028j). Available from: <http://dx.doi.org/10.1039/C9TA14028J> (**Minor contribution**, see Section 2.1.)
- OLIVEIRA, B. L. et al. Platinum-Triggered Bond-Cleavage of Pentynoyl Amide and N-Propargyl Handles for Drug-Activation. **Journal of the American Chemical Society**, American Chemical Society (ACS), v. 142, n. 24, p. 10869–10880, May 2020. ISSN 1520-5126. DOI: [10.1021/jacs.0c01622](https://doi.org/10.1021/jacs.0c01622). Available from: <http://dx.doi.org/10.1021/jacs.0c01622> (**Major contribution**, see Section 2.2 and Chapter 4.)

2021

Software

- SCHNEIDER, F. S. S. **schneiderfelipe/doi2bib: doi2bib v1.1**. [S.l.]: Zenodo, Mar. 2021. <https://doi.org/10.5281/ZENODO.4625655>. Accessed: 2022-07-29. DOI: [10.5281/zenodo.4625655](https://doi.org/10.5281/zenodo.4625655). Available from: <https://zenodo.org/record/4625655>
- SCHNEIDER, F. S. S. **geem-lab/overreact: overreact v1.0.2**. [S.l.]: Zenodo, Nov. 2021. <https://doi.org/10.5281/ZENODO.5730603>. Accessed: 2022-07-29. DOI: [10.5281/zenodo.5730603](https://doi.org/10.5281/zenodo.5730603). Available from: <https://zenodo.org/record/5730603> (**Major contribution**, see Section 2.2 and Chapter 5.)

2022

- SCHNEIDER, F. S. S.; CARAMORI, G. F. Overreact, an *in silico* lab: Automatic quantum chemical microkinetic simulations for complex chemical reactions. **Journal of Computational Chemistry**, Wiley, Apr. 2022. ISSN 1096-987x. DOI: [10.1002/jcc.26861](https://doi.org/10.1002/jcc.26861). Available from: <http://dx.doi.org/10.1002/jcc.26861> (**Major contribution**, see Section 2.2 and Chapter 5.)

Annexes

Annex A – Rights for Chapter 1



Home



Help ▾



Live Chat



Sign in



Create Account

Mechanism of Palladium(II)-Mediated Uncaging Reactions of Propargylic Substrates



Author: Sara E. Coelho, Felipe S. S. Schneider, Daniela C. de Oliveira, et al

Publication: ACS Catalysis

Publisher: American Chemical Society

Date: May 1, 2019

Copyright © 2019, American Chemical Society

PERMISSION/LICENSE IS GRANTED FOR YOUR ORDER AT NO CHARGE

This type of permission/license, instead of the standard Terms and Conditions, is sent to you because no fee is being charged for your order. Please note the following:

- Permission is granted for your request in both print and electronic formats, and translations.
- If figures and/or tables were requested, they may be adapted or used in part.
- Please print this page for your records and send a copy of it to your publisher/graduate school.
- Appropriate credit for the requested material should be given as follows: "Reprinted (adapted) with permission from {COMPLETE REFERENCE CITATION}. Copyright {YEAR} American Chemical Society." Insert appropriate information in place of the capitalized words.
- One-time permission is granted only for the use specified in your RightsLink request. No additional uses are granted (such as derivative works or other editions). For any uses, please submit a new request.

If credit is given to another source for the material you requested from RightsLink, permission must be obtained from that source.

[BACK](#)

[CLOSE WINDOW](#)

Annex B – Rights for Chapter 2

ACS AuthorChoice/Editors' Choice via Creative Commons CC-BY Usage Agreement

Note

ACS Publications has now ceased using this license for newly published articles, but the license remains valid for select articles published previously.

This ACS article is provided to You under the terms of this *ACS AuthorChoice/Editors' Choice* via Creative Commons CC-BY agreement between You and the American Chemical Society ("ACS"), a federally-chartered nonprofit located at 1155 16th Street NW, Washington DC 20036. Your access and use of this ACS article means that you have accepted and agreed to the Terms and Conditions of this Agreement. ACS and You are collectively referred to in this Agreement as "the Parties").

1. SCOPE OF GRANT

ACS grants You a non-exclusive and nontransferable permission to access and use this ACS article subject to the terms and conditions set forth in this Agreement.

2. PERMITTED USES

a. ACS grants You the rights in the attached Creative Commons Attribution 4.0 International license. Consistent with the Creative Commons Attribution 4.0 license we note that any use of the article is subject to the following conditions:

- i. The authors' moral right to the integrity of their work under the Berne Convention (Article 6bis) is not compromised.
- ii. Where content in the article is identified as belonging to a third party, it is your responsibility to ensure that any reuse complies with copyright policies of the owner.

3. TERMINATION

ACS reserves the right to limit, suspend, or terminate your access to and use of the ACS Publications Division website and/or all ACS articles immediately upon detecting a breach of this License.

4. COPYRIGHTS; OTHER INTELLECTUAL PROPERTY RIGHTS

Codified in Title 17 of the U.S. Code and subject to the Universal Copyright Convention and the Berne Copyright Convention. You agree not to remove or obscure copyright notices. You acknowledge that You have no claim to ownership of any part of this ACS article or other proprietary information accessed under this Agreement. The names "American Chemical Society," "ACS" and the titles of the journals and other ACS products are trademarks of ACS.

5. DISCLAIMER OF WARRANTIES; LIMITATION OF LIABILITY

ACS warrants that it is entitled to grant this Agreement.

EXCEPT AS SET FORTH IN THE PRECEDING SENTENCE, ACS MAKES NO WARRANTY OR REPRESENTATION OF ANY KIND, EXPRESS OR IMPLIED, WITH RESPECT TO THIS ACS ARTICLE INCLUDING, BUT NOT LIMITED TO WARRANTIES AS TO THE ACCURACY OR COMPLETENESS OF THE ACS ARTICLE, ITS QUALITY, ORIGINALITY, SUITABILITY, SEARCHABILITY, OPERATION, PERFORMANCE, COMPLIANCE WITH ANY COMPUTATIONAL PROCESS, MERCHANTABILITY OR FITNESS FOR A PARTICULAR PURPOSE.

ACS SHALL NOT BE LIABLE FOR: EXEMPLARY, SPECIAL, INDIRECT, INCIDENTAL, CONSEQUENTIAL OR OTHER DAMAGES ARISING OUT OF OR IN CONNECTION WITH THE AGREEMENT GRANTED HEREUNDER, THE USE OR INABILITY TO USE ANY ACS PRODUCT, ACS'S PERFORMANCE UNDER THIS AGREEMENT, TERMINATION OF THIS AGREEMENT BY ACS OR THE LOSS OF DATA, BUSINESS OR GOODWILL EVEN IF ACS IS ADVISED OR AWARE OF THE POSSIBILITY OF SUCH DAMAGES. IN NO EVENT SHALL THE TOTAL AGGREGATE LIABILITY OF ACS OUT OF ANY BREACH OR TERMINATION OF THIS AGREEMENT EXCEED THE TOTAL AMOUNT PAID BY YOU TO ACS FOR ACCESS TO THIS ACS ARTICLE FOR THE CURRENT YEAR IN WHICH SUCH CLAIM, LOSS OR DAMAGE OCCURRED, WHETHER IN CONTRACT, TORT OR OTHERWISE, INCLUDING, WITHOUT LIMITATION, DUE TO NEGLIGENCE.

The foregoing limitations and exclusions of certain damages shall apply regardless of the success or effectiveness of other remedies. No claim may be made against ACS unless suit is filed within one (1) year after the event giving rise to the claim.

6. GENERAL

This Agreement sets forth the entire understanding of the Parties. The validity, construction and performance of this Agreement shall be governed by and construed in accordance with the laws of the District of Columbia, USA without reference to its conflicts of laws principles. You acknowledge that the delivery of the ACS article will occur in the District of Columbia, USA. You shall pay any taxes lawfully due from it, other than taxes on ACS's net income, arising out of your use of this ACS article and/or other rights granted under this Agreement.

7. ACCEPTANCE

constitute acceptance of the terms and conditions as modified.

Creative Commons Attribution 4.0 International Public License

By exercising the Licensed Rights (defined below), You accept and agree to be bound by the terms and conditions of this Creative Commons Attribution 4.0 International Public License ("Public License"). To the extent this Public License may be interpreted as a contract, You are granted the Licensed Rights in consideration of Your acceptance of these terms and conditions, and the Licensor grants You such rights in consideration of benefits the Licensor receives from making the Licensed Material available under these terms and conditions.

Section 1 – Definitions

- a. **Adapted Material** means material subject to Copyright and Similar Rights that is derived from or based upon the Licensed Material and in which the Licensed Material is translated, altered, arranged, transformed, or otherwise modified in a manner requiring permission under the Copyright and Similar Rights held by the Licensor. For purposes of this Public License, where the Licensed Material is a musical work, performance, or sound recording, Adapted Material is always produced where the Licensed Material is synched in timed relation with a moving image.
- b. **Adapter's License** means the license You apply to Your Copyright and Similar Rights in Your contributions to Adapted Material in accordance with the terms and conditions of this Public License.
- c. **Copyright and Similar Rights** means copyright and/or similar rights closely related to copyright including, without limitation, performance, broadcast, sound recording, and Sui Generis Database Rights, without regard to how the rights are labeled or categorized. For purposes of this Public License, the rights specified in Section 2(b)(1)-(2) are not Copyright and Similar Rights.
- d. **Effective Technological Measures** means those measures that, in the absence of proper authority, may not be circumvented under laws fulfilling obligations under Article 11 of the WIPO Copyright Treaty adopted on December 20, 1996, and/or similar international agreements.
- e. **Exceptions and Limitations** means fair use, fair dealing, and/or any other exception or limitation to Copyright and Similar Rights that applies to Your use of the Licensed Material.
- f. **Licensed Material** means the artistic or literary work, database, or other material to which the Licensor applied this Public License.
- g. **Licensed Rights** means the rights granted to You subject to the terms and conditions of this Public License, which are limited to all Copyright and Similar Rights that apply to Your use of the Licensed Material and that the Licensor has authority to license.
- h. **Licensor** means the individual(s) or entity(ies) granting rights under this Public License.

ways that members of the public may access the material from a place and at a time individually chosen by them.

j. **Sui Generis Database Rights** means rights other than copyright resulting from Directive 96/9/EC of the European Parliament and of the Council of 11 March 1996 on the legal protection of databases, as amended and/or succeeded, as well as other essentially equivalent rights anywhere in the world.

k. **You** means the individual or entity exercising the Licensed Rights under this Public License. **Your** has a corresponding meaning.

Section 2 – Scope

a. License grant.

1. Subject to the terms and conditions of this Public License, the Licensor hereby grants You a worldwide, royalty-free, non-sublicensable, non-exclusive, irrevocable license to exercise the Licensed Rights in the Licensed Material to:

- A. reproduce and Share the Licensed Material, in whole or in part; and
- B. produce, reproduce, and Share Adapted Material.

2. *Exceptions and Limitations.* For the avoidance of doubt, where Exceptions and Limitations apply to Your use, this Public License does not apply, and You do not need to comply with its terms and conditions.

3. *Term.* The term of this Public License is specified in Section 6(a).

4. *Media and formats;* technical modifications allowed. The Licensor authorizes You to exercise the Licensed Rights in all media and formats whether now known or hereafter created, and to make technical modifications necessary to do so. The Licensor waives and/or agrees not to assert any right or authority to forbid You from making technical modifications necessary to exercise the Licensed Rights, including technical modifications necessary to circumvent Effective Technological Measures. For purposes of this Public License, simply making modifications authorized by this Section 2(a)(4) never produces Adapted Material.

5. *Downstream recipients*

A. *Offer from the Licensor – Licensed Material.* Every recipient of the Licensed Material automatically receives an offer from the Licensor to exercise the Licensed Rights under the terms and conditions of this Public License.

B. *No downstream restrictions.* You may not offer or impose any additional or different terms or conditions on, or apply any Effective Technological Measures to, the Licensed Material if doing so restricts exercise of the Licensed Rights by any recipient of the Licensed Material.

provided in Section 3(a)(1)(A)(I).

b. Other rights.

1. Moral rights, such as the right of integrity, are not licensed under this Public License, nor are publicity, privacy, and/or other similar personality rights; however, to the extent possible, the Licensor waives and/or agrees not to assert any such rights held by the Licensor to the limited extent necessary to allow You to exercise the Licensed Rights, but not otherwise.
2. Patent and trademark rights are not licensed under this Public License.
3. To the extent possible, the Licensor waives any right to collect royalties from You for the exercise of the Licensed Rights, whether directly or through a collecting society under any voluntary or waivable statutory or compulsory licensing scheme. In all other cases the Licensor expressly reserves any right to collect such royalties.

Section 3 – License Conditions

Your exercise of the Licensed Rights is expressly made subject to the following conditions.

a. Attribution

1. If You Share the Licensed Material (including in modified form), You must:

A. retain the following if it is supplied by the Licensor with the Licensed Material:

- i. identification of the creator(s) of the Licensed Material and any others designated to receive attribution, in any reasonable manner requested by the Licensor (including by pseudonym if designated);
- ii. a copyright notice;
- iii. a notice that refers to this Public License;
- iv. a notice that refers to the disclaimer of warranties;
- v. a URI or hyperlink to the Licensed Material to the extent reasonably practicable;

B. indicate if You modified the Licensed Material and retain an indication of any previous modifications; and

C. indicate the Licensed Material is licensed under this Public License, and include the text of, or the URI or hyperlink to, this Public License.

2. You may satisfy the conditions in Section 3(a)(1) in any reasonable manner based on the medium, means, and context in which You Share the Licensed Material. For example, it may be reasonable to satisfy the conditions by providing a URI or hyperlink to a resource that includes the required information.

recipients of the Adapted Material from complying with this Public License.

Section 4 – Sui Generis Database Rights

Where the Licensed Rights include Sui Generis Database Rights that apply to Your use of the Licensed Material:

- a. for the avoidance of doubt, Section 2(a)(1) grants You the right to extract, reuse, reproduce, and Share all or a substantial portion of the contents of the database;
- b. if You include all or a substantial portion of the database contents in a database in which You have Sui Generis Database Rights, then the database in which You have Sui Generis Database Rights (but not its individual contents) is Adapted Material; and
- c. You must comply with the conditions in Section 3(a) if You Share all or a substantial portion of the contents of the database.

For the avoidance of doubt, this Section 4 supplements and does not replace Your obligations under this Public License where the Licensed Rights include other Copyright and Similar Rights.

Section 5 – Disclaimer of Warranties and Limitation of Liability

- a. **Unless otherwise separately undertaken by the Licensor, to the extent possible, the Licensor offers the Licensed Material as-is and as-available, and makes no representations or warranties of any kind concerning the Licensed Material, whether express, implied, statutory, or other. This includes, without limitation, warranties of title, merchantability, fitness for a particular purpose, non-infringement, absence of latent or other defects, accuracy, or the presence or absence of errors, whether or not known or discoverable. Where disclaimers of warranties are not allowed in full or in part, this disclaimer may not apply to You.**
- b. **To the extent possible, in no event will the Licensor be liable to You on any legal theory (including, without limitation, negligence) or otherwise for any direct, special, indirect, incidental, consequential, punitive, exemplary, or other losses, costs, expenses, or damages arising out of this Public License or use of the Licensed Material, even if the Licensor has been advised of the possibility of such losses, costs, expenses, or damages. Where a limitation of liability is not allowed in full or in part, this limitation may not apply to You.**
- c. The disclaimer of warranties and limitation of liability provided above shall be interpreted in a manner that, to the extent possible, most closely approximates an absolute disclaimer and waiver of all liability.

Section 6 – Term and Termination

- a. This Public License applies for the term of the Copyright and Similar Rights licensed here. However, if

1. automatically as of the date the violation is cured, provided it is cured within 30 days of Your discovery of the violation; or
2. upon express reinstatement by the Licensor. For the avoidance of doubt, this Section 6(b) does not affect any right the Licensor may have to seek remedies for Your violations of this Public License.
- c. For the avoidance of doubt, the Licensor may also offer the Licensed Material under separate terms or conditions or stop distributing the Licensed Material at any time; however, doing so will not terminate this Public License.
- d. Sections 1, 5, 6, 7, and 8 survive termination of this Public License.

Section 7 – Other Terms and Conditions

- a. The Licensor shall not be bound by any additional or different terms or conditions communicated by You unless expressly agreed.
- b. Any arrangements, understandings, or agreements regarding the Licensed Material not stated herein are separate from and independent of the terms and conditions of this Public License.

Section 8 – Interpretation

- a. For the avoidance of doubt, this Public License does not, and shall not be interpreted to, reduce, limit, restrict, or impose conditions on any use of the Licensed Material that could lawfully be made without permission under this Public License.
- b. To the extent possible, if any provision of this Public License is deemed unenforceable, it shall be automatically reformed to the minimum extent necessary to make it enforceable. If the provision cannot be reformed, it shall be severed from this Public License without affecting the enforceability of the remaining terms and conditions.
- c. No term or condition of this Public License will be waived and no failure to comply consented to unless expressly agreed to by the Licensor.
- d. Nothing in this Public License constitutes or may be interpreted as a limitation upon, or waiver of, any privileges and immunities that apply to the Licensor or You, including from the legal processes of any jurisdiction or authority.

[Back to ACS Publishing Policies](#)

Posted: 03/06/2014

Master the fundamentals of peer review in our free online course. [Click here to sign up.](#)



Connect with our language editors and scientific illustrators to help showcase your science at its best. [Click here to learn more.](#)



Get expert advice from the ACS editor community in this brand-new video series. [Click here to watch.](#)

Partners



1155 Sixteenth Street N.W.
Washington, DC 20036

ABOUT

About ACS Publications
ACS & Open Access
ACS Membership

**RESOURCES AND
INFORMATION**

Journals A-Z
Books and Reference
Advertising Media Kit
Institutional Sales
ACS Publishing Center
Privacy Policy
Terms of Use

SUPPORT & CONTACT

Help
Live Chat
FAQ

Connect with ACS Publications

Annex C – Rights for Chapter 3

JOHN WILEY AND SONS LICENSE TERMS AND CONDITIONS

Nov 30, 2022

This Agreement between Felipe S. S. Schneider ("You") and John Wiley and Sons ("John Wiley and Sons") consists of your license details and the terms and conditions provided by John Wiley and Sons and Copyright Clearance Center.

License Number 5438920643292

License date Nov 30, 2022

Licensed Content
Publisher John Wiley and Sons

Licensed Content
Publication Journal of Computational Chemistry

Licensed Content
Title Overreact, an in silico lab: Automative quantum
chemical microkinetic simulations for complex
chemical reactions

Licensed Content
Author Giovanni F. Caramori, Felipe S. S. Schneider

Licensed Content
Date Apr 11, 2022

Licensed Content
Volume 0

Licensed Content
Issue 0

Licensed Content
Pages 9

Type of use	Dissertation/Thesis
Requestor type	Author of this Wiley article
Format	Print and electronic
Portion	Full article
Will you be translating?	No
Title	Quantitative computational contributions to the elucidation of chemical reaction mechanisms
Institution name	Federal University of Santa Catarina
Expected presentation date	Jan 2023
Order reference number	07021351941
Requestor Location	Felipe S. S. Schneider Luis Oscar de Carvalho, 75 Apto 14 B6, Trindade Florianópolis, Santa Catarina 88036400 Brazil Attn: Felipe S. S. Schneider
Publisher Tax ID	EU826007151
Customer VAT ID	BR07021351941
Total	0.00 USD
Terms and Conditions	

TERMS AND CONDITIONS

This copyrighted material is owned by or exclusively licensed to John Wiley & Sons, Inc. or one of its group companies (each a "Wiley Company") or handled on behalf of a society with which a Wiley Company has exclusive publishing rights in relation to a particular work (collectively "WILEY"). By clicking "accept" in connection with completing this licensing transaction, you agree that the following terms and conditions apply to this transaction (along with the billing and payment terms and conditions established by the Copyright Clearance Center Inc., ("CCC's Billing and Payment terms and conditions"), at the time that you opened your RightsLink account (these are available at any time at <http://myaccount.copyright.com>).

Terms and Conditions

- The materials you have requested permission to reproduce or reuse (the "Wiley Materials") are protected by copyright.
- You are hereby granted a personal, non-exclusive, non-sub licensable (on a stand-alone basis), non-transferable, worldwide, limited license to reproduce the Wiley Materials for the purpose specified in the licensing process. This license, **and any CONTENT (PDF or image file) purchased as part of your order**, is for a one-time use only and limited to any maximum distribution number specified in the license. The first instance of republication or reuse granted by this license must be completed within two years of the date of the grant of this license (although copies prepared before the end date may be distributed thereafter). The Wiley Materials shall not be used in any other manner or for any other purpose, beyond what is granted in the license. Permission is granted subject to an appropriate acknowledgement given to the author, title of the material/book/journal and the publisher. You shall also duplicate the copyright notice that appears in the Wiley publication in your use of the Wiley Material. Permission is also granted on the understanding that nowhere in the text is a previously published source acknowledged for all or part of this Wiley Material. Any third party content is expressly excluded from this permission.
- With respect to the Wiley Materials, all rights are reserved. Except as expressly granted by the terms of the license, no part of the Wiley Materials may be copied, modified, adapted (except for minor reformatting required by the new Publication), translated, reproduced, transferred or distributed, in any form or by any means, and no derivative works may be made based on the Wiley Materials without the prior permission of the respective copyright owner. **For STM Signatory Publishers clearing permission under the terms of the [STM Permissions Guidelines](#) only, the terms of the license are extended to include subsequent editions and for editions in other languages, provided such editions are for the work as a whole in situ and does not involve the separate exploitation of the permitted figures or extracts**, You may not alter, remove or suppress in any manner any

copyright, trademark or other notices displayed by the Wiley Materials. You may not license, rent, sell, loan, lease, pledge, offer as security, transfer or assign the Wiley Materials on a stand-alone basis, or any of the rights granted to you hereunder to any other person.

- The Wiley Materials and all of the intellectual property rights therein shall at all times remain the exclusive property of John Wiley & Sons Inc, the Wiley Companies, or their respective licensors, and your interest therein is only that of having possession of and the right to reproduce the Wiley Materials pursuant to Section 2 herein during the continuance of this Agreement. You agree that you own no right, title or interest in or to the Wiley Materials or any of the intellectual property rights therein. You shall have no rights hereunder other than the license as provided for above in Section 2. No right, license or interest to any trademark, trade name, service mark or other branding ("Marks") of WILEY or its licensors is granted hereunder, and you agree that you shall not assert any such right, license or interest with respect thereto
- NEITHER WILEY NOR ITS LICENSORS MAKES ANY WARRANTY OR REPRESENTATION OF ANY KIND TO YOU OR ANY THIRD PARTY, EXPRESS, IMPLIED OR STATUTORY, WITH RESPECT TO THE MATERIALS OR THE ACCURACY OF ANY INFORMATION CONTAINED IN THE MATERIALS, INCLUDING, WITHOUT LIMITATION, ANY IMPLIED WARRANTY OF MERCHANTABILITY, ACCURACY, SATISFACTORY QUALITY, FITNESS FOR A PARTICULAR PURPOSE, USABILITY, INTEGRATION OR NON-INFRINGEMENT AND ALL SUCH WARRANTIES ARE HEREBY EXCLUDED BY WILEY AND ITS LICENSORS AND WAIVED BY YOU.
- WILEY shall have the right to terminate this Agreement immediately upon breach of this Agreement by you.
- You shall indemnify, defend and hold harmless WILEY, its Licensors and their respective directors, officers, agents and employees, from and against any actual or threatened claims, demands, causes of action or proceedings arising from any breach of this Agreement by you.
- IN NO EVENT SHALL WILEY OR ITS LICENSORS BE LIABLE TO YOU OR ANY OTHER PARTY OR ANY OTHER PERSON OR ENTITY FOR ANY SPECIAL, CONSEQUENTIAL, INCIDENTAL, INDIRECT, EXEMPLARY OR PUNITIVE DAMAGES, HOWEVER CAUSED, ARISING OUT OF OR IN CONNECTION WITH THE DOWNLOADING, PROVISIONING, VIEWING OR USE OF THE MATERIALS REGARDLESS OF THE FORM OF ACTION, WHETHER FOR BREACH OF CONTRACT, BREACH OF WARRANTY, TORT, NEGLIGENCE, INFRINGEMENT OR OTHERWISE (INCLUDING, WITHOUT LIMITATION, DAMAGES BASED ON LOSS OF PROFITS, DATA, FILES, USE, BUSINESS OPPORTUNITY OR CLAIMS OF

THIRD PARTIES), AND WHETHER OR NOT THE PARTY HAS BEEN ADVISED OF THE POSSIBILITY OF SUCH DAMAGES. THIS LIMITATION SHALL APPLY NOTWITHSTANDING ANY FAILURE OF ESSENTIAL PURPOSE OF ANY LIMITED REMEDY PROVIDED HEREIN.

- Should any provision of this Agreement be held by a court of competent jurisdiction to be illegal, invalid, or unenforceable, that provision shall be deemed amended to achieve as nearly as possible the same economic effect as the original provision, and the legality, validity and enforceability of the remaining provisions of this Agreement shall not be affected or impaired thereby.
- The failure of either party to enforce any term or condition of this Agreement shall not constitute a waiver of either party's right to enforce each and every term and condition of this Agreement. No breach under this agreement shall be deemed waived or excused by either party unless such waiver or consent is in writing signed by the party granting such waiver or consent. The waiver by or consent of a party to a breach of any provision of this Agreement shall not operate or be construed as a waiver of or consent to any other or subsequent breach by such other party.
- This Agreement may not be assigned (including by operation of law or otherwise) by you without WILEY's prior written consent.
- Any fee required for this permission shall be non-refundable after thirty (30) days from receipt by the CCC.
- These terms and conditions together with CCC's Billing and Payment terms and conditions (which are incorporated herein) form the entire agreement between you and WILEY concerning this licensing transaction and (in the absence of fraud) supersedes all prior agreements and representations of the parties, oral or written. This Agreement may not be amended except in writing signed by both parties. This Agreement shall be binding upon and inure to the benefit of the parties' successors, legal representatives, and authorized assigns.
- In the event of any conflict between your obligations established by these terms and conditions and those established by CCC's Billing and Payment terms and conditions, these terms and conditions shall prevail.
- WILEY expressly reserves all rights not specifically granted in the combination of (i) the license details provided by you and accepted in the course of this licensing transaction, (ii) these terms and conditions and (iii) CCC's Billing and Payment terms and conditions.
- This Agreement will be void if the Type of Use, Format, Circulation, or Requestor Type was misrepresented during the licensing process.

- This Agreement shall be governed by and construed in accordance with the laws of the State of New York, USA, without regards to such state's conflict of law rules. Any legal action, suit or proceeding arising out of or relating to these Terms and Conditions or the breach thereof shall be instituted in a court of competent jurisdiction in New York County in the State of New York in the United States of America and each party hereby consents and submits to the personal jurisdiction of such court, waives any objection to venue in such court and consents to service of process by registered or certified mail, return receipt requested, at the last known address of such party.

WILEY OPEN ACCESS TERMS AND CONDITIONS

Wiley Publishes Open Access Articles in fully Open Access Journals and in Subscription journals offering Online Open. Although most of the fully Open Access journals publish open access articles under the terms of the Creative Commons Attribution (CC BY) License only, the subscription journals and a few of the Open Access Journals offer a choice of Creative Commons Licenses. The license type is clearly identified on the article.

The Creative Commons Attribution License

The [Creative Commons Attribution License \(CC-BY\)](#) allows users to copy, distribute and transmit an article, adapt the article and make commercial use of the article. The CC-BY license permits commercial and non-

Creative Commons Attribution Non-Commercial License

The [Creative Commons Attribution Non-Commercial \(CC-BY-NC\) License](#) permits use, distribution and reproduction in any medium, provided the original work is properly cited and is not used for commercial purposes.(see below)

Creative Commons Attribution-Non-Commercial-NoDerivs License

The [Creative Commons Attribution Non-Commercial-NoDerivs License](#) (CC-BY-NC-ND) permits use, distribution and reproduction in any medium, provided the original work is properly cited, is not used for commercial purposes and no modifications or adaptations are made. (see below)

Use by commercial "for-profit" organizations

Use of Wiley Open Access articles for commercial, promotional, or marketing purposes requires further explicit permission from Wiley and will be subject to a fee.

Further details can be found on Wiley Online Library
<http://olabout.wiley.com/WileyCDA/Section/id-410895.html>

Other Terms and Conditions:

v1.10 Last updated September 2015

**Questions? customercare@copyright.com or +1-855-239-3415
(toll free in the US) or +1-978-646-2777.**

